Review article: Polymer-matrix Nanocomposites, Processing, Manufacturing, and Application: An Overview

FARZANA HUSSAIN*
MEHDI HOJJATI

*Aerospace Manufacturing Technology Center (AMTC)
Institute for Aerospace Research (IAR), National Research
Council Canada (NRC), Montreal, QC, Canada*

MASAMI OKAMOTO

*Advanced Polymeric Nanostructured Materials Engineering
Graduate School of Engineering Toyota Technological Institute, Japan*

RUSSELL E. GORGA

*North Carolina State University, Fiber and
Polymer Science Raleigh, NC, USA*

ABSTRACT: This review is designed to be a comprehensive source for polymer nanocomposite research, including fundamental structure/property relationships, manufacturing techniques, and applications of polymer nanocomposite materials. In addition to presenting the scientific framework for the advances in polymer nanocomposite research, this review focuses on the scientific principles and mechanisms in relation to the methods of processing and manufacturing with a discussion on commercial applications and health/safety concerns (a critical issue for production and scale-up). Hence, this review offers a comprehensive discussion on technology, modeling, characterization, processing, manufacturing, applications, and health/safety concerns for polymer nanocomposites.

---

*Author to whom correspondence should be addressed. E-mail: farzssain@gmail.com
Figures 1, 4, 5, 9, 11, 12, 15, 20–22, 25, 27–32 and 34 appear in color online: http://jcm.sagepub.com

Table of Contents

INTRODUCTION AND BACKGROUND

Overview

THE USE OF organic or inorganic filler has become ubiquitous in polymeric systems. Polymer composites are manufactured commercially for many diverse applications such as sporting goods, aerospace components, automobiles, etc. In the last 20 years, there has been a strong emphasis on the development of polymeric nanocomposites, where at least one of the dimensions of the filler material is of the order of a nanometer. The final product does not have to be in nanoscale, but can be micro- or macroscopic in size [1]. This surge in the field of nanotechnology has been greatly facilitated by the advent of scanning tunneling microscopy and scanning probe microscopy in the early 1980s. With these powerful tools, scientists are able to see the nature of the surface structure with atomic resolution [2]. Simultaneously, the rapid growth of computer technology has made it easier to characterize and predict the properties at the nanoscale via modeling and simulation [1]. In general, the unique combination of the nanomaterial's characteristics, such as size, mechanical properties, and low concentrations necessary to effect change in a polymer

matrix, coupled with the advanced characterization and simulation techniques now available, have generated much interest in the field of nanocomposites. In addition, many polymer nanocomposites can be fabricated and processed in ways similar to that of conventional polymer composites, making them particularly attractive from a manufacturing point of view.

Nature has mastered the use of nanocomposites, and researchers, as usual, are learning from their natural surroundings. In 1998, Chemistry in Britain published an article titled 'Nano sandwiches' [3], stating, 'Nature is a master chemist with incredible talent'. Using natural reagents and polymers such as carbohydrates, lipids, and proteins, nature makes strong composites such as bones, shells, and wood. These are examples of nanocomposites, made by mixing two or more phases such as particles, layers or fibers, where at least one of the phases is in the nanometer size range. Nanoscale science and technology research is progressing with the use of a combination of atomic scale characterization and detailed modeling [1]. In the early 1990s, Toyota Central Research Laboratories in Japan reported work on a Nylon-6 nanocomposite [4], for which a very small amount of nano filler loading resulted in a pronounced improvement of thermal and mechanical properties. 'The properties of nanocomposite materials depend not only on the properties of their individual parents (nano filler and nylon, in this case), but also on their morphology and interfacial characteristics', says Kanartzidis [3].

Due to the potential promise that nanotechnology holds, federal funding for nanotechnology R&D has increased substantially since inception of the *National Nanotechnology Initiative* (NNI), from $464 million in 2001 to an estimated $982 million in 2005. The 2006 budget request that President Bush sent to Congress calls for a total NNI budget of $1.052 billion [5]. These tremendous funding opportunities in nanotechnology are geared toward new and improved products and more efficient manufacturing processes for a wide range of applications.

Background

The transition from microparticles to nanoparticles yields dramatic changes in physical properties. Nanoscale materials have a large surface area for a given volume [6]. Since many important chemical and physical interactions are governed by surfaces and surface properties [1], a nanostructured material can have substantially different properties from a larger-dimensional material of the same composition. In the case of particles and fibers, the surface area per unit volume is inversely proportional to the material's diameter, thus, the smaller the diameter, the greater the surface area per unit volume [6]. Common particle geometries and their respective surface area-to-volume ratios are shown in Figure 1. For the fiber and layered material, the surface area/volume is dominated, especially for nanomaterials, by the first term in the equation. The second term ($2/l$ and $4/l$) has a very small influence (and is often omitted) compared to the first term. Therefore, logically, a change in particle diameter, layer thickness, or fibrous material diameter from the micrometer to nanometer range, will affect the surface area-to-volume ratio by three orders of magnitude [7]. Typical nanomaterials currently under investigation include, nanoparticles, nanotubes, nanofibers, fullerenes, and nanowires. In general, these materials are classified by their geometries [8]; broadly the three classes are particle, layered, and fibrous materials [7,8]. Carbon black, silica nanoparticle, polyhedral oligomeric sislesquioxanes (POSS) can be classified as nanoparticle reinforcing agents while nanofibers and carbon nanotubes are examples of fibrous materials [8]. When
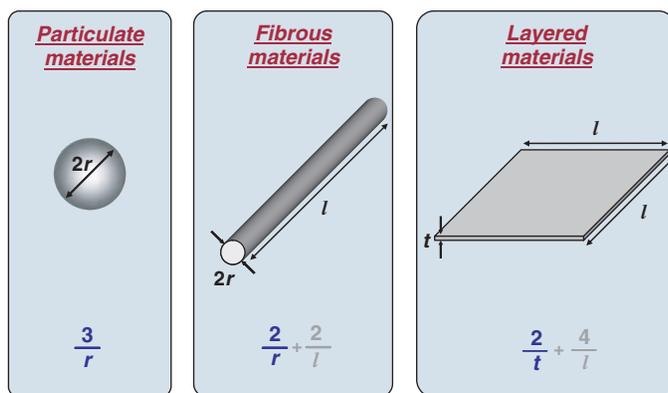
Figure 1. *Common particle reinforcements/geometries and their respective surface area-to-volume ratios. (Reproduced from [7]. © 2005, Elsevier.)*
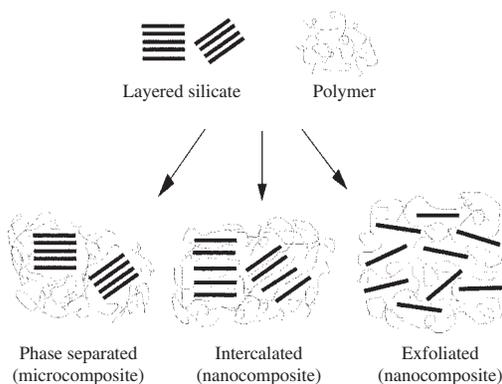

Figure 2. *Scheme of three main types of layered silicates in polymer matrix. (Reprinted with permission [9]. © 2005 Elsevier.)*

the filler has a nanometer thickness and a high aspect ratio (30–1000) plate-like structure, it is classified as a layered nanomaterial (such as an organosilicate) [9].

In general, nanomaterials provide reinforcing efficiency because of their high aspect ratios [6]. The properties of a nanocomposite are greatly influenced by the size scale of its component phases and the degree of mixing between the two phases. Depending on the nature of the components used (layered silicate or nanofiber, cation exchange capacity, and polymer matrix) and the method of preparation, significant differences in composite properties may be obtained [10]. For example, Figure 2 represents three main types of composites for layered silicate materials. When the polymer is unable to intercalate (or penetrate) between the silicate sheets, a phase-separated composite is obtained, and the properties stay in the same range as those for traditional microcomposites [9]. In an intercalated structure, where a single extended polymer chain can penetrate between the silicate layers, a well-ordered multilayer morphology results with alternating polymeric and inorganic layers. When the silicate layers are completely and uniformly dispersed in a continuous polymer matrix, an exfoliated or delaminated structure is obtained [9].

In each case, the physical properties of the resultant composite are significantly different, as discussed in the following sections.

Analogously, in fibrous or particle-reinforced polymer nanocomposites (PNCs), dispersion of the nanoparticle and adhesion at the particle–matrix interface play crucial roles in determining the mechanical properties of the nanocomposite. Without proper dispersion, the nanomaterial will not offer improved mechanical properties over that of conventional composites, in fact, a poorly dispersed nanomaterial may degrade the mechanical properties [11]. Additionally, optimizing the interfacial bond between the particle and the matrix, one can tailor the properties of the overall composite, similar to what is done in macrocomposites. For example, good adhesion at the interface will improve properties such as interlaminar shear strength, delamination resistance, fatigue, and corrosion resistance.

Finally, it is important to recognize that nanocomposites research is extremely broad, encompassing areas such as electronics and computing, data storage, communications, aerospace and sporting materials, health and medicine, energy, environmental, transportation, and national defense applications [1]. The focus of this review is to highlight the state of knowledge in processing, manufacturing, characterization, material properties, challenges, and potential applications for the most common polymer nanocomposites (while numerous products utilizing nanoscale materials are currently available, such as automotive, textile, and cosmetic applications, the major impact for nanomaterials is anticipated to be at least a decade away [1]). Comparisons are made with traditional composites, as well, especially since there has been a revived interest in these materials.

POLYMERIC NANOCOMPOSITES

Conventional Composite Manufacturing Techniques using Nanocomposites

An improvement in a property arises when the length scale of the morphology (i.e., nano) and fundamental physics associated with a property coincide. Two principal factors cause the properties of nanomaterials to differ significantly from other materials: increased relative surface area and quantum effects [2]. Some nanocomposites may show properties predominated by the interfacial interactions and others may exhibit the quantum effects associated with nanodimensional structures [12]. In the Introduction and Background section, it was mentioned that nanocomposites research is extremely broad; for the real world applications, instead of a single novel property, a set of properties is of interest [1]. In some of these areas, fundamental studies of mechanical, electrical, thermal, optical, and chemical properties are required along with related research for real applications. For manufacturing of nano-phased structural polymer composite material, the first step will be choice of a fabrication method. Some of the widely used methods for manufacturing conventional composite parts are wet lay-up, pultrusion, resin transfer molding (RTM), vacuum assisted resin transfer molding (VARTM), autoclave processing, resin film infusion (RFI), prepreg method, filament winding, fiber placement technology, etc. [13].

Wet lay-up is a simple method compared to other composite manufacturing methods; it allows the resin to be applied only in the mold, but the mechanical properties of the product are poor due to voids and the final product is nonuniform. Pultrusion is a low cost continuous process with a high production rate. But near the die assembly, the prepreg or

materials accumulate and can create a jam. Voids can be also created if the dies run with too much opening for the fiber volume input. Moreover, a constant cross section is a limitation of this process [13]. But the fibers in pultruded material are generally well aligned [14]; it helps to reduce fiber misalignment in the composite through optimization of manufacturing process variables, such as pull-speed, preformer temperature, nanoparticle alignment and/or dispersion. The RTM is a closed mold operation [13]. In this process, resin flow and fiber wet-out are critical issues; resin flows in the plane as well as in the transverse directions of the preform. Fiber wet-out depends on the fiber architecture and permeability of the preform. Recent developments in textile and resin technology have allowed the designer and manufacturer to use RTM for the fabrication of parts for the primary and secondary structures [15]. Advanced textile technology has helped to increase the wetability of the preforms. A fiber volume fraction of 55–60% can be achieved. Higher toughness can be achieved by using three-dimensional weaving and stitching technology. The VARTM is an adaptation of the RTM; a widely used single-sided tooling process such as open molds are used to make the parts using vacuum [13]. This process has certain advantages like a relatively low cost for high volume production, very large and complex parts are possible with improved surface finish, higher fiber volume fraction than hand lay-up and as it is a closed system, it reduces environmental concerns more than hand lay-up. Both in RTM and VARTM, if the resin viscosity is high it restricts the flow of resin. The effect of nanoconstituents on the matrix resins creates a problem in the altered resin viscosity and cure kinetics [16], and there is a possibility of dry spots or uneven distribution of resin over the entire volume of the reinforcement [17].

Autoclave processing is a promising technique to process and manufacture different complex shapes of high-quality composite structures [13]. It has the ability to process both thermoset and thermoplastic composites with uniform thickness and minimum porosity. However, the major difficulty in this process is the higher capitalization cost. But with the increasing requirement for high-performance composite materials for new generation aircrafts, autoclave applications remains one of the most widely used techniques in the aerospace industry [18].

Resin film infusion (RFI) is similar to RTM where a thin film or sheet of solid resin is laid into the mold and preform is laid on top of the resin film under heat and pressure. Resin impregnated unidirectional or woven fabric (partially cured) is used in the prepreg method with vacuum bagging and autoclave processing. Although the method is labor intensive, resin distribution in preform is usually uniform.

In filament winding, resin impregnated fibers are wrapped over a mandrel at the same or different winding angles to form a part. Complicated cylindrical parts, pressure vessels, fuel and water tanks for storage and transportation, and pipes can be manufactured by this method. The viscosity-related problems of the resin systems can be eliminated in this technique [19]. But the critical task is programming the wet winding in this technique. Filament winding is a cost-effective alternative for fabricating spherical and cylindrical parts (even those with varying diameters and surface contours). However, it cannot lay tow on a concave surface. Fiber placement is one of the technologies developed for automation and affordability of composite manufacturing. Fiber placement developed as a logical combination of filament winding and automated tape placement technique to overcome many of the limitations of each manufacturing method. Although tape laying systems generally are more efficient than fiber placement in making large flat panels and components with simple curvatures, fiber placement can accommodate much more severe curvature as well as complex contours. Fiber placement eliminates the

crossover points produced in filament winding, can crimp fibers, and reduce mechanical properties.

For advanced structural applications, it is required to incorporate nano-reinforcements into macroscopic functions and validate them at the nanometric level. Recently, nanocomposites have been introduced in structural applications, such as automotive parts, gas barrier films, scratch-resistant coating, flame-retardant cables, etc. Also RTM, VARTM, RFI, and filament winding techniques can be used to manufacture nanocomposite parts for various applications including commercial aircraft structures for Boeing, Airbus, as well as many products in the industrial markets. Routine use of nanocomposites in automotive and aerospace industries is a long-term prospect as these are risk-averse sectors and extensive testing and characterization alone takes significant time [1]. But more emphasis should be given to technology development and for this issue participation from engineering communities are urgently needed. Hence, it will be easier to develop a product and bring out a product from the lab [1].

Characterization Techniques for Nanocomposites

Characterization tools are crucial to comprehend the basic physical and chemical properties of PNCs. For structural applications, it facilitates the study of emerging materials by giving information on some intrinsic properties [20]. Various techniques for characterization have been used extensively in polymer nanocomposite research [20]. The commonly used powerful techniques are wide-angle X-ray diffraction (WAXD), small-angle X-ray scattering (SAXS), scanning electron microscopy (SEM), and transmission electron microscopy (TEM) [9,21].

The SEM provides images of surface features associated with a sample. However, there are two other microscopies, scanning probe microscopy (SPM) and scanning tunneling microscopy (STM), which are indispensable in nanotube research [20]. The SPM uses the interaction between a sharp tip and a surface to obtain an image. In STM, a sharp conducting tip is held sufficiently close to a surface (typically about 0.5 nm), such that electrons can 'tunnel' across the gap [2]. This method provides surface structural and electronic information at atomic level. The invention of the STM inspired the development of other 'scanning probe' microscopes, such as the atomic force microscope (AFM) [2]. The AFM uses a sharp tip to scan across the sample. Raman spectroscopy has also proved a useful probe of carbon-based material properties [20].

Due to the easiness and availability, WAXD is the most commonly used to probe the nanocomposite structure [22,23] and occasionally to study the kinetics of the polymer melt intercalation [24]. In layered silicate nanocomposite systems, a fully exfoliated system is characterized by the absence of intensity peaks in WAXD pattern e.g., in the range $1.5° \leq 2\theta \leq 10°$, which corresponds to a d-spacing of at least 6 nm [25]. Therefore, a WAXD pattern concerning the mechanism of nanocomposite formation and their structure are tentative issues for making any conclusion. On the other hand, TEM allows a qualitative understanding of the internal structure, spatial distribution of the various phases, and views of the defective structure through direct visualization, in some cases of individual atoms. Therefore, TEM complements WAXD data [26]. Small-angle X-ray scattering (SAXS) is typically used to observe structures on the order of 10 Å or larger, in the range of 0° or 0.5–5°. The TEM, AFM, and SEM, are also required to characterize nanoparticle, carbon nanofiber dispersion, or distribution. However, X-ray diffraction

has found relatively limited success in CNT research [20]. For thermal characterization and to study the cure behavior (typically for thermoset resin systems) of PNCs, the commonly used techniques are differential scanning calorimeter (DSC), thermogravimetric analysis (TGA), thermomechanical analysis (TMA), Fourier-transform infrared (FTIR), dynamic modulus analysis (DMA), rheometer, etc.

The next section will discuss the structure, properties, processing, and manufacturing of different PNCs with relevant applications.

Nanoplatelet-reinforced Systems

Two types of nanoplatelet particle composites are reviewed in this article: silicate clay minerals and graphite.

Historically, the term clay has been understood to be made of small inorganic particles (part of soil fraction less than 2 μm), without any definite composition or crystallinity. The clay mineral (also called a phyllosilicate) is usually of a layered type and a fraction of hydrous, magnesium, or aluminum silicates [27]. Every clay mineral contains two types of sheets, tetrahedral (T) and octahedral (O) [27]. For a better understanding the major clay mineral groups, along with ideal structural chemical compositions are listed in Table 1 [9]. Hectorite, saponite, and montmorillonite are the most commonly used smectite type layered silicates for the preparation of nanocomposites. Montmorillonite (MMT) has the widest acceptability for use in polymers because of their high surface area, and surface reactivity [28]. It is a hydrous aluminosilicate clay mineral with a 2:1 expanding layered crystal structure, with aluminum octahedron sandwiched between two layers of silicon tetrahedron. Each layered sheet is approximately 1 nm thick (10 Å), the lateral dimensions of these layers may vary from 30 nm to several microns or larger, depending on the particular layered silicate. The aspect ratio is about 10–1000 and the surface area is in the range of 750 m^2/g [27]. When one octahedral sheet is bonded to one tetrahedral sheet, a 1:1 clay mineral results. The 2:1 clays are formed when two tetrahedral sheets bond with one octahedral sheet, [27,28]. The aspect ratio of 1000 is possible when a clay platelet is well-dispersed into the polymeric matrix without breaking. Practically, breaking up of clay platelets during mixing process at high shear and large shear stress condition results in an aspect ratio of 30–300.

As mentioned earlier, graphite has a similar geometry (layered structure) with nanoclay therefore a clay polymer reinforcement concept is applicable [29]. Graphite flakes have

Table 1. Classification and example of clay minerals. (Reprinted with permission [9]. © 2005 Elsevier.)

Structure type	Group	Mineral examples	Ideal composition	Basal spacing (Å)
2:1(TOT)	Smectite	Montmorillonite Hectorite Saponite	$[(Al_{3.5-2.8}Mg_{0.5-0.2})(Si_8)O_{20}(OH)_4]$ $Ex_{0.5-1.2}$ $[(Mg_{5.5-4.8}Li_{0.5-1.2})(Si_8)O_{20}(OH)_4]$ $Ex_{0.5-1.2}$ $[(Mg_6)(Si_{7.5-6.8}Al_{0.5-1.2})O_{20}(OH)_4]$ $Ex_{0.5-1.2}$	12.4–17
2:1(TOT)	Illite	Illite	$[(Al_4)(Si_{7.5-6.5}Al_{0.5-1.5})O_{20}(OH)_4]K_{0.5-1.5}$	10
2:1(TOT)	Vermiculite	Vermiculite	$[(Al_4)(Si_{6.8-6.2}Al_{.1.2-1.8})O_{20}(OH)_4]Ex_{1.2-1.8}$	9.3–14
1:1(TO)	Kaolin-serpentine	Kaolinite, dickite, nacrite	$Al_4Si_4O_{10}(OH)_8$	7.14

been known as host materials for intercalated compounds. By applying rapid heating some of the graphite-intercalated compounds (GICs) expanded and a significant increase in volume takes place. Many literature citations identify the expanded graphite flakes with polymer systems for 'lightweight and conductive polymer composites' [30–34].

STRUCTURE AND PROPERTIES
Organically Modified Clay Platelets

In polymer layered silicate (PLS) nanocomposites, stacking of the layers leads to a regular van der Waals gap between the layers called the interlayer or gallery. Isomeric substitution (for example tetrahedral Si^{4+} by Al^{3+} or octahedral Al^{3+} by Mg^{2+} or Fe^{2+}) within the layers generates negative charges that are counterbalanced by alkali and alkaline earth cations (typically Na^+ or Ca^{2+}) situated inside the galleries [28]. This type of layered silicate is characterized by a moderate surface charge known as the cation exchange capacity (CEC). Details regarding the structure and chemical formula of the layered silicates are provided in Figure 3 [28,35].

In general, the organically modified silicate nanolayers are referred as 'nanoclays' or 'organosilicates' [8]. It is important to know that the physical mixture of a polymer and layered silicate may not form nanocomposites [28]. Pristine-layered silicates usually contain hydrated Na^+ or K^+ ions [28]. To render layered silicates miscible with other polymer matrices, it is required to convert the normally hydrophilic silicate surface to an organophilic one, which can be carried out by ion exchange reactions with cationic surfactants [28]. Sodium montmorillonite $(Na_x(Al_2\text{-}xMg_x)(Si_4O_{10})(OH)_2 \cdot mH_2O)$ type layered silicate clays are available as micron size tactoids, which consists of several hundreds of individual plate-like structures with dimensions of $1\,\mu m \times 1\,\mu m \times 1\,nm$. These are held together by electrostatic forces (gap in between two adjacent particles $\approx 0.3\,nm$). The MMT particles, which are not separated, are often referred to as tactoids. The most difficult task is to break down the tactoids to the scale of individual particles in the dispersion process to form true nanocomposites, which has been a critical issue in current research in different literatures [4,36–45]. In immiscible systems, which typically
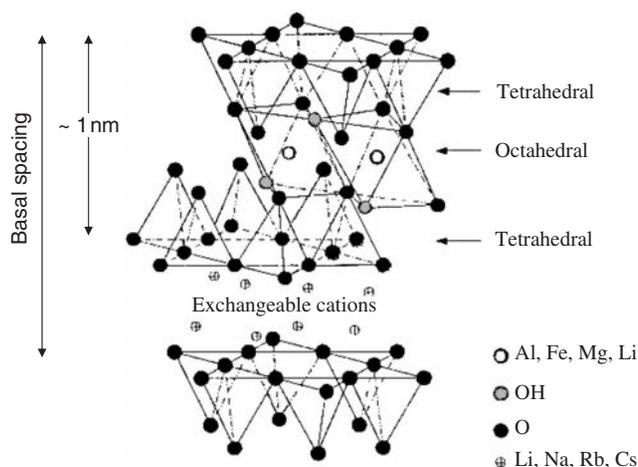

Figure 3. *Basic structures of 2 : 1 clay minerals. (Reproduced with permission [9,28]. © 2005 Elsevier.)*

correspond to the more conventionally filled polymers, the poor physical interaction between organic and inorganic components leads to poor mechanical and thermal properties. In contrast, the dispersion of the individual nanosheets of the layered silicates in the polymer matrix creates a large contact area. Moreover, uniform dispersion constructs interfacial coupling between the individual sheets and the polymer matrix facilitating the stress transfer to the reinforcement phase. This reduces the weak points present in conventional polymer composites [46,47].

Graphite Nanoplatelet

Natural flake graphite (NFG) is also composed of layered nanosheets [48], where carbon atoms positioned on the NFG layer are tightened by covalent bonds, while those positioned in adjacent planes are bound by much weaker van der Waals forces. The weak interplanar forces allow for certain atoms, molecules, and ions to intercalate into the interplanar spaces of the graphite. The interplanar spacing is thus increased [48]. As it does not bear any net charge, intercalation of graphite cannot be carried out by ion exchange reactions into the galleries like layered silicates [48].

The original graphite flakes with a thickness of 0.4–60 μm may expand up to 2–20,000 μm in length [49]. These sheets/layers get separated down to 1 nm thickness, forming a high aspect ratio (200–1500) and high modulus (~1 TPa) graphite nanosheets. Furthermore, when dispersed in the matrix, the nanosheet exposes an enormous interface surface area (2630 m^2/g) and plays a key role in the improvement of both the physical and mechanical properties of the resultant nanocomposite [50]. Expanded graphite (EG) can be easily prepared by rapid heating of intercalation compound (GIC), which is initially prepared from an NFG [48] (Figure 4). The black lines shown in the figure represent the graphite sheets when they are viewed from a direction parallel to the sheets. Basically, the structure of EG has parallel boards, which collapse and deform desultorily [51] and form many pores of different sizes ranging from 10 nm to 10 μm [52]. As it has a high expansion ratio [53,54], the galleries of EG can be easily intercalated through physical adsorption [55].
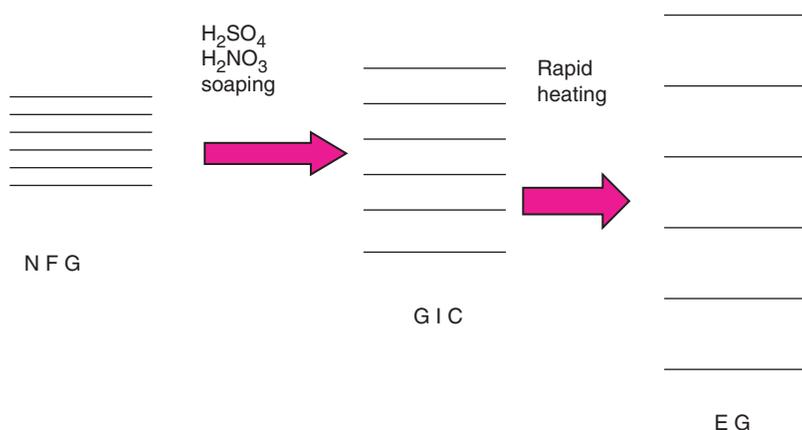

Figure 4. *Schematic illustration of making expanded graphite (EG). (Reproduced with permission [48]. © 2005 John Wiley & Sons, Inc.)*

PREPARATION AND PROCESSING

For preparing polymer–clay nanocomposites, the interaction mechanism (pressure drop into the nano gallery, miscibility between polymer and clay, hydrogen bonding, electrostatic, coordination, etc.) of the polymer and clay depends on the polarity, molecular weight, hydrophobicity, reactive groups, etc. of the polymer, and the type of solvent, i.e., water, polar, or nonpolar organic liquids and clay mineral type [27]. In this section some fabrication methodologies will be discussed, which have been developed with the layered silicates [56] and graphite nanoplatelet.

Nanoclay-reinforced Composites

In situ *intercalative polymerization*: Using this technique, polymer formation can occur in between the intercalated sheets. *In situ* polymerization is based on the following procedure: swelling of the layered silicate within the liquid monomer and the polymerization can be initiated either by heat or radiation, by the diffusion of a suitable initiator, or by an organic initiator [4,9,56–59]. At first this approach was successfully applied in manufacturing of nylon–montmorrillonite nanocomposite, and later it was extended to other thermoplastics [35]. This is a convenient method for thermoset–clay nanocomposites [41]. Messermith and Giannelis [60] have modified MMT by bis(2-hydroxyethyl) methyl hydrogenated tallow alkyl ammonium cation and they found the modified clay dispersed readily in diglycidyl ether of bisphenol A (DGEBA) by using this process. One obvious advantage of *in situ* polymerization is the tethering effect, which enables the nanoclay's surface organic chemical, such as 12-aminododecanoic acid (ADA), to link with nylon-6 polymer chains during polymerization, as illustrated in Figure 5 [61].

Exfoliation-Adsorption: This is based on a solvent system in which the polymer or pre-polymer is soluble and the silicate layers are swellable. The layered silicates, owing to the weak forces that stack the layers together, can be easily dispersed in an adequate solvent such as water, acetone, chloroform, or toluene. The polymer then adsorbs onto the
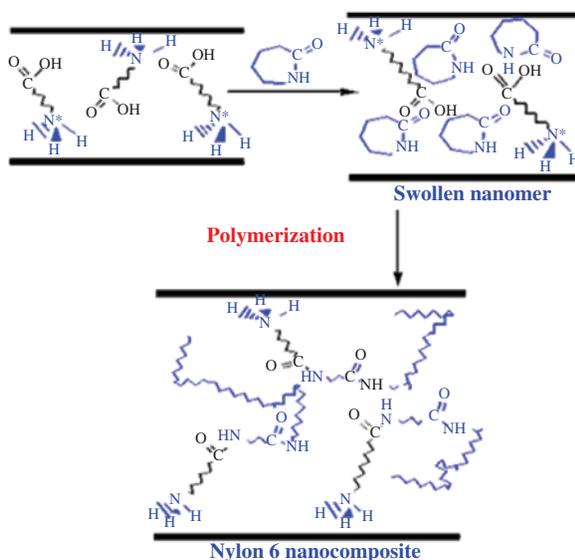

Figure 5. *Nylon-6 nanocomposite formed through* in situ *polymerization with ADA–MMT [61] with permission.*
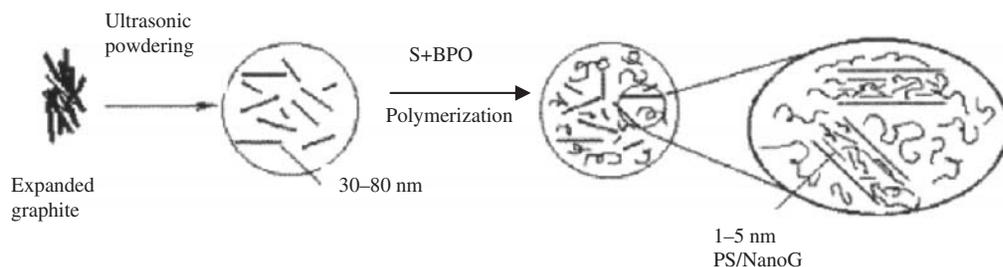
Figure 6. Schematic illustration of the process for the formation of nanocomposites of polystyrene-nano graphite. (Reproduced from [66]. © 2005 Elsevier.)

delaminated sheets and when the solvent is evaporated, the sheets reassemble, sandwiching the polymer to form. This strategy can be used to synthesize epoxy–clay nanocomposites [62], but removal of solvent is a critical issue here. Moreover, there is a disadvantage in using a large amount of solvent in the resin system [37]. This process also includes the emulsion polymerization where the layered silicate is dispersed in the aqueous solution [56]. The Toyota Research Group has been the first to use this method to produce polyimide (PI) nanocomposites [9,23].

Melt Intercalation: In this technique, no solvent is required [39,44,56,63] and the layered silicate is mixed within the polymer matrix in the molten state. A thermoplastic polymer is mechanically mixed by conventional methods such as extrusion and injection molding [37] with organophillic clay at an elevated temperature. The polymer chains are then intercalated or exfoliated to form nanocomposites. This is a popular method for preparing thermoplastic nanocomposites. The polymers, which are not suitable for adsorption or *in situ* polymerization, can be processed using this technique [28].

Expanded Graphite-reinforced Composites

An expanded graphite (EG) preparation method has been reported in different literatures (Figure 4) [49,64]. Concentrated sulfuric acid and concentrated nitric acid (industrial grade) were used as chemical oxidizers to prepare the EG [48]. Chung [53] mentioned intercalation of NFG using an intercalating agent. For an intercalated compound (GIC), the stacking could be of the form –C–C–I–C–C–I–C–C–I–C–C–, where C is a carbon layer and I an intercalated layer. Pan et al. [65] used intercalation polymerization to prepare nylon-6–EG nanocomposites. Shen et al. [29] developed a process to prepare EG by solution intercalation. Chen et al. [66] sonicated the expanded graphite to make graphite nanosheets (thickness of 30–80 nm) and dispersed in a polystyrene matrix via *in situ* polymerization. They achieved excellent conducting property through this method (Figure 6).

Exfoliation

Exfoliation of nanoclay-reinforced composites: Exfoliated nanocomposites have higher phase homogeneity than the intercalated counterpart. Hence the exfoliated structure is more desirable in enhancing the properties of nanocomposites [67]. Some factors (i.e., length and number of modifier chain, structure of clay, curing agent, curing conditions: temperature and time, viscosity, functionality of resin matrix, etc.) need to be considered to process the exfoliated thermoset polymer–nanoclay nanocomposites.
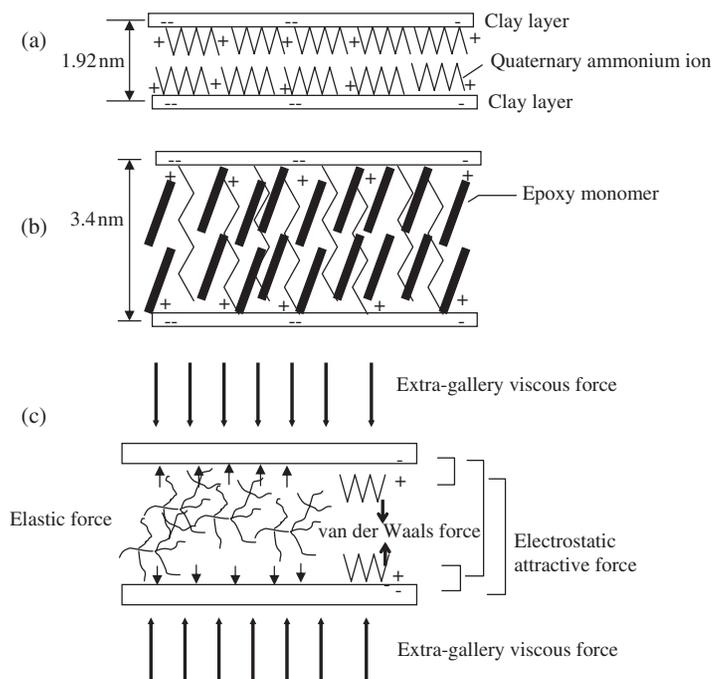
Figure 7. *Schematic illustrations of the forces acting on a pair of clay layers for intercalation and exfoliation. (Reproduced from [25]. © 2005 American Chemical Society.)*

Typically, these factors should be considered before polymer network formation and matrix gelation, in order to achieve a high degree of exfoliation [36,68,69]. Therefore, it is a technical challenge to achieve full exfoliation of clay, due to the large lateral dimensions of the layers (1 μm or larger), high intrinsic viscosity of the resin, and strong tendency of clay platelets to agglomerate [70]. Park and Jana [25] hypothesized that the elastic force developed in the clay galleries during epoxy curing is responsible for exfoliation. They explained that (Figure 7) the sum of the viscous force and attractive forces arising due to electrostatic attraction and van der Waals force work against exfoliation, while elastic force due to conformational entropy work for clay layer separation. If the elastic force overcomes the attractive forces and viscous force, exfoliation of clay occurs [25]. In an uncured system, exfoliation is not expected, because the magnitude of the entropic force is small for separating the clay layers [25]. As shown schematically in Figure 8 [25], the inner layers have a higher ionic bonding energy than the surface layers [71]; hence, the separation of the clay layers from the tactoid structures begins with the outermost clay layers. Full exfoliation results if all layers are separated from all tactoids [25]. Jiankun et al. [72] have found a few factors that promote the exfoliating ability, such as catalytic effect during cross-linking, penetrating ability of curing agent to clay, long alkyl-chain of the organocation, etc. Besides these they presented a thermodynamic analysis of exfoliation [68,73,74], which is determined by the change of free energy (∇G) of the system during the curing process. They suggested that, when $\nabla G = \nabla H - T \nabla S < 0$, the exfoliation can occur [69]; where ∇H is the change of enthalpy and ∇S is the change of entropy.

(a)   Clay layers

x

(b)

Bonding
energy

Surface   Center   Surface

Distance from the surface (x) ⟶
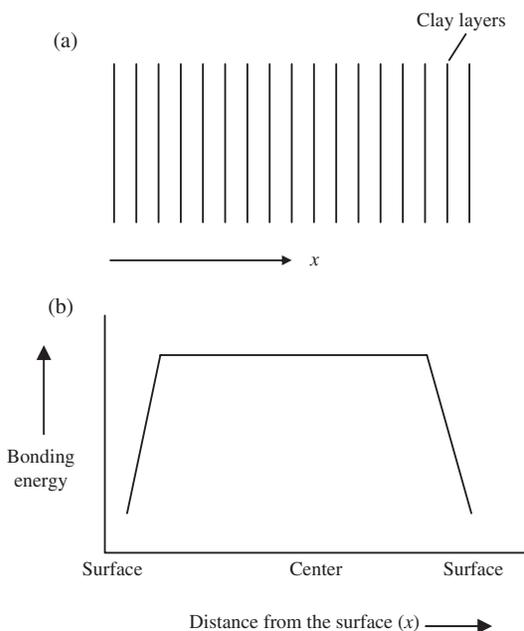
Figure 8. *Schematic diagram showing the relationship between the ionic bonding energy and the location of the layers in the tactoid. (a) Tactoid and (b) Variation of bonding energy along the thickness of the tactoid [25]. (© 2005 American Chemical Society.)*

   Tolle and Anderson [75] investigated the sensitivity of exfoliation for processing. They found that both at lower temperatures for isothermal cure and at higher heating rate for nonisothermal cure cause an inhibition of exfoliated morphology. Messermith and Giannelis [60] prepared exfoliated layered silicate epoxy nanocomposites from diglycidyl ether of bisphenol A (DGEBA) and a nadic methyl anhydride-curing agent and found that the dynamic storage modulus improved. Kormann et al. [36] investigated the effect of three different curing agents upon the organoclay exfoliation in the DGEBA-based system. In their work, exfoliation of organoclay occurred in cycloaliphatic diamine-cured DGEBA nanocomposites only at higher temperatures. The speed of diffusion of curing agents and increased curing temperatures also influenced the degree of exfoliation [36,67,75,76]. Lan et al. [41–43] reported that the balancing of intra and extra gallery polymerization rates is a primary concern to obtain exfoliated thermoset/layered silicate nanocomposites. Pinnavaia et al. [77] achieved exfoliated morphologies in epoxy resins by gradual diffusion of monomeric epoxy into the gallery. They suggest that faster intragallery polymerization produced exfoliated structures by pushing out the individual clay layers from the tactoids [25,77]. Wang et al. [78] mentioned that the relative curing speed between the interlayer and extralayer is the most important factor for clay exfoliation. Messermith and Giannelis [60] used anhydride species curing agents to prepare exfoliated nanocomposites, whereas the use of amine curing agents allowed them to prepare only intercalated composites. Lan et al. [41–43] used amine-curing agents and they achieved exfoliation only at an appropriate temperature, when the curing speed of the interlayer and extralayer is almost the same. Exfoliated nanocomposites have been prepared by preaging of an intercalated epoxy/layered silicate prepolymer mixture before curing and it showed enhancement of

toughness [79]. Vaia et al. [44] mentioned that, the degree of exfoliation can be improved by the use of conventional shear devices such as extruders, mixers, sonicators etc. Park and Jana [25] observed that hydroxylated quaternary ammonium ions and quaternary ammonium ions with nonpolar functional groups produced exfoliated structures. High levels of exfoliation and dispersion of the silicate clay layers in the epoxy matrix gave improved dynamic modulus using a three-roll mill as a means of applying external shearing forces [50]. Improved impact, flexural, and tensile properties have been achieved from exfoliated epoxy nanocomposites by using ball milling [80]. A combination of both using higher shear forces and improved cure temperature during the curing process or the use of swelling agents [81], are the effective issues for exfoliation.

For the fabrication of thermoplastic polymer nanocomposites, Dennis et al. [39] found that increasing the mean residence time in the extruder generally promotes exfoliation, but excessive shear intensity or back mixing causes poor delamination and dispersion. Ahn et al. [82] prepared the exfoliated polypropylene–clay nanocomposites under an electric field (with a function of generator and high voltage amplifier). Silicate layer exfoliation in polyolefins such as PP and polyethylene is achieved by the introduction of small amounts of polar groups to nonpolar polyolefins [35,83–85]. The degree of delamination and dispersion of the layered silicates have been achieved in polyamide 6 by melt compounding [39] using an extruder.

Complete exfoliation (single platelet dispersion) is a very difficult issue, but all researchers easily say 'exfoliation' and 'exfoliated structure of the dispersed clays'. At this point, the meaning of full exfoliation has to be taken into consideration. For example, exfoliation due to 'parallel stacking or layer registry of the nanoclay is disrupted'. Nanoclay has a terminal hydroxylated edge group. Therefore, the edge–edge interaction of the silicates takes place and then the flocculated structure is developed at high clay content loading (2 wt% corresponding to about 0.75 vol.%). To achieve the finer dispersion (near to exfoliation), the volume fraction of clay must be less than 1/(aspect ratio). Most of the nanocomposite researchers believe that the preparation of a completely exfoliated structure is the ultimate goal for better properties. However, these significant improvements are not observed in every nanocomposite system, including systems where the silicate layers are nearly exfoliated [86].

Exfoliation of graphite-reinforced composites: Exfoliated graphite consists of a large number of delaminated graphite sheets [87,88]. Du et al. [87] prepared expandable polyaniline/graphite nanocomposites by chemical and physical treatments, especially by microwave irradiation. Instead of the usual HNO_3–H_2SO_4 route [87], they prepared the nanocomposites through the H_2O_2–H_2SO_4 route to avoid the evolution of poisonous NO_x. 1–2 wt% of EG were fabricated using epoxy resin (DGEBA) by sonication, shear, and a combination of sonication and shear mixing methods [50]. Shioyama [89] reported improved exfoliation at weight fractions of graphite below 1 wt% through polymerization with vaporized monomers such as styrene and isoprene. Fukushima and Drazal [90] used O_2 plasma treated graphite nanoplatelet in an acrylamide/benzene solution. After applying heat treatment (80°C for 5 h) they produced grafted graphite; which was used as reinforcement in an epoxy matrix with a high aspect ratio and better thermal and mechanical properties. For better exfoliation Cho et al. [91] pulverized EG nanoplatelets after heat treatment (900°C) using ultrasonication, ball-milling, and vibratory ball-milling techniques to fabricate the phenylethynyl-terminated polyimide (PETI)-5/EG composites. Li et al. proposed [92] UV/ozone treatment on expanded graphite at room temperature and atmospheric pressure. After ultrasonication they achieved uniform dispersion and

interfacial adhesion of EG with the epoxy matrix. Improved mechanical and electrical properties were achieved using this technique.

In the case of graphite, the term 'complete exfoliation' has no exact meaning. It does not mean a single layer sheet as in the case of polymer–clay nanocomposites; it may mean a separated graphite flake which is completely delaminated layer by layer. The EG is somewhat partially exfoliated graphite, because the graphite sheets are interlinked with each other [93]. But in polymer–EG nanocomposites, it is impossible to completely delaminate the carbon layer, because EG is fragile and breaks down during processing of the mixture of EG and polymer [66]. Each graphite layer is theoretically separated by a $3.354\,\text{Å}$ space. Chen et al. [66] conducted research on graphite nanosheets of $50\,\text{nm}$ thickness. They [94] tried to get one-layer carbon film, which is not related to the field of polymer nanocomposite.

Thostenson et al. [7] gave a summary of the properties between exfoliated graphite platelets and exfoliated clay platelets from different literatures [6,90,95].

PROPERTIES, MANUFACTURING, AND APPLICATION

In the early 1990s, Toyota researchers reported work based on true nylon-6–clay thermoplastic nanocomposites technology [3,40,96] and now it has a broad-based proprietary patent technology that is licensed to companies in Japan and the USA [12]. In their work, mechanical properties showed significant improvement at a loading of only $4.2\,\text{wt}\%$ clay, the modulus doubled, and the increase in strength was more than 50%. Also an improvement in thermal properties was observed with the increase of heat distortion temperature (HDT) by $80°C$ compared to the pristine polymer [4,40]. In recent years, for nanocomposite formation, organoclay has been used in various polymer systems including epoxy, polyurethanes, vinyl ester, etc. [36,47,60,97,98]. Ballistic performance is an important issue for the survivability and damage tolerance studies for aerospace and automotive structures. The US Army research laboratory investigated the ballistic impact strength of polycarbonate-layered silicate nanocomposites [99]. Boeing, USA demonstrated the potential for aerospace application in a workshop in 2004 in FL, USA. According to their description, nanocomposites can play an important role in longer-range missiles and a greater payload for aircraft. Koo and Pilato [100] investigated the polymer nanocomposite for high-temperature applications using cyanate ester, epoxy, phenolic, nylon 11, etc. and described the feasibility of using these materials for fire retardant coatings, rocket propulsion insulation, rocket nozzle ablative materials, damage tolerant performance, etc. Ablatives are required to protect aerospace launching systems against solid rocket exhaust plumes ($3600°C$) at very high velocity. They demonstrated that nanoclay plays a key role in reducing the flammability on coating systems [100]. Flammability is another important issue for many applications. Other studies show that nanocomposites prepared from he nylon family, epoxy, polystyrene or vinyl ester, exhibit reduced flammability compared to pure polymers [12].

Fiber-reinforced nanocomposites are manufactured through affordable RTM, and VARTM processes described in different literatures [16,17,97,101]. Hussain et al. [17] achieved an almost (by dispersing only 1% by weight nanosilicates) 18 and 24% improvement in flexural strength and fracture toughness respectively in S2 glass/ vinylester–clay nanocomposites compared to conventional composites [17]. Roy and Hussain [14,102] manufactured E-glass/PP clay nanocomposites using prepreg tapes with extruder and pultrusion machine. They achieved improvements in compressive strength and modulus using this technique. Fielding et al. [16] achieved uniform dispersion of the

Table 2. Mechanical properties of organoclay and polyamide 6 nanocomposites with respect to extruders/screw configurations. (Reproduced from [39]. © 2005 Elsevier.)

Extruder type	Tensile modulus (GPa)	Tensile yield strength (MPa)
Single screw	3.3	77
Twin screw co-rotating intermeshing	3.7	81
Twin screw counter-rotating intermeshing	3.6	75
Twin screw counter-rotating non-intermeshing	4.0	85

(a)   (b)

Figure 9. *TPO nanocomposites: application for automotive parts [109]: (a) M-Van step Assist: 1st commercial launch and (b) impala: 2nd nanocomposite application. Through the courtesy of M. Verbrugge, General Motors.*

nanoclay of carbon fiber reinforced epoxy nanocomposites using RFI in the autoclave. Nanocomposites formed by melt blending have been described in different literatures [45,103,104]. Dennis et al. [39] described how the type of extruder and screw design affects the degree of dispersion of nanoclay in a polyamide matrix (Table 2).

The first commercial example of polymeric nanocomposites in automotive applications was clay–nylon-6 nanocomposites used for making timing belt covers (the Toyota Motor Company, 1991) [105]. More significantly, these composites have been in use in under the hood applications in the Toyota Camry [9]. Unitika, Japan introduced nylon-6 for engine covers on Mitsubishi's GDI engines [105,106]. Chevrolet Impalas [107,108] developed doors with thermoplastic polyolefin nanocomposite (TPO). After that General Motors and Basell published the application of clay/polyolefin nanocomposites as a step assistant component for GMC Safari and Chevrolet Astro vans in 2001 (Figure 9) [107]. Recently, Honda Acura developed clay–PP nanocomposites for structural seat backs [109] and with clay–nylon-12 nanocomposites Ube developed fuel lines and fuel system components for automotives [105].

Organically modified clays dispersed in a nylon-6–polymer matrix greatly improved the dimensional stability and the barrier properties [96,110,111]. Improvement in barrier resistance in nanocomposites plays an important role in beverage applications [105]. When the layers are delaminated, it increases the effective path length for molecular diffusion and the path becomes highly tortuous to reduce the effect of gas and moisture transmission through the film [12]. Based on the barrier properties, nanocomposite packaging films made in polyethylene terephthalate (PET) have been studied as replacements for conventional polymer films [12]. Honeywell developed commercial clay–nylon-6

nanocomposite products for drink packaging applications [105]. More recently Mitsubishi Gas Chemical and Nanocor have co-developed nylon-MXD6 nanocomposites with multilayered PET for bottle applications [105].

Researchers at NASA Langley Center developed transparent nanocomposites with chemically modified clay, which is lightweight and durable and suitable for a variety of aerospace applications [112]. For space applications, some critical issues are important, such as temperature extremes of -196 to $125°C$, higher toughness, dimensional stability (i.e., resistance to micro cracking), etc. Timmerman et al. [113] used nanoclays in carbon fiber/epoxy reinforced composites for cryogenic storage systems with improved mechanical and thermal expansion (CTE) characteristics thereby avoiding micro cracking and thermal cycling. The Air Force Office of Scientific Research (AFOSR) used aerospace grade resins and organoclays to understand the mechanism of the toughening effects at ambient and sub-ambient temperatures. For practical applications in polymer nanocomposites, whether it is aerospace or automobile (where constant or cyclic stresses are applied), creep and fatigue properties have to be considered to estimate the overall mechanical performance. In different studies [114–116], researchers investigated the effect of particles on the fatigue performance using various polymers like polyamide 6, epoxy, and PP nanocomposites.

Different literatures studied the thermal behavior as well as cure in the layered silicate nanocomposites [36,59,117–127]. Chen et al. [123] synthesized epoxy–MMT nanocomposites to understand the interlayer expansion mechanism and thermal–mechanical properties. They verified the cross-linking reactions and showed that the nanocomposites are predominantly cured via initiation by the surfactant hydroxyl groups and not by the catalyst. Kornmann et al. [37] investigated the influence of cure temperature; various cure agents, and their concentration on the structure of epoxy–clay nanocomposites. Hussain and her coworkers achieved higher primary onset of decomposition around $30°C$ in S2 glass vinylester nanocomposites, which showed the formation of a char layer [17]. Cure behavior study has been carried out basically for thermoset resin systems. Hussain and Chen investigated the cure behavior of epoxy–silicate nanocomposites using a dielectric online cure monitoring technique [128]. In the aerospace manufacturing point of view, authors mentioned that this technique helps to improve the consistency, quality assurance, process development, and efficiency of the parts of the composite [128]. Cure monitoring of epoxy organoclay nanocomposites was also demonstrated by Chen and He [129] by using a resin cure meter. Reaction kinetics of unsaturated polyester resins with clay was investigated using DSC and FTIR [130]. Xu et al. [131] predicted the cure behavior of epoxy clay nanocomposites using different theories (Flory's gelation, nonequilibrium thermodynamic fluctuation, etc.) and the Avrami equation and suggested that there is no special curing process required for the formation of epoxy nanocomposites.

Foam Processing Using Supercritical CO₂

Very recently, the first successful nanocomposite foam, processed by using supercritical CO_2 as a physical foaming agent, appeared through a pioneering effort by Okamoto and his colleagues [132,133]. They used intercalated polycarbonate (PC)–layered silicate nanocomposites (PCCNs) and PC/SMA (polycarbonate/poly styrene-co-maleic anhydride) blend (matrix) without clay foamed at $160°C$ under different isobaric saturation conditions of supercritical CO_2 (10, 14, and 18 MPa) [134]. The PC/ SMA foams exhibit the polygon closed-cell structures having pentagonal and hexagonal faces, which express the most energetically stable state of polygon cells. Such a foam

structure was obtained probably because these foams belong to the polymeric foams having a high gas phase volume (>0.6) [135]. High CO_2 pressure (~18 MPa) provides a large supply of CO_2 molecules, which can subsequently form a large population of cell nuclei upon depressurization. The PC/SMA/MAE1 ($2C_{12}C_{18}$-fluorohectrite) (including 1 wt% of organoclay) foam shows smaller cell size, i.e., larger cell density compared to PC/SMA foam, suggesting that the dispersed clay particles act as nucleating sites for cell formation and the lowering of d-spacing with clay. The incorporation of nanoclay hinders CO_2 diffusion and simultaneously induces heterogeneous nucleation because of a lower activation energy barrier compared to homogeneous nucleation [136]. The nanocomposite foams exhibit high modulus compared to neat PP–MA foam. The residual strain is 17% for polypropylene-based nanocomposite (including 2 wt% of organoclay) as well as neat PP foam, providing an excellent strain recovery and energy dissipation mechanism.

Biodegradability

Another interesting aspect of nanocomposite technology is the significant improvements of biodegradability of biodegradable polymers after nanocomposite preparation with organoclay [137,138]. **TOYOTA** Technological Institute are commercializing PLA/layered silicate nanocomposites for packaging materials and also for short-term disposable applications. Now it is commercially available through Unitika Ltd., Kyoto, Japan. Aliphatic polyesters are among the most promising materials for the production of environmentally friendly biodegradable plastics. Biodegradation of aliphatic polyester is well known, in that some bacteria degrades them by producing enzymes, which attack the polymer. Tetto et al. [139] first reported some results about the biodegradability of nanocomposites based on PCL, where the authors found that the poly (ε-caprolactone) (PCL)/layered silicate nanocomposites showed improved biodegradability compared to pure PCL. According to them, the improved biodegradability of PCL after the formation of nanocomposites may be due to the catalytic role of the organoclay in the biodegradation mechanism. But it is still not clear how the clay increases the biodegradation rate of PCL. Recently, Lee et al. [140] reported the biodegradation of aliphatic polyester (APES) based nanocomposites under compost. They assumed that the retardation of biodegradation is due to the improvement of the barrier properties of the aliphatic APES after the preparation of nanocomposites with clay. However, there are no data available about permeability. Very recently, Ray et al. [141] reported the biodegradability of neat PLA and corresponding nanocomposites prepared with trimethyl octadecylammonium modified MMT ($3C1C_{18}$-MMT) with details of the mechanism involved. The used compost was prepared from food waste and tests were carried out at a temperature of $58 \pm 2°C$. Figure 10 shows the decrease in molecular weight M_w and residual weight percentage R_w of the initial test samples (neat PLA and PLACN4 ($3C1C_{18}$-MMT = 4 wt%) from the compost with time.

After 1 month, a sharp change occurred in the weight loss of PLACN4 (containing organo-clay of 4 wt%), and within 2 months, it was completely degraded in the compost. The degradation of PLA in the compost is a complex process involving four main phenomena, namely: water absorption, ester cleavage and formation of oligomer fragments, solubilization of oligomer fragments, and finally diffusion of soluble oligomers by bacteria [142]. Therefore, the factor, which increases the hydrolysing tendency of PLA, ultimately controls the degradation of PLA.

Further details regrading the mechanism of biodegradability are presented in relevant literature [141,143]. Okamoto et al. [144] also investigated the biodegradability of neat PBS
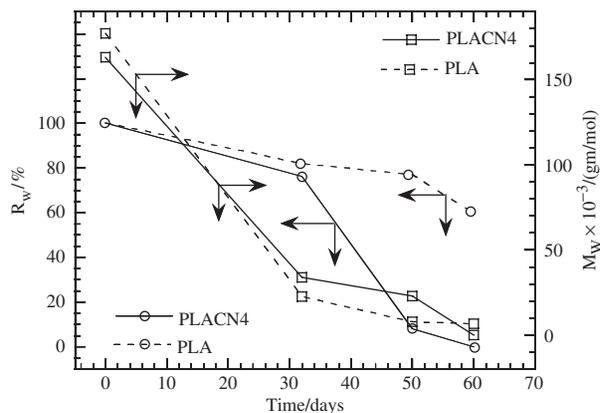
Figure 10. *Time dependence of residual weight, R_w and of matrix, M_w of PLA and PLACN4 under compost at $58 \pm 2°C$. (Reprinted from [141]. © 2006 American Chemical Society.)*
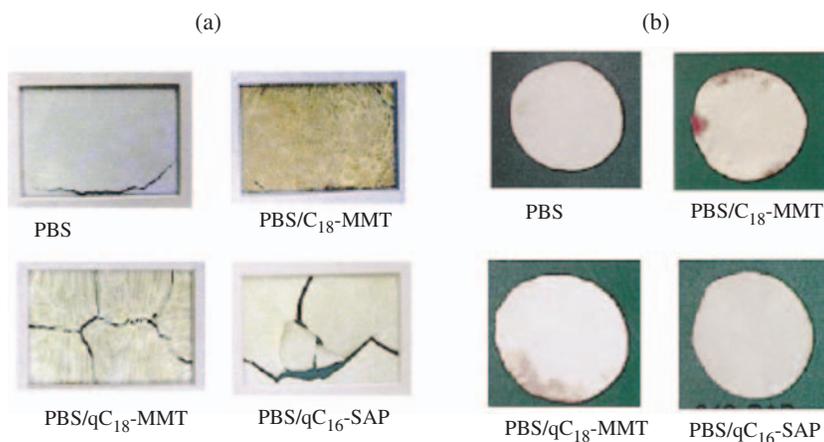

Figure 11. *Biodegradability of neat PBS and various nanocomposites sheets: (a) under compost and (b) under soil field. (Reproduced [144], © 2006 John Wiley & Sons, Inc.)*

before and after the preparation of nanocomposites with three different types of organoclay. They used alkylammonium or alkylphosphonium salts for the modification of pristine-layered silicates, and these surfactants are toxic for microorganisms. Figure 11(a) shows the real pictures of the recovered samples of neat PBS and various nanocomposites from the compost after 35 days. From the figure it is clearly observed that many cracks appeared in nanocomposite samples compared to that of the neat PBS. This observation indicates the improved degradability of nanocomposites in the compost. This kind of fracture has an advantage for biodegradation because they are easy to mix with compost and create a larger surface area for further attack by microorganisms, and it should be noted here that the extent of fragmentation is directly related to the nature of organoclay used for nanocomposites preparation. Figure 11(b) presents the results of degradation of neat PBS and various nanocomposite sheets recovered from a soil field after 6 months. They reported that these spots on the sample surface are due to fungus attack, because when they put these parts into the slurry they observed a clear growth of fungus.
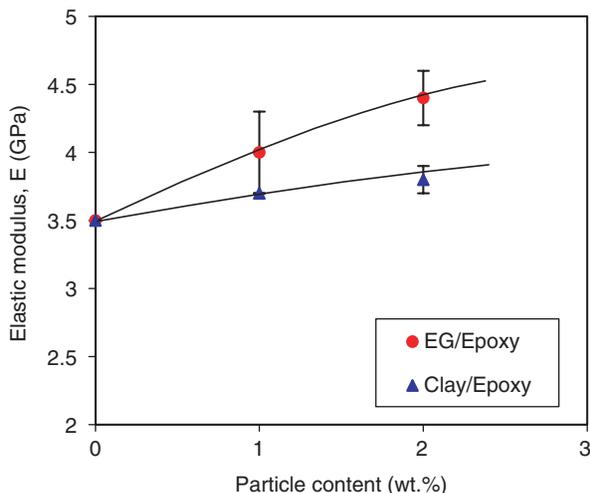
Figure 12. *Variation of elastic modulus as a function of particle content. (Reproduced from [50] with permission. © Elsevier 2006.)*

These results also indicate that the nanocomposites exhibit the same or a higher level of biodegradability compared with the PBS matrix.

Graphite Nanoplatelet Polymer Composites

Improvement in electrical conductivity is achieved by adding a graphite platelet in a polystyrene. It basically represents the sharp transition of the polymer from an electrical insulator to an electrical semiconductor with the addition of a graphite nanoplatelet [88]. The percolation threshold value of the conducting composite (with 1.8 wt% of expanded graphite) was much lower than that of conventional composites [48,88,145]. A graphite platelet is used as reinforcement in both epoxy and PP systems to investigate the mechanical, thermal, and electrical properties of the nanocomposites [146]. Fukushima and Drazal [90] showed better flexural and tensile properties of chemically functionalized graphite nanoplatelet in the epoxy matrix. In addition they achieved lower CTE and electrical resistivity compared to other carbon materials like carbon fiber, carbon black, etc. These properties of graphite nanoplatelet combined with low cost make it useful in electromagnetic interference (EMI) shields, thermal conductors, etc. Graphite is well known for its stiffness and excellent thermal and electrical conductivity, which are absent in clay materials. Yasmin et al. [50] used both graphite/epoxy and clay/epoxy nanocomposites to investigate the performance of reinforcement and they found that graphite/epoxy has a higher (16% for 2 wt% particle content) elastic modulus compared to the clay/epoxy for the same particle content (Figure 12).

CHARACTERIZATION

The WAXD patterns and corresponding TEM images of three different types of nanocomposites are presented in Figure 13 [28]. A closer observation of the micrograph at higher magnification reveals that each dark line often corresponds to several clay layers [28,97,147,148]. Chen et al. [26], Wang and Pinnavaia [149], and Yao et al. [150] reported the WAXD analysis of polyurethane/clay nanocomposites using the *in situ* intercalative polymerization technique. Chenggang and David [151] used SAXS to
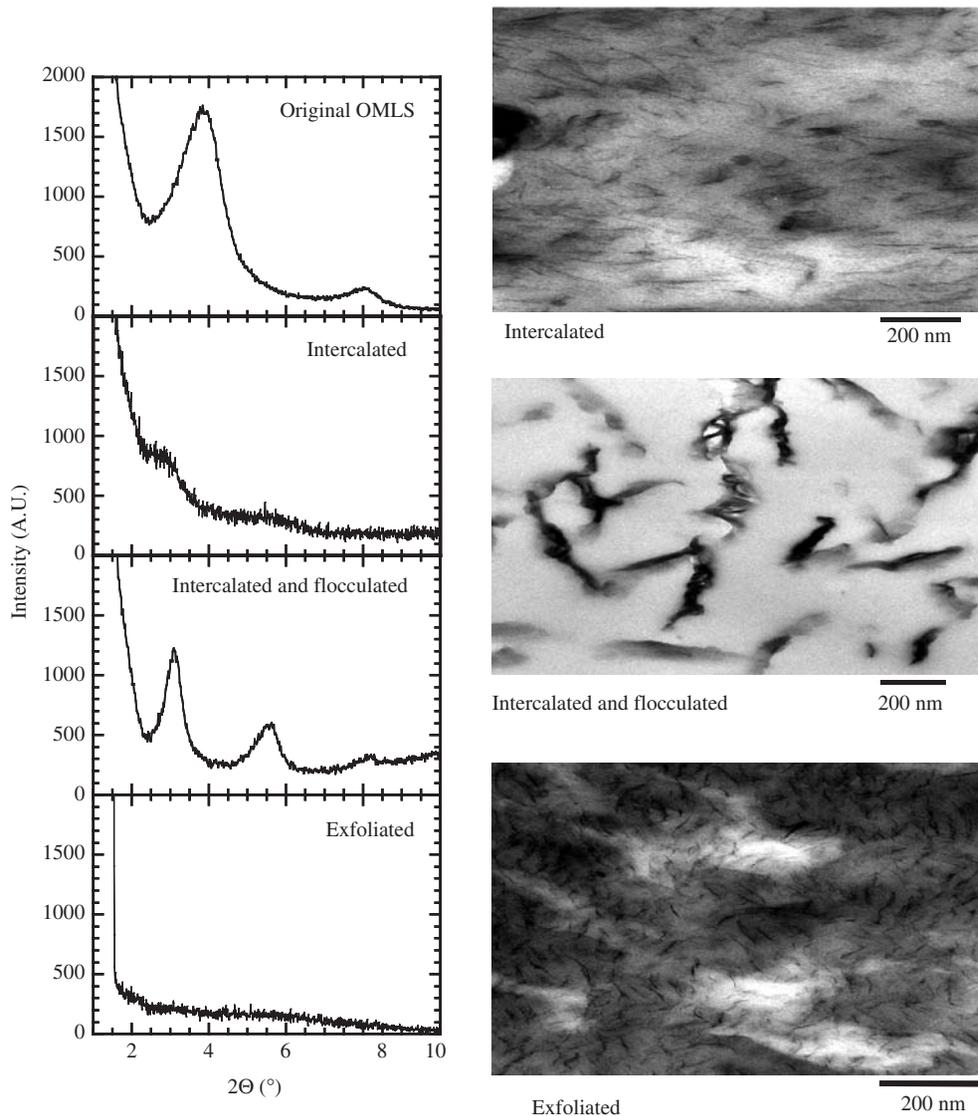
Figure 13. WAXD patterns and TEM images of three different types of nanocomposites. (Reproduced with permission [28]. © 2005 Elsevier.)

characterize the morphologies of epoxy nanocomposites. Figure 14 gives an example of the clay–fiber interaction, where nanosized clay particles are embedded in the matrix of vinyl ester and are in contact with S2 glass fibers [17]. Hussain et al [17] assumed that these interactions presumably give rise to enhanced interfacial properties [17]. Dean et al. [68] showed that interlayer spacing increases with the increase in cure temperature and a higher cure temperature allows sufficient mass diffusion into the layers before gelation. A plot of intergallery spacing (from WAXD and SAXS) for a sample cure at lower and higher temperatures is displayed in Figure 15.
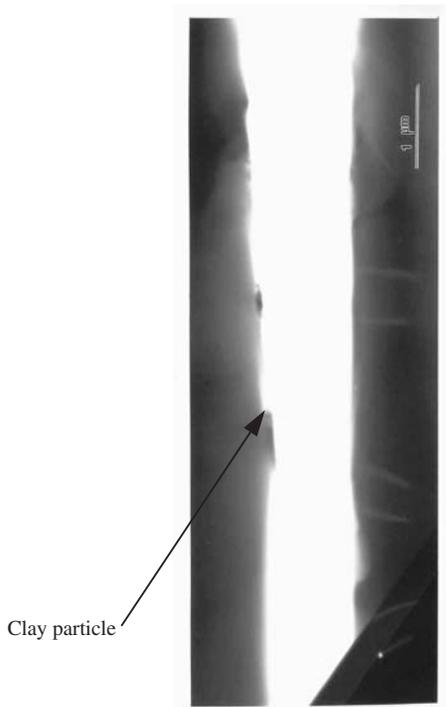
Figure 14. *The isolated existence of a clay particle embedded in the vinyl ester in contact with the S2 glass fiber [17]. (Reproduced with permission [17]. © 2006 SAMPE, JCM.)*
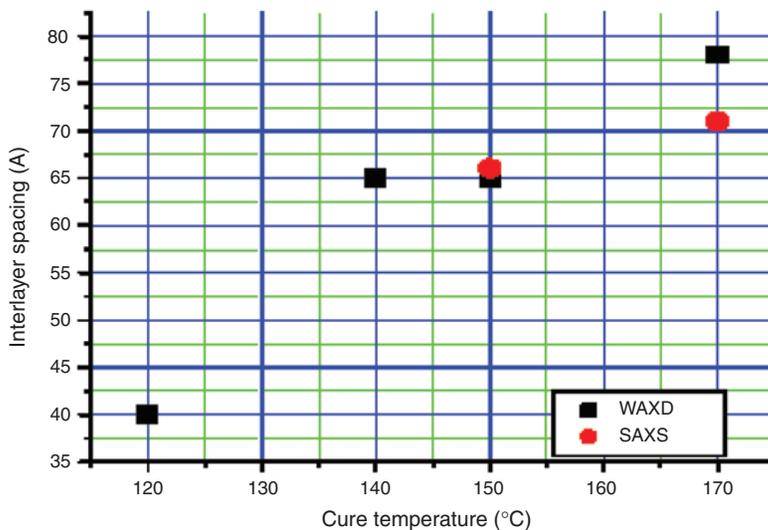

Figure 15. *Effect of cure temperature on the intergallery spacing. (Reproduced with permission [68]. © 2005 Elsevier.)*

SIMULATION AND MODELING

Multiscale Micromechanical Modeling for Clay

   Very recently, Sheng et al. [152] reported a multiscale modeling strategy to account for the hierarchical morphology of the nanocomposite: at a length scale of thousands of microns, the structure is one of the high aspect ratio particles within a matrix; at the length scale of microns, the clay particle structure is either (a) exfoliated clay sheets of nanometer level thickness or (b) stacks of parallel clay sheets separated from one another by interlayer galleries of nanometer level height, and the matrix, if semicrystalline, consists of fine lamella, oriented with respect to the polymer/nanoclay interfaces. Models of various representative volume elements of the underlying structure of the clay-filled polymer are constructed. Figure 16 [152] represents the influence of internal clay structural parameters (the average number of silicate layers per clay stack: N, d (001)) on the macroscopic modulus of the polymer layered silicate nanocomposite (PLSNC). The enhancement of modulus (E_{11}/E_m) is plotted as a function of clay content (W_c) and N at fixed d (001). The strong dependence of modulus on N is clearly demonstrated; at a fixed W_c, modulus increases with decreasing N; the amount of increase gradually expands as $N \rightarrow 1$. On the other hand, the effect d (001) on the modulus for two different values of N ($N = 2$ and 5). Compared with N, the influence of d (001) on the modulus is rather small, and depends on the specific value of N. This increment is rather negligible when N is small; however, when the nanocomposite is highly intercalated (e.g., $N = 5$), the increase of a few nanometers in d (001) can cause a considerable increase in modulus. Micromechanical models (numerical as well as analytical) based on the 'effective clay particle' were employed to calculate the overall elastic modulus of the amorphous and semicrystalline PLSNCs and to compute their dependence on the matrix and clay properties as well as internal clay structural parameters. The proposed modeling technique captures the strong modulus enhancements observed in elastomer/clay nanocomposites as compared with the moderate enhancements observed in glassy and semicrystalline PLSNCs. Note that in order to determine the modulus of the nanocomposite, the modulus of the nanoclay of 400 GPa is employed. Most of the nanocomposite researchers believe that the nanoclay has a high modulus of 170 GPa [153]. But this value is absolutely acceptable or not acceptable, even if in the case of a mono-layered clay sheet.
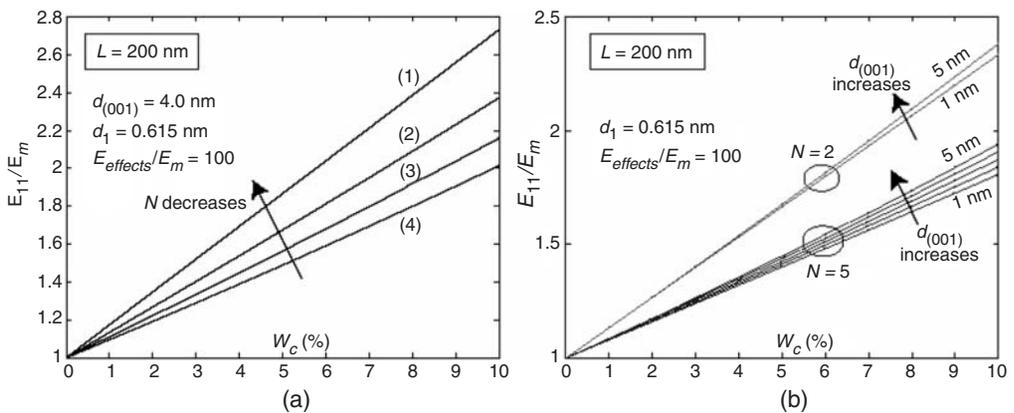

Figure 16. *Effect of clay structural parameters (N, d$_{(001)}$) on the macroscopic modulus predicted by Mori-Tanaka model. (a) Effect of N at fixed d$_{(001)}$ = 4.0 nm and (b) Effect of d$_{(001)}$ at two fixed values N = 2 and N = 5. (Reproduced from [152]. © 2006 Elsevier.)*

Flexibility of a Single Clay Layer

A large degree of flexibility of the monolayered clay sheet is reported [27]. Two TEM images are evident (Figure 17). One arises from the clay layers that appear as ~150–200 nm curved sheets. When viewed edge-on as in Figure 17(b), several 5–8 nm stacked sheets are apparent. The curved nature of the sheet is observed, for it is well known that a smectite clay sheet has a large degree of flexibility [27]. Sato et al. [154] reported the study of the flexibility of smectite clay minerals by using molecular dynamics (MD) simulations. They took into account the quantitative understanding of the mechanical behavior of a single clay layer in a completely exfoliated state. The repeating unit of a layer is taken to be $a_0 = 0.52$ nm and $b_0 = 0.902$ nm with a formula of $2Na_{1/3} Al_2[Si_{11/3} Al_{1/3}]O_{10}(OH)_2$, which corresponds to that of beidellite. When the size of the basic cell ($A = 9.3$ nm, $B = 2.6$ nm, and $C = 5$ nm) (A-type cell) is reduced by 3–40% in the A-direction, the stationary structure of a clay layer is obtained as a curved sheet with a 2:1 smectite-type layer. In such a curved state, the layer experiences an external stress of 0.5–0.7 GPa. The layer structure of a clay fractures when the size of the same basic cell is reduced by more than 40%. This value is much lower than that of moscovite (~2 GPa), which is also reported by the same authors [155]. The simulation has also been carried out by reducing the size of the basic cell ($A = 3.1$ nm, $B = 10.7$ nm, and $C = 5$ nm) (B-type) in the B-direction. The clay layer is found to be more flexible along the A-direction than along the B-direction. When the microscopic structure of a curved clay layer is examined, it is concluded that the main origin of the flexibility lies in the change of Si-O-Si angle in the silicate tetrahedral sheets rather than in the change of bond lengths. These simulation results agree with the AFM observations [156].
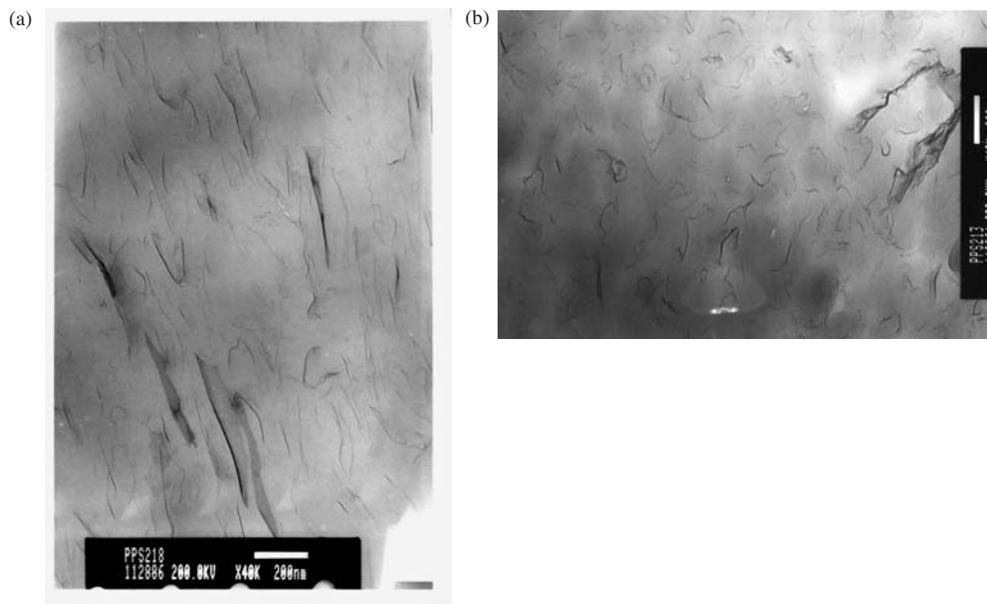

Figure 17. *For flexibility of nanoclay, both are poly (p-phenylenesulfide/layer titanate nanocomposites: loading filler = 5.35 wt%, unpublished data from Okamoto).*

Alignment (Orientation) of Silicate Layers

The orientation of silicate layers and nylon-6 crystallites in injection molded N6CN using WAXD and TEM is examined [157,158]. Kojima et al. [157] have found three regions of different orientations in the sample as a function of depth. Near the center of the sample, where the shear forces are minimal, the silicate layers are oriented randomly and the nylon-6 crystallites are perpendicular to the silicate layers. In the surface region, shear stresses are very high, so both the clay layers and the nylon-6 crystallites are parallel to the surface. In the intermediate region, the clay layers, presumably due to their higher aspect ratio, still orient parallel to the surface and the nylon-6 crystallites assume an orientation perpendicular to the silicate. Okamoto and his colleagues conducted the TEM observation for the sheared N6CN3.7 with $\gamma = 0.0006\,\mathrm{s}^{-1}$ for 1000 s [153]. The edges of the silicate layers lying along the z-axis (marked with the arrows (A)) or parallel alignment of the silicate edges to the shear direction (x-axis) (marked with the arrows (B)) rather than assumingly random orientation in the nylon-6 matrix is observed, but in fact, one cannot see these faces in this plane (Figure 18) [153]. Here, it should be emphasized that the planar orientation of the silicate faces along the x–z plane does not take place prominently. For the case of rapid shear flow, the commonly applicable conjecture of the planar orientation of the silicate faces along the shear direction was first demonstrated to be true by Kojima and his colleagues [157]. Recently, Bafna et al. [159] developed a technique to determine the three-dimensional (3D) orientation of the various hierarchical organic and inorganic structures in PLSNCs. They studied the effect of the compatibilizer concentration on the orientation of various structures in PLSNCs using 2D small angle X-ray scattering (SAXS) and 2D WAXD. Quantitative data on the orientation of these structural units in the nanocomposite film was also determined [160,161].

Theoretical Phase Diagram of Polymer Layered Silicate Nanocomposites (PLSNCs)

Recently, Ginzburg and Balazs developed simple models that describe the liquid crystalline ordering in the polymer–platelet systems [162–165]. They combined a density functional theory (DFT) with a self-consistent field (SCF) model to calculate the phase behavior of thin, oblate colloidal particles that are coated with surfactants and dispersed in a polymer melt. These coated particles represent organoclay sheets. By intergrafting the two methods, they investigated the effect of the surfactant characteristics (grafting density and length of surfactants) and the polymer–intercalant interaction energy on the polymer/clay phase diagram [163]. The system can also form a smectic, crystal (Cr), as well as a two-phase immiscible mixture. Using this model they isolated conditions that lead to the stabilization of the exfoliated nanocomposite system and to the narrowing of the immiscible two-phase regions. Figure 19 corresponds when the surface/sticker attraction is increased even further, the system exhibits a plastic solid at low φ, and a columnar phase at very high φ. The resulting phase diagrams can be used as guidelines for the nanocomposite formation with thermodynamically stable morphologies. In Figure 19, I, Col, N, PS, and S means isotropic, columnar which is (the structure made up of columns consisted of the aligned clay particles), nematic phase, plastic solid (house-of-cards structure), smectic (lamellar) respectively.

Atomic Scale Structure and Binding Energy in PLSNCs

Molecular simulation techniques are used to explore and characterize the atomic scale structure and to predict the binding energies and basal spacing of PLSNCs based on PP and maleated (MA), (PP–MA), MMT, and different alkylammonium ions as
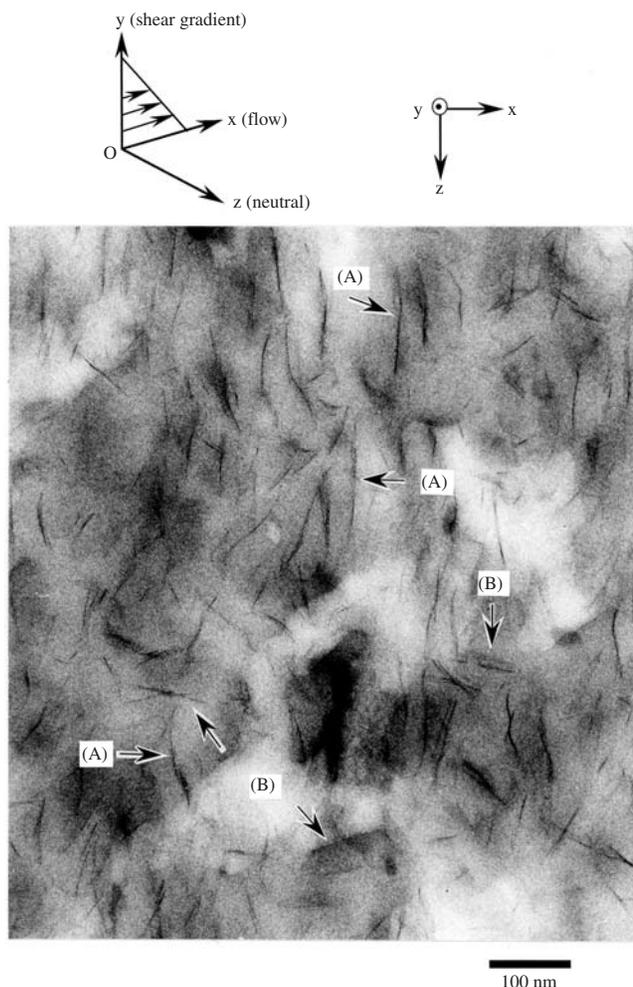
Figure 18. *TEM micrograph in the x–z plane showing N6CN3.7 sheared at 225°C with $\gamma = 0.0006\,s^{-1}$ for 1000 s. The x, y, and z-axes correspond respectively to flow, shear gradient, and neutral direction. (Reproduced from [153]. © 2006 Elsevier.)*

intercalants [166]. The basic machinery of the procedure consists of building a molecular model comprising PP, a given intercalant and MMT, refining and equilibrating it by molecular mechanics/molecular dynamics (MM/MD), and calculating the binding energies as guidelines for screening among different intercalants to make PPLSNCs characterized by a strong interface between dispersed clay platelets and the PP matrix (Figure 20). Figure 21 shows the predicted binding energy versus volume of the intercalant. From a global interpretation of all these molecular dynamics simulation results, they concluded that intercalants with a smaller volume are more effective for clay modification as they improve the thermodynamics of the system by increasing the binding energy, while on the other hand intercalants with longer tails are more effective for intercalation and exfoliation processes, as they lead to higher basal spacing. Similarly, for a given surfactant molecule, the use of PP-MA in the preparation of
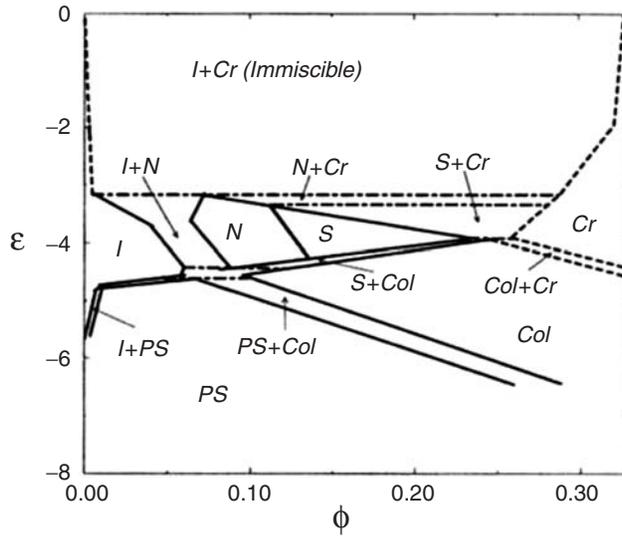
Figure 19. Phase diagram for polymer/clay mixture. Here ε is the sticker–clay adhesion energy. (Reproduced from [164]. John Wiley & Sons, Inc. © 2006.)
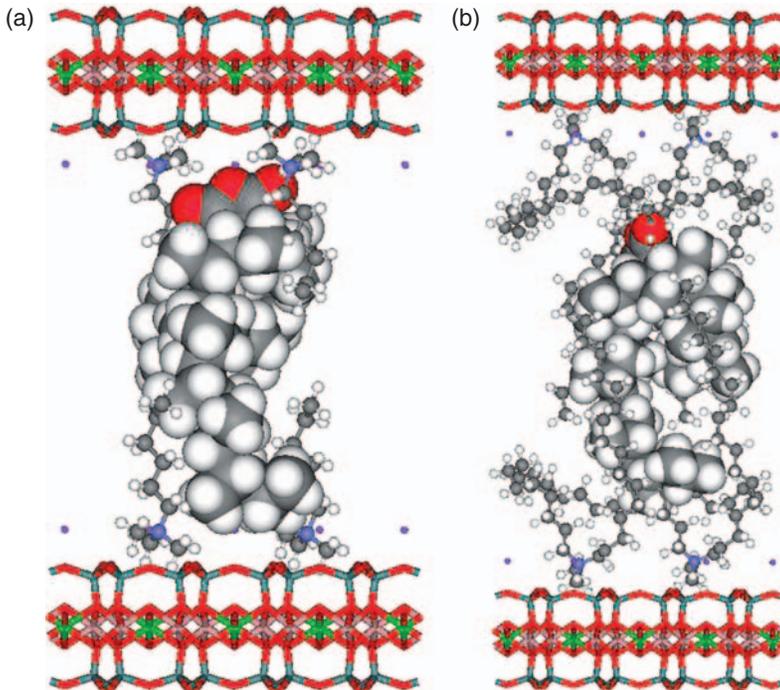
Figure 20. Three component model used for basal spacing simulations, consisting of two layers of MMT with K^+ cations (stick model), (a) four molecules of trimethylammonium cation: or (b) dimethylstearylammonium cation (stick and ball model), and one molecule of maleated PP (PP-MA) (ball model). (Reprinted from [166]. © 2006 Elsevier.)
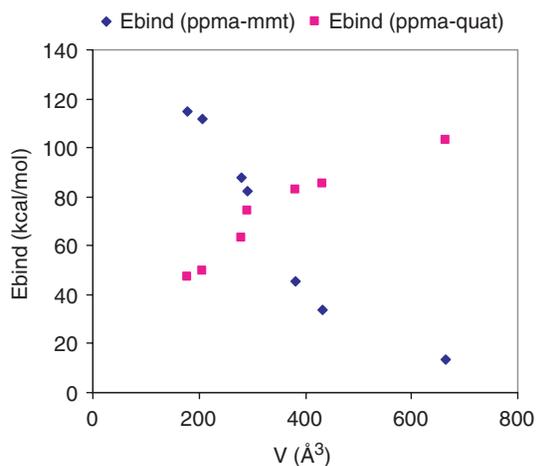
Figure 21. *Predicted binding energy vs volume of the intercalant. (■) E_{bind} (PP-MA/intercalant); (▲) E_{bind} (PP-MA/MMT). (Reprinted from [166]. © 2006 Elsevier.)*

PPLSNCs results in a system with the most favorable interaction energy but with a lower basal spacing. Under the hypothesis, the MMT platelets are uniformly dispersed in a polymer matrix; the PP-MA yields higher interfacial strength with clay than neat PP. The use of neat PP and intercalants with higher molecular volume offers the higher values of the basal spacing and thus, in principle, they should be more effective in the exfoliation process. Recently, some literature is also available [167–170] related to the confinement of polymer chains in the silicate galleries by using coarse-grained MD simulation.

Carbon Nanotube-reinforced Systems

Carbon nanotubes are graphitic sheets rolled into seamless tubes (i.e., arrangements of carbon hexagons into tube-like fullerenes) and have diameters ranging from about a nanometer to tens of nanometers with lengths up to centimeters. Nanotubes have received much attention due to their interesting properties (high modulus and electrical/thermal conductivity) since their discovery by Iijima in 1991 [171,172]. Since then, significant effort has been made to incorporate nanotubes into conventional materials (such as polymers) for improved strength and conductivity [173–182]. Moreover, many potential applications have been proposed for carbon nanotubes, including conductive and high-strength composites; energy storage and energy conversion devices; sensors; field emission displays and radiation sources; hydrogen storage media and nanometer-sized semiconductor devices; probes and interconnects [183].

STRUCTURE AND PROPERTIES OF CNTs

Nanotubes can be synthesized in two structural forms, single-wall and multiwall (as shown in Figure 22). The first tubules Iijima discovered exhibited the multiwall structure of concentric nanotubes forming one tube defining a multiwall nanotube (MWNT) (with a constant interlayer separation of 0.34 Å) [171]. Figures 23 and 24 show electron microscopy images of MWNTs from Nano-Lab (Newton, MA) produced via
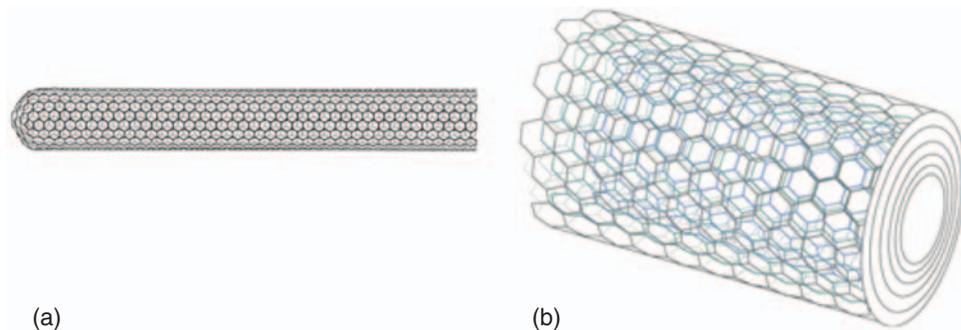
Figure 22. *Schematic of a: (a) single-wall and (b) multiwall nanotube. (With permission. http://www.cnanotech.com and http://www.fibrils.com)*
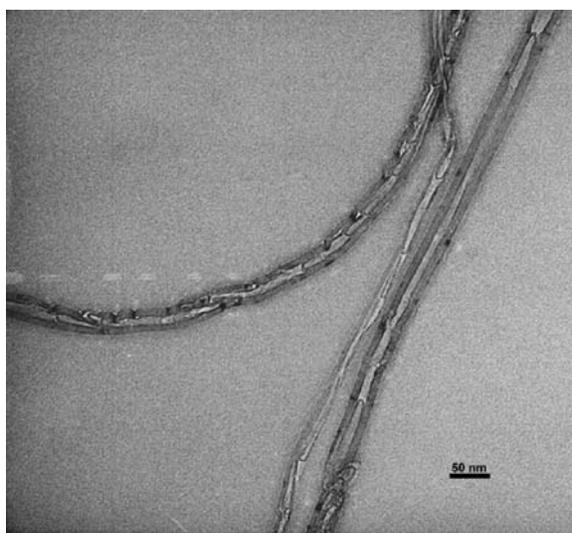
Figure 23. *TEM image for nanotubes on a substrate (lacey carbon), cast from a dispersion in acetone (from Gorga, previously unpublished).*

plasma enhanced chemical vapor deposition (PE-CVD) using acetylene and ammonia with iron catalyst particles on a mesoporous silica substrate. Two years later, Iijima observed a single-shell structure believed to be the precursor to the MWNTs [172]. This single graphitic sheet, rolled into a tube with a cap at either end and a diameter of around 1 nm, is defined as a single-wall nanotube (SWNT) [172,184]. Additionally, nanotubes are described using one of three different morphologies: armchair, zigzag, and chiral (as shown in Figure 25) [183,185].

The packing of the carbon hexagons in the graphitic sheets defines a chiral vector (m, n) and angle. The indices of the vector determine the morphology of the nanotube. Variations in the nanotube morphology can lead to changes in the properties of the nanotube. When $m - n/3$ is an integer, the resulting structure is metallic; otherwise, it is a semiconducting nanotube [1]. For instance, the electronic properties of an armchair nanotube are metallic; however, the electronic properties of zigzag and chiral nanotubes are semiconducting
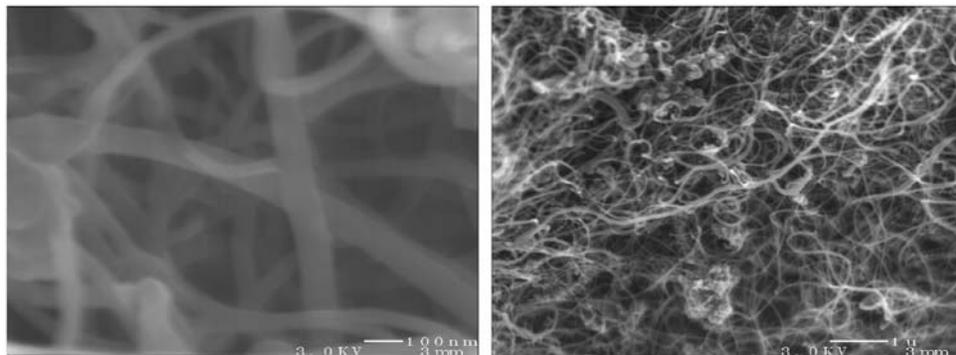
Figure 24. *SEM images of nanotubes on a substrate (Si); cast from dispersion in acetone (from Gorga, previously unpublished).*

(a)

(b)

(c)
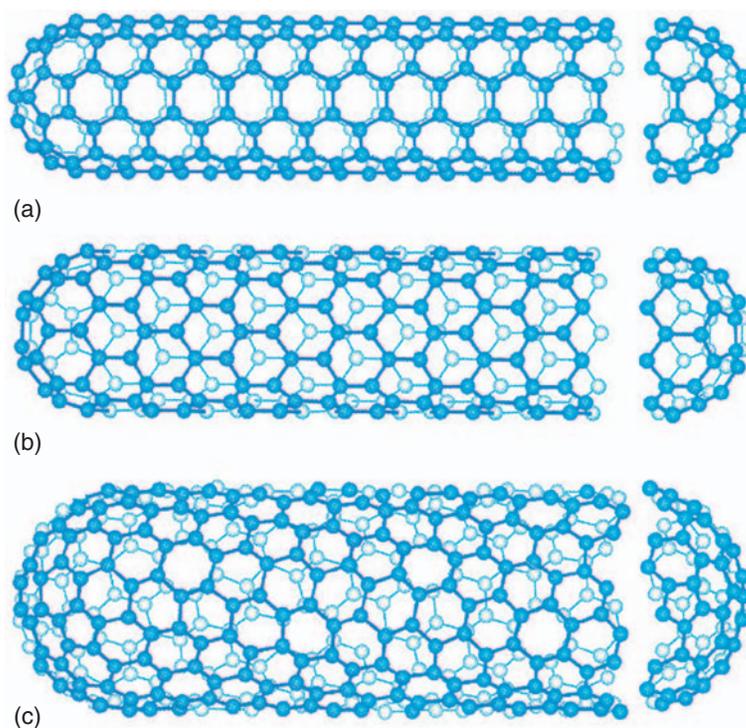
Figure 25. *Schematic of nanotube morphologies. (a) Armchair, (b) zig-zag, and (c) chiral. (Reprinted with permission [183]. © 2005 Elsevier.)*

[186]. Lau and Hui [183] gave a comprehensive review on the structures of nanotubes and three types of nanotube structures: zigzag $(n, 0)$, armchair (n, n), and chiral $(n, m$ where $n \neq m)$. The behavior is determined based on a mathematical model developed using the chiral vector indices [172]. All arm-chair and one-third of zig-zag nanotubes are metallic having a continuous conduction band. The remaining two-thirds of the zig-zag nanotubes are semiconductors, having an energy gap in the conduction band [187]. Based on their

very high aspect ratio (>1000), carbon nanotubes possess an interesting combination of physical properties. Attempts to determine the physical properties of the carbon nanotubes have been conducted both experimentally and theoretically. Originally, researchers used the vibration of the nanotubes as a function of temperature to calculate a Young's modulus of 1 TPa [188]. Such high strength as compared to other materials, as shown in Figure 26 below, led to a pronounced interest in carbon nanotube enabled materials. Common methods to measure the elastic properties of individual nanotubes include micro-Raman spectroscopy [189], thermal oscillations by TEM [188,190], and the application of a force to a nanotube rope suspended across a pit using an atomic force microscope cantilever [191,192]. Other groups measured the properties of a rope and obtained an average value for each tube based on the number of nanotubes in the rope [193,194]. The experimental values measured ranged from significantly below theoretical values to values in agreement with the theory. These methods have produced tensile modulus and strength values for single- and multiwall nanotubes ranging from 270 GPa to 1 TPa and 11 GPa to 200 GPa respectively [183].

Modeling techniques such as molecular dynamics, empirical potentials, and first-principles total-energy, continuum shell, and empirical lattice model have been used to describe the elastic properties of the nanotubes [195–197]. The empirical lattice models, previously used to calculate the elastic properties of graphite, led to tensile modulus values in the range of 1 TPa for multi- and single-wall nanotubes [195]. These values compared well with the diamond structure and outperform conventional carbon fibers. In addition to the mechanical properties, researchers have investigated the electrical and thermal conductivity of nanotubes. In a similar fashion, modeling has been used to determine the conductivity via the structure of the nanotubes as compared with graphite. Much of the theoretical work found that conductivity is greatly dependent on the small structural variations in the nanotubes [198]. For example Berber et al. [199] found unusually high thermal conductance of 6600 W/m K at room temperature for a particular nanotube structure using nonequilibrium and equilibrium molecular dynamics. In addition, the static electrical conductive and superconductive nature of nanotubes were modeled based
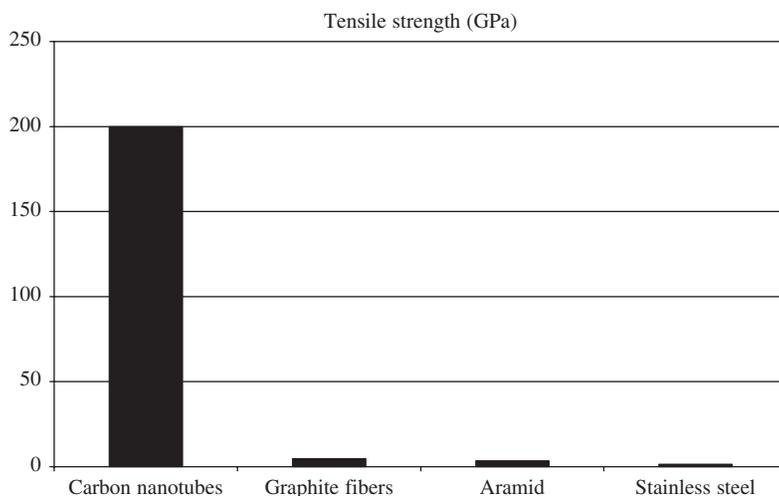

Figure 26. *Tensile strength comparison of common engineering materials. (Reprinted permission from [183]. © 2005 Elsevier.)*

on the conductivity of the graphite sheet structure [200]. Experimentally, Hone et al., reported slightly lower values in the range of 1750–5800 W/m K for the room temperature of a single nanotube rope by comparing the temperature drop across a constantan rod of known thermal conductance to a nanotube mat sample in series with the rod [201]. For electrical conductivity, experimental four-probe measurements of individual nanotubes showed resistivities in the range of 5.1×10^{-6}–5.8 Ωcm (or conductivities ranging from 0.17 to 196,078 S/cm) [198].

CARBON NANOTUBE SYNTHESIS

The three main methods of manufacturing nanotubes include direct-current arc discharge, laser ablation, and chemical vapor deposition (CVD). A thorough discussion on each of these production methods can be found in the April 2004 MRS Bulletin [202]. Direct-arc discharge and laser ablation were the first techniques used to produce gram quantities of SWNTs. In both methods, the evaporation of solid carbon is used to condense carbon gas. The products of such methods are normally tangled and poorly oriented. The CVD produces nanotubes from the decomposition of a continuously supplied carbon containing gas onto a substrate. Due to the continuous supply of the gas, high-purity nanotubes can be produced on a larger (or industrial) volume scale. Producing the nanotubes in an ordered array with controlled length and diameter can also be achieved via CVD methods. Furthermore, plasma enhanced chemical vapor deposition (PECVD) results in further nanotube uniformity within the array [203]. In 2001, a team led by Schlittler developed a self-assembly method for making an ordered array of nanotubes with identical geometry and high purity [204]. More recently, the McGill university researchers in Canada developed a new method and apparatus to produce CNTs with the possibility of a scale up to large industrial levels that is based on thermal plasma technology (having temperatures between 4000 and 25,000°C, which is created by electric arcs or magnetic induction discharges) to overcome the current low-volume production methods and high production costs [205,206].

CARBON NANOTUBE ENABLED MATERIALS

Currently many methods of producing nanotube-enabled materials are under investigation. Some methods attempt to form fibers from nanotubes alone; whereas, other procedures use a matrix to support the nanotubes. Without a support medium, research teams expect to achieve property values closer to the values of individual nanotubes. However, the use of a matrix or binder often makes production of macroscale materials more feasible. Forming fibers directly from nanotube production methods, such as arc discharge [207] and CVD [208], have been investigated. Furthermore, research has shown the ability to create nanotube yarns by twisting them together as they are pulled out of a nanotube forest [209]. Other studies have proposed using super-acid solutions as a medium to support the fiber through a conventional spinning process followed by the removal of the medium [210,211]. However, the most common method has been to incorporate them in a polymer matrix as a reinforcing material. The combined polymer/ nanotube structure is often referred to as a nanocomposite. Research has proposed that the nanotubes will provide load transfer in the same way as non-continuous fibers in conventional composite systems. Experimentally, the property improvement in nanotube-enabled materials has been marginal. The mechanical properties have varied from no change [175,212] to moderate increases (25–50% modulus increase; 80–150% toughness increase) [213,214], electrical properties in the range of 2 S/m (with a percolation threshold

of 0.0025 wt%) [213], and 125% increase in thermal properties at room temperature [187]. However, optimal property improvements have not been achieved due to deficiencies in nanotube dispersion and alignment. The remaining parts of this section will focus on the processing, manufacturing, properties, and applications of carbon nanotube/polymer composites.

CNTs PROCESSING: DISPERSION AND ORIENTATION

Two essential components for optimal reinforcement in particle-reinforced composite systems are filler dispersion and orientation. Dispersion of single-wall carbon nanotubes (SWNTs) and higher concentrations of multi-wall carbon nanotubes (MWNTs) into a polymer matrix has been one of the largest challenges to date [175], due to the aggregation of the nanotubes as a result of the van der Waals interactions between individual tubes. Consistent dispersion of reinforcing material throughout the matrix leads to consistent load transfer from matrix to particle. Moreover, it can assist with the realization of a network for conductivity of electrical and thermal energy. Many composite researchers believe that SWNTs will be the ultimate reinforcements for the next generation high-performance structural and multifunctional composite materials. Thostenson et al. [203] stated some critical issues in the processing of CNT polymer composites in their review; uniform dispersion [215–217], wetting, and alignment of the carbon nanotubes [217,218] in the polymer matrix and functionalization of CNT for the nanotube/matrix interfacial bonding [203]. The SWNTs agglomerate more easily than MWNTs due to their size difference (i.e., greater surface area) and can form ropes or aligned bundles of SWNTs. The SWNTs often require more specialization to produce than MWNTs. Therefore, the cost of purified SWNTs tends to be greater than that for MWNTs. The MWNTs, on the other hand, have been found to demonstrate lower mechanical, electrical, and thermal properties due to the ability of the concentric nanotubes to slide past each other. Due to the inherent tube within a tube structure, the MWNTs tend to have a larger diameter (10 nm) as compared with SWNTs (∼1 nm). However, improvements in nanotube fabrication have led to MWNTs with more precise, smaller diameters. This may lead the nanotubes with improved properties over larger diameter MWNTs with less agglomeration than SWNTs.

Similarly, orientation in the direction of applied forces allows for greater load transfer. If the particle is oriented in a direction other than the direction of the applied force, the full potential of the particle cannot be realized. In addition, having all the particles oriented in the same direction allows for easier transfer of energy (electrical or thermal). Achieving consistent dispersion and orientation will allow optimal property improvements. Researchers have used many different techniques in an attempt to disperse nanotubes in polymer matrices including solution chemistry to functionalize the nanotube surface [219–223], the use of polymers to coat the nanotube surface [224] *in situ* polymerization of the nanocomposite [225,226], ultrasonic dispersion in solution [181,227], melt processing [11,228–232], the use of surfactants [233,234], electrospinning [235], electrode chemistry [236], and gelation/crystallization [237]. In gelation/crystallization experiments, the nanotubes were dissolved in a solvent, polymer solution was added, a gel was formed, the gel was formed into a film, and finally the solvent was evaporated [237]. Nanotube surface modifications used plasma treatment or chemical oxidation to attach the functional groups. These groups allowed the nanotubes to bond better to the matrix and overcome the van der Waals interactions between nanotubes [223]. Melt compounding involves creating a preblend by dry mixing polymer powder with

nanotube powder. The preblend is fed into an extruder allowing for control of shear, temperature, and residence time. After the residence time, the material is extruded in the film or fiber form [11]. Good dispersion alone has shown moderate property improvements, but nanotube alignment, or orientation, has led to further improvements. Using melt compounding followed by melt drawing, has shown a significant increase in mechanical properties [229,238]. Transmission and scanning electron microscopy have shown good dispersion and orientation using such methodology [11,228,238]. These improvements have been shown to increase until an optimal loading level and then decrease above this concentration [11,239]. In addition to mechanical drawing, the inherent conductive nature of carbon nanotubes has been utilized to induce alignment. For example, the application of a magnetic field to a nanocomposite sample during or after processing has shown nanotube alignment [240–245]. To bring out the anisotropic nature of nanotubes, Walters et al., prepared a freestanding aligned SWNT film by filtering the nanotube dispersion under a high magnetic field up to 19 T [244]. Kimura and Ago [245] applied this technique to MWNT–polymer composites and obtained anisotropic composites, with a better percolation path and higher elastic modulus and glass transition temperature. Fan and Advani [246] subjected the vinylester resin system to shear flow for MWNT orientation and used a second-order orientation tensor to describe the orientation in 2D plane. Again, the optimal properties, as predicted by such models as Halpin–Tsai, have not been achieved due to poor interfacial bonding, variations in nanotube structure, and variations in properties.

PROPERTIES, MANUFACTURING, AND APPLICATION

Most of the researchers have incorporated nanotubes into thermoplastic polymers due to their ease of processibility. This allows fibers or films to be made and other objects to be easily melt processed into molded parts. Research has been performed using both amorphous and semicyrstalline polymers with varying degrees of success. The nanotubes have been shown to toughen and stiffen amorphous brittle materials such as polymethyl methacrylate (PMMA) [11,177,247] as well as in semicrystalline polymers such as PP [238]. In addition to the toughening and stiffening effects, morphological changes are the subject of discussion for semicrystalline polymers such as PP. Research literature has suggested that nanotubes act as nucleating agents in these materials leading to new crystallographic morphologies and ultimately increased strength [228,248–250]. Although, most polymer/ nanotube composite research has utilized thermoplastic matrices, research has also been conducted with thermosetting materials [182,251–259]. The change in viscosity as a function of cross-linking can be problematic for optimizing dispersion and orientation. Research has been carried out to study mechanical [182,251,257–259], thermal [257], and electrical [252,253,255,259] properties of thermosetting polymer/nanotube composites with various results. Of the various thermosetting polymers that have been reported in the literature, epoxies have been the most commonly used.

Recent research has shown that the tensile toughness of 1 wt% MWNTs in PMMA exhibited the same tensile properties as composites fabricated with 1 wt% SWNTs in PMMA [260] using the dispersion process outlined by Sabba and Thomas [261]. Both samples were drawn to a 12 : 1 draw ratio. In each case, the dispersion of nanotubes was excellent (as shown by electron microscopy); however, no special dispersion treatment (other than melt mixing) was needed for the MWNT composite, therefore making the MWNTs the favorable toughening particle for PMMA. Research has shown mechanical property improvements with the addition of both SWNTs and MWNTs

to PP. As discussed earlier, dispersion of the nanotubes plays a large role in property improvements. One study showed that the addition of 1 wt% SWNTs via melt blending did not significantly improve the mechanical properties [228]. In the study, SEM images showed micrometer scale aggregates and nanotube ropes within the sample. Some research has suggested that the aggregates could act as stress concentrators inhibiting the property improvement. However, from the slight increases, the aggregates were either not big enough to create stress concentrations, or the strength of the ropes was greater than the losses from the stress concentrations. The research concluded that better nanotube dispersion would lead to more rope, less aggregates, and ultimately significant mechanical property improvements.

In another study, significant property improvements were observed when adding SWNTs to PP [262]. The nanotubes were first dispersed in the polymer using solution processing. After removing the solvent, the fibers were melt spun and post drawn for improved dispersion and orientation. The addition of 0.5 and 1 wt% demonstrated an increase in tensile strength and modulus values. At 1 wt%, the tensile strength and modulus were 40 and 55% higher than neat PP fibers. However, additions of 1.5 and 2 wt% made spinning of the fibers difficult and led to lower mechanical properties.

A similar maximum in mechanical properties as a function of nanotube loading was also noted in another study in both conventional tensile experiments and dynamic mechanical analysis [263]. The study looked at the properties of both as-spun fiber and postdrawn PP/SWNT fibers. Additionally, the studies investigated many differences in low melt flow rate and high melt flow rate PP. The basic tensile qualitative behavior of neat PP (high initial modulus, sharp yield, and stretching to very long elongations) was observed in the as-spun nanocomposites. However, the nanocomposites exhibited lower elongation to break values. Increased tensile strength was noted for the low melt flow rate samples and the opposite for the high melt flow rate samples. Furthermore, the postdrawn low flow rate samples increased in tensile strength up to 1% and then decreased. The higher concentrations caused the fibers to become brittle and difficult to draw. All of the high melt flow rate samples exhibited a decrease in ultimate tensile strength. The dynamic mechanical analysis produced results similar to conventional tensile tests. Within the temperature limits, the storage modulus, E', increased with increasing nanotube additions. At higher temperatures, E' of postdrawn samples started to decrease. The concentration of 1% was found to be the optimal value for E'. Moreover, as evidenced by the tensile test, the postdrawing process created a far stiffer material. In contrast, the loss modulus, E'', shows little to no discernible trend as related to molecular weight of PP or nanotube concentration.

Research of PP/MWNTs has been preformed to a lesser extent than SWNTs. In one study, functionalized nanotubes were added to chlorinated PP to create composite films [264]. The study noted an upward shift in the yield point on the stress–strain curve and consequently increased yield strength. Additionally, the Young's modulus, ultimate tensile strength, and toughness increased with increasing nanotube volume fraction by a factor of 3.1, 3.9, and 4.4, respectively. From the data and previously derived composite models, mathematical models based on volume fraction were developed for the Young's modulus and composite strength. In another study, PP/multi-wall nanotube powder was created using a pan milling process [265]. The pan milling of the neat PP reduced the elongation to break significantly. However, the addition of nanotubes increased the elongation to break (over pan-milled PP) through crystal structure changes and induced PP orientation. Again an optimal 1% nanotube loading exhibited increased Young's modulus and yield strength.

The pan milling allows for better dispersion, reduces the number of defects, curvature, and entanglements, and enhances the polymer/nanotube adhesion.

Most recently, Dondero and Gorga [238] showed that 0.25 wt% MWNTs in drawn PP (with a 12:1 draw ratio) increased tensile toughness by 32% and modulus by 138% over drawn PP. The DSC supported the conclusion of modulus increases via load transfer rather than increased crystallinity. However, WAXD indicated a crystal structure change from α and mesophase to α phase only with the addition of nanotubes in oriented samples. The activation energy, calculated from dynamic mechanical experiments, also revealed an increasing trend to a maximum as a function of nanotube loading. In drawn samples, TEM and SEM showed well-dispersed and highly oriented nanotubes.

Johnson et al. [266] manufactured CNT/polyethylene composites using extrusion to determine mechanical properties such as stiffness, work to failure, wear resistance, etc. Ren et al. [267] investigated the fatigue behavior (under repeated mechanical loads) of unidirectional, aligned SWNT reinforced epoxy composite, which is demonstrated in long-term structural applications as well as in aerospace application. O'Donnell and Sprong [268] investigated the potential impact of carbon nanotube reinforced polymer (CNRP) composites on commercial aircraft. The CNRP composite structured airframes are modeled through the utilization of Euro Control's Base of Aircraft Data and from traditional flight dynamics theory. They considered notional Boeing 747-400 and 757-200; Airbus A320 and Embraer E145 with CNRP and replaced the entire volume of structural aluminum with CNRP composites, without including any modifications to the geometry or design of the airframe. In their model, weight reduction affects aircraft performance, fuel saving, and efficiency. Hsiao et al. [269] showed the potential of CNT to reinforce the adhesives. They joined two composite laminates with toughened epoxy adhesives and MWNT for bonding graphite fiber/epoxy composite laminates with improved shear strength [268].

Jihua and Liang and other coworkers proposed a bucky paper/resin infiltration (wetted in epoxy) approach for fabricating nanocomposite [270,271]. They suggested that bucky paper can provide a number of advantages for controlling dispersion, alignment, and high tube loading and is also easy for composite processing. Through a filtration process, SWNTs were fabricated into thin membranes called bucky papers to form networks of SWNT ropes. The heavy curvature of the composite sample is an example of tube alignment as shown in Figure 27 [241]. This is the effective approach for bulk polymeric composites with controlled in plane SWNT alignment and high nanotube content [241].


Magnetically aligned bucky paper composite

Random bucky paper composite

US quarter coin to show the sample dimension
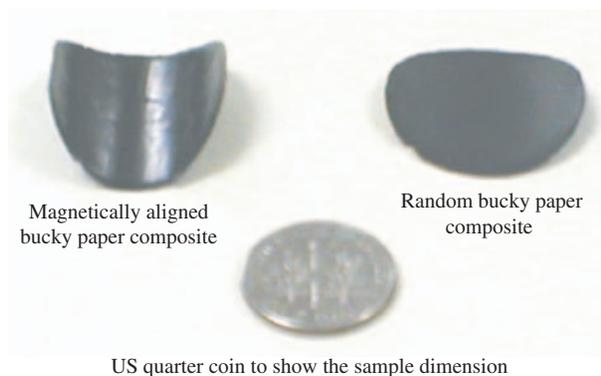
Figure 27. *Heavy curvature of magnetically aligned bucky paper. (Reproduced from [241] with the permission of SAMPE.)*

SIMULATION AND MODELING

Li and Chou [272,273] have worked out the contributions of van der Waals interactions between individual carbon atoms within nanotubes within the finite element modeling (FEM) truss model (Figure 28). Nonlinear truss elements were used in simulations, as the force between two carbon atoms is also nonlinear. It was found that the Young's modulus of the nanotubes increases as the diameter of the nanotube is increased. Frankland et al. [274] investigated the effect of cross-links on the interfacial bonding strength between a SWNT and polymer–matrix (crystalline or amorphous) with MD simulations. They found that even a relatively low density of cross-links could have a large influence on the properties of a nanotube–polymer interface. Recently, Lau [275] conducted an analytical study on the interfacial bonding properties of nanotube/polymer composites by using a well-developed local density approximation model [276], classical elastic shell theory and conventional fiber-pullout model. In his study, several important parameters such as the nanotube wall thickness, Young's modulus, volume fraction, and chiral vectors of the nanotubes were considered. It was found that the decrease of the maximum shear stress occurs with the increase in the size of the nanotubes. Increasing the number of wall layers of the nanotubes will cause: (1) a decrease in Young's modulus of the nanotubes; (2) an increase in effective cross-sectional area; and (3) thus an increase in total contact surface area at the bond interface and the allowable pullout force of the nanotube/polymer system (Figure 29). In the figure, it shows that the maximum shear stress of zigzag nanotube (5,0) is comparatively higher than those of chiral (5,3) and armchair (5,5). The FEM method associated with the molecular dynamic (MD) or equivalent-continuum (EC) model has been recently adopted to calculate the mechanical properties of nanotubes. Odegard et al. [277] have developed an equivalent-
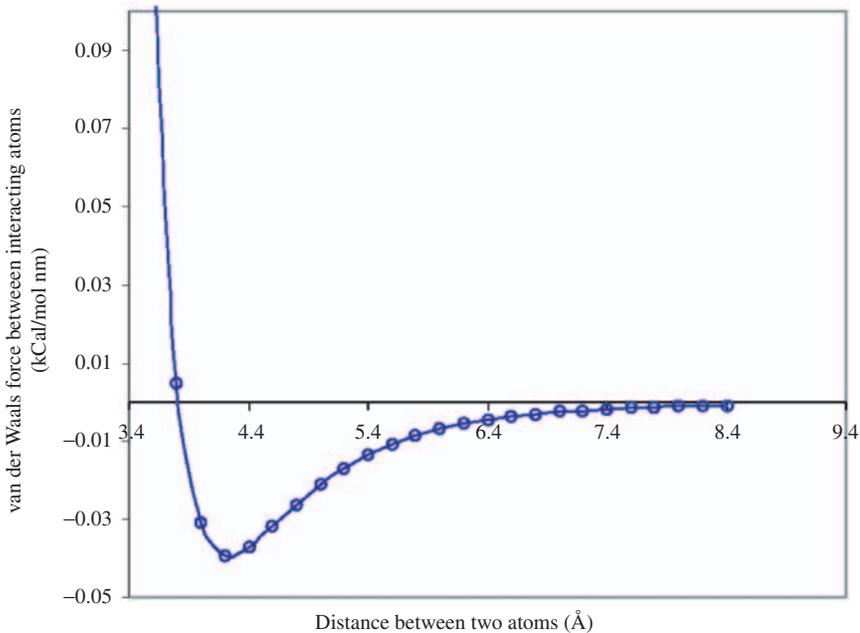
Figure 28. *van der Waals force vs the distance between two carbon atoms. (Reproduced with permission [278]. © 2006 Taylor and Francis.)*
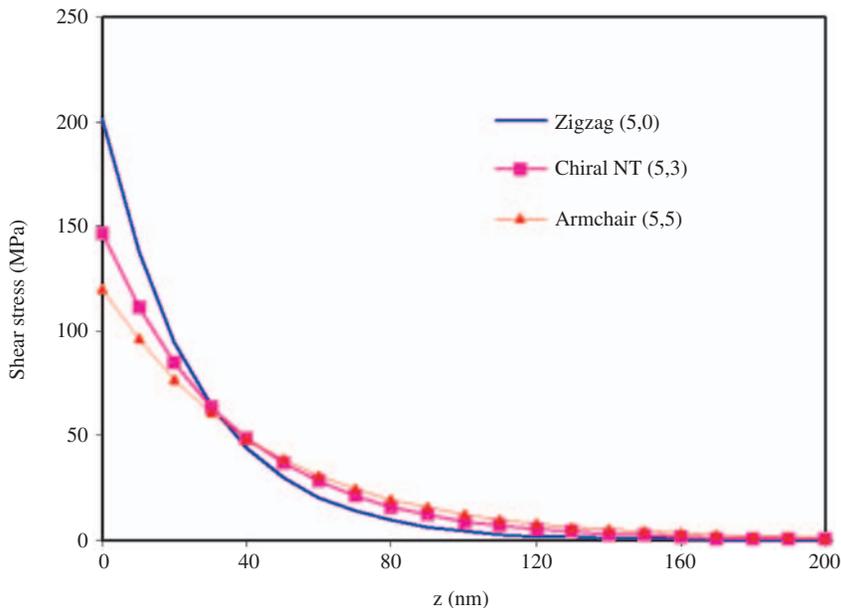
Figure 29. *Plot of interfacial shear stress vs different types of nanotube. (Reproduced with permission [275]. © 2005 Elsevier.)*
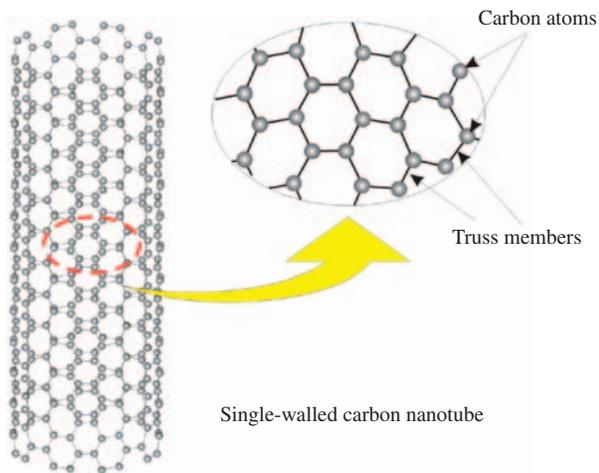
Figure 30. *Truss model of a carbon nanotube's structure. (Reproduced with permission [278]. © 2006 Taylor and Francis.)*

continuum tube model to determine the effective geometry and effective bending rigidity of a graphene structure. Molecular mechanics considerations were first used to determine the linking forces between individual carbon atoms. This molecular force field was simulated by using a pin-joint truss model, i.e., each truss member represents the force between two atoms, as shown in Figure 30 [278]. Therefore, the truss model allows the accurate simulation of the mechanical behavior of nanotubes in terms of atoms displacements.

Other Nanocomposite Systems

POLYMER-INORGANIC PARTICLE NANOCOMPOSITES
Particles of Interest

Nanoparticles are often defined as particles of less than 100 nm in diameter [2]. Nanometer-sized particles have been made from different organic–inorganic particles and impart composite materials improved properties [279]. Different particles have been used to prepare polymer/inorganic particle nanocomposites, including:

- Metal (Al, Fe, Au, Ag, etc.)
- Metal oxide (ZnO, Al_2O_3, $CaCO_3$, TiO_2 etc.)
- Nonmetal oxide (SiO_2) [280]
- Other (SiC)

The selection of nanoparticles depends on the desired thermal, mechanical, and electrical properties of the nanocomposites. For example, Al nanoparticles are often selected due to their high conductivity; calcium carbonate particles are chosen because of the relative low cost of the material, and silicon carbide (SiC) nanoparticles are used because of their high hardness, corrosion resistance, and strength [281].

Preparation and Processing

In the case of organic–inorganic nanocomposites, the strength or level of interaction between the organic and inorganic phases is an important issue. Physical or simple mechanical mixing causes a weak phase interaction, e.g., hydrogen bonding, van der Waals forces. On the other hand, a strong chemical covalent or ionic–covalent bond between the organic and inorganic phases or sol gel technique is the typical preparation method for the organic–inorganic nanocomposites [282]. Surface chemistry has been studied for understanding the effect of nanoparticles on a polymer matrix, particle–matrix adhesion etc. in different studies [279,282–285]. Yong and Hahn used a dispersant and coupling agent in an SiC/vinylester nanocomposite system to improve the dispersion quality and strength [286]. Different methods have been used to prepare polymer/inorganic particle nanocomposites, including: *in situ* polymerization [284], melt compounding by twin-screw extrusion [287–289], solution blending [282], high shear mixing [290] with three roll milling [291,292], etc. Tang et al. [279] used two traditional polymer-processing techniques (free cast and spinning) to prepare polyacrylonitrile matrix and nano-ZnO composites.

Properties, Manufacturing, and Application

Polymer/inorganic particle-based nanocomposites have shown significant improvement in mechanical, thermal and electrical properties. For example, in nylon-6 filled with 5 wt% 50 nm silica nanoparticles, an increase in tensile strength by 15%, strain-to-failure by 150%, Young's modulus by 23%, and impact strength by 78% were reported [293]. Jiang and coworkers [294] investigated ABS (acrylonitrile butadiene styrene) reinforced with both microsized and nanosized calcium carbonate particles through melt compounding. It was found that the ABS/micron-sized particle composites had higher modulus but lower tensile and impact strength than neat ABS. However, the ABS/nano-sized particle composites increased the modulus as well as impact strength. Chen et al. [296] found that different particle sizes influence the glass transition temperature (T_g) of the nanocomposites (Figure 31). Ma et al. [283] showed an improvement in electrical properties of polyethylene nanocomposites by introducing functional groups at TiO_2 nanoparticles.
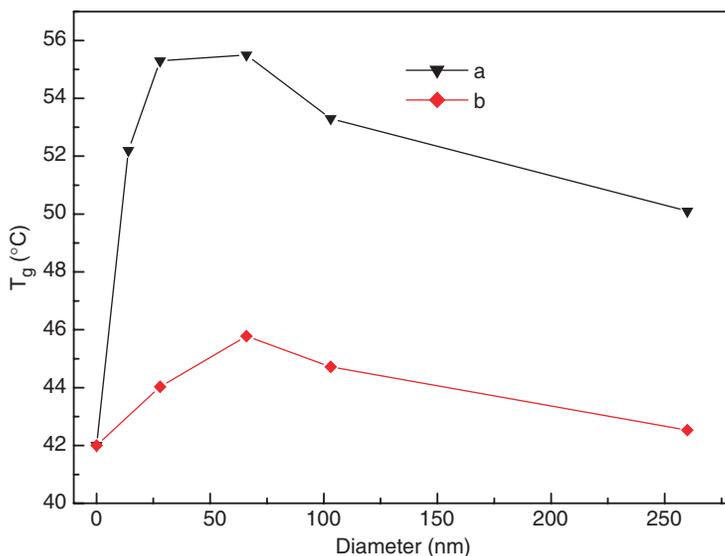
Figure 31. *Effect of particle size on* T_g *of silica/polyurethane nanocomposites: (a)* in situ *polymerization; (b) blending methods. (Reprinted from [296] with permission. © 2006 Elsevier.)*

Zhang and Singh [285] improved the fracture toughness of nominally brittle polyester resin systems by incorporating Al_2O_3 (15 nm). An Al_2O_3 particle has been found to be effective in improving the dielectric constant of polymer in other studies [295] also. Koo et al. [290–292] used AEROSIL (silicon dioxide, 7–40 nm) silica nanoparticles to process different nanocomposites with different resin systems (phenolic, epoxy, cyanate ester) for high temperature application. Recently creep tests were performed on TiO_2/PA6,6 nanocomposites by Zhang and Yang [289]. Poor creep resistance and dimensional stability have been improved by adding TiO_2 in polyamide 6,6 thermoplastic composites.

Chisholm et al. [298] investigated micro- and nano-sized SiC in an epoxy matrix system. In their study, an equal amount of loading, nanoparticle infusion brings superior thermal and mechanical properties than microsized particle-based composites. They utilized VARTM with satin weave carbon preforms to fabricate nanoparticle infused laminated composites. Li et al. [297] performed a low velocity impact test with improved impact strength using TiO_2 and nanoclay in an epoxy system. They also showed a linear relationship with impact energy and corresponding initial velocity.

Polymeric foams are extensively used in different applications such as aerospace, marine, automotive, packaging, and cushioning due to their energy absorption capabilities especially in the event of impact loading [299], good moisture resistance, dampening characteristics (sound, vibration, and oscillation). Mahfuz et al. [300,301] modified polyurethane foam by infusing 3% TiO_2 nanoparticles (spherical shape, diameter: 29 nm) through ultrasonic cavitation process. They found that nanophased foams are thermally stable and their strength and stiffness are greatly improved. It also showed higher absorbed energy [301]. On the basis of research results, it can be said that nanocomposite foam plays an important role in packaging industries and also for short-term disposal applications.

Figure 32. *Casting of foam in aluminum mold. (Reprinted from [301] with the permission of SAMPE.)*

Table 3. Experimental Data for core materials in High Velocity Impact Test *[303].
(Reproduced with permission.)

Material	Average striking velocity (m/s)	Average residual velocity (m/s)	Average energy absorbed per aerial density (Nm^3/kg)	Ballistic limit per aerial density (m^3/kgs)
Neat	802.05	752.78	40.69	22.39
Nanophased (TiO_2)	784.23	724.95	48.84	24.98
		Gain	20%	12%

Impacted (velocity $\approx$ 800 m/s) by a 13 g fragment simulating projectiles (FSP) made from hardened steel [303].

Sandwich composites have been used in the aerospace industry and as load bearing members in naval structures. As the core plays an important role in enhancing the flexural rigidity, Mahfuz et al. [302] studied about strengthening the core materials by using nanophased polyurethane foam (infused TiO_2) for a better performance of the structural sandwich. They used a VARTM set up for sandwich construction and investigated the static [302] and dynamic behavior of the nanophased foams (Figure 32, Table 3) [303]. Mahfuz and coworkers assumed that, several energy-dissipating mechanisms (matrix shear yielding, crack front pinning or blocking) play an important role in higher energy absorption in a nanophased sandwich. Very recently, Mahfuz et al. [19] impregnated SiC nanoparticles (30 nm diameter) in continuous prepreg tapes by the solution impregnation method. These partially cured tapes were used to fabricate nanophased unidirectional laminates using a filament winding machine. They achieved improved flexural strength and stiffness of approximately 32 and 20% respectively, on nanophased laminate. These types of nanophased prepreg can be used in pultrusion and fiber placement technology for manufacturing nanocomposites with improved properties for structural applications.

NANOFIBER-REINFORCED SYSTEMS

Carbon nanofibers (CNF) are a unique form of vapor-grown carbon fibers that fill the gap in physical properties between conventional carbon fibers (5–10 μm) and carbon

nanotubes (1–10 nm). The reduced diameter of nanofiber provides a larger surface area with surface functionalities in the fiber [304]. Typically CNF are not concentric cylinders; the length of the fiber can be varied from about 100 µ to several centimeters, and the diameter is of the order of 100–200 nm with an average aspect ratio greater than 100. The most common structure of CNF is the truncated cones, but there are wide ranges of morphologies (cone, stacked coins, etc). The CNF have the morphology where they are hollow at the center (much like a multi-wall nanotube) and have a larger diameter than MWNT but the individual layers are not arranged in concentric tubes.

Polymer nanofibers can be synthesized by a number of techniques, such as drawing, template synthesis, phase separation, electro spinning, self-assembly, etc. [304,305,306,307, 308,309,310]. Applied Sciences, Incorporated used CNF in the form of VGCF, which is a discontinuous graphitic filament, produced in the gas phase from the pyrolysis of hydrocarbons [311,312]. They developed Pyrograf-III carbon nanofiber for different aerospace applications like aircraft engine anti-icing, fire retardant coatings (forming a char layer over combustible composites), lightning strike protection, solid rocket motor nozzles, conductive aerospace adhesives, thermo-oxidative resistant structures, missile/airframe structures [290–292], etc.

Processing, Manufacturing, Properties, and Application

Tandon and Ran [313] enhanced the thermomechanical properties of conventional aerospace carbon fiber-reinforced (IM7) composites by using carbon nanofiber. They manufactured IM7/CNF matrix unidirectional laminate aerospace structures by using the filament winding technique. Glasgow and Tibbetts [314] oxidized the surface of carbon nanofiber to improve the tensile behavior in PP composites. Lafdi and coworkers [315] showed improved flexural strength and modulus in epoxy-based composites with oxidized nanofibers. Finegan and Tibbetts [316] incorporated CNF in a PP with improved strength and stiffness. Thermal transport across bonded radiator panels is important where thermally conductive adhesives play an important role. Electrically conductive bonded joints are needed in spacecraft to eliminate the buildup of static charge on the structure due to the impingement of charged particles. Gibson et al. [317] modified the epoxy-based adhesives formulated with silver coated and uncoated vapor-grown carbon nanofibers for several aerospace applications such as electrical conductivity, thermal transport, and mechanical properties. But they concluded that it does not help to remove the waste heat [317]. Lao et al. [287] used CNF, clay platelets, and silica nanoparticles to find the relationship between the flammability and mechanical properties of nylon-11. They achieved a combination of enhanced mechanical and flammability properties in clay platelets and CNF. In their analysis, clay-based nanocomposites showed better flammability, while the CNF-based nanocomposites showed better mechanical property. Koo and his co-workers achieved better dispersion using oxidized CNF in [292] CYCOM 977-3 (epoxy type) resin (Figure 33). In another paper [290] they mentioned the poor dispersion of CNF by TEM image using phenolic resin, whereby they observed poor performance in the nanomodified phenolic resin. Carbon fiber-reinforced PMC was produced by Cytec Engineered Materials using their proprietary procedures. Here an image is inserted (Figure 34) to compare short beam shear strength values of the five different nanomodified epoxy carbon fiber-reinforced PMCs [290].
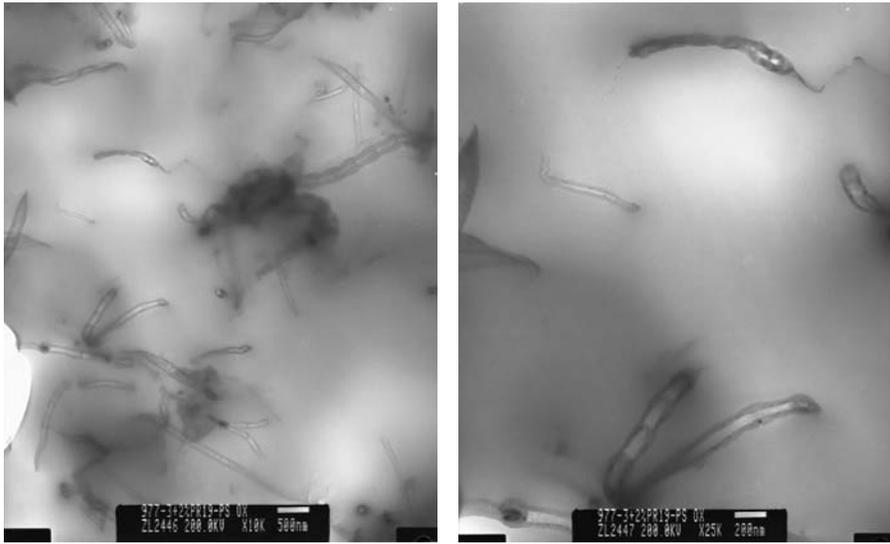
Figure 33. *TEM micrograph showing good dispersion of 2% (PR-19-PS Ox) CNF in the CYCOM 977-3 (epoxy type). Reproduced with the permission of SAMPE [292].*
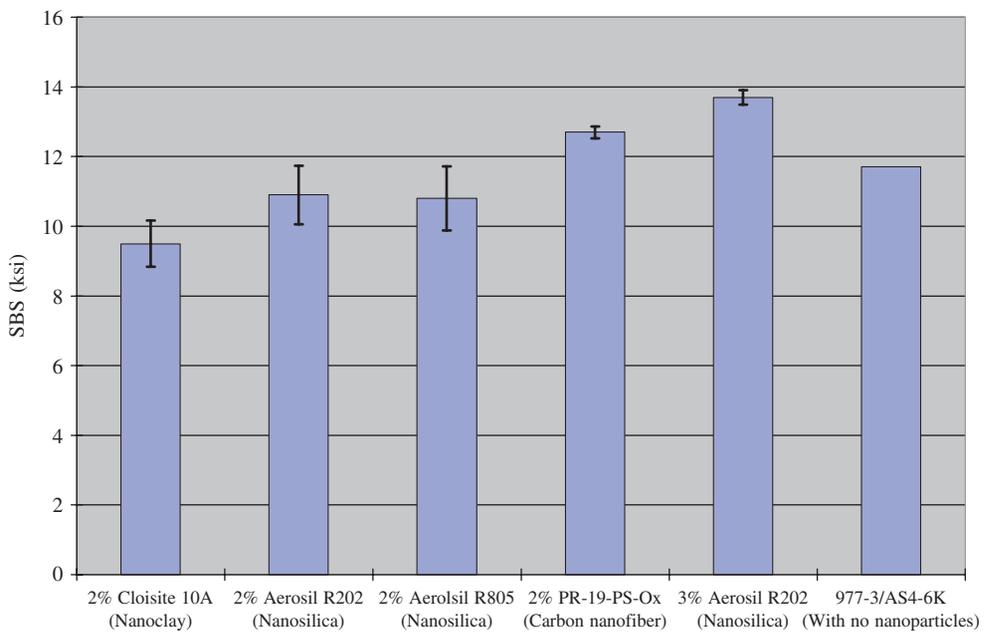

Figure 34. *Comparison of SBS values of the five nanomodified epoxy carbon fiber-reinforced PMCs with the 977-3/carbon fiber baseline composites. Reproduced with the permission of AIAA [290].*

CURRENT CHALLENGES

Challenges in Processing and Manufacturing of Nanocomposites

Nanocomposite materials hold the potential to redefine the field of traditional composite materials both in terms of performance and potential applications. There is little doubt that polymer nanocomposites have tremendous market potential both as replacements for current composites and in the creation of new markets through their outstanding properties. But developing the processing–manufacturing technologies in terms of quantity and value for commercialization will be one of the biggest challenges. For example, dispersion of nanoparticles or chemical compatibility with matrix materials is the important issue. A homogeneous dispersion of nanoparticles in a polymer by using existing/traditional compounding techniques is very difficult due to the strong tendency of fine particles to agglomerate [318,319]. At the same time if it is subjected to force, there is a possibility of splitting of agglomerate nanoparticle. Therefore, premature failure takes place in the final product [319]. Degassing is another critical problem while processing a nanocomposite. The air trapped while pouring the highly viscous material in the mold (5–10 wt% of clay in the matrix), initiates crack and failure of specimen can take place under low strains [319]. The alignment of nanoparticles in the composite matrix can be critical to maximize unidirectional properties such as strength, modulus, and toughness [320]. As in the case for traditional composites, it is even more challenging to determine the strength, composition and functionality of the interfacial region.

The goal of improving the carbon nanofiber matrix interfacial adhesion issue and complete dispersion must be solved before achieving the full potential of CNF nanocomposites. McMorrow and Chartoff [321] used a two-roll mill for dispersing carbon nanofibers in vinyl ester resin via continuous shearing. They found a dry and brittle mixture after 6 min of milling and incomplete dispersion because of the viscosity limitations. However, they mentioned that the technique holds promise for lower viscosity resins if the temperature and/or added diluents help to reduce the viscosity of the mixture. They did not achieve a good trend in the mechanical and thermomechanical results as a function of CNF loading, which were opposite to what was expected for a well-dispersed nanocomposite with good fiber–matrix adhesion.

In addition to the composite integrity, the nature of the nanoparticle is also critical for property improvement. Han et al. [20,322–324] looked at the defective structures and properties of carbon nanotubes. They generated model configurations of nanotubes [322–324]. They found SWNTs to be relatively defect-free whereas, MWNTs typically had more defects, such as topological defects (pentagon, heptagon) and structural defects (discontinuous, cone shaped walls, or bamboo structure). To improve dispersion and compatibility in polymer matrices, nanotube is being functionalized. There are still some concerns remaining like whether functionalization of a nanotube will affect the properties to improve the final product.

The SWNTs and SWNT bucky paper are highly radiation tolerant for high-energy neutrons (upper atmosphere), medium, and high-energy protons, which would be the environments that one would expect to encounter in aerospace application [325]. But Wilkins et al. [325] suggest that in the case of composites, there might be a limitation of using these materials in aerospace application as matrix response with the radiation.

Scale up is needed to produce large quantities of nanomaterials for manufacturing purposes. There is still a lack of real-time characterization methods, instrumentation, tools, as well as a lack of affordable infrastructure (facilities, equipment, design tools, skilled personnel). To move nanotechnology forward, education is needed for both scientists and engineers in academics and industry. At the same time, researchers must continue to prove the disruptive and confusing nature of this technology and urge industry not to let the Innovator's Dilemma slow the introduction of nanoproducts [326]. For example the change in T_g by using nanofiller composites has been controversial [128,327,328].

Molecular dynamics simulation (MD) and theoretical analyses are mainly based on certain assumptions that may not be practically applied to a real situation in nanotube/polymer composites [278]. The mechanical and dispersion properties, and alignment of nanotubes are mainly involved in enhancing the properties of nanotube/polymer composites. However, it is also hard to achieve this without a good interfacial bonding between nanotubes and matrix. Presently, no reports are available to obtain the best solution for these points. Two opening problems exist and have not yet been solved: (1) whether the chemical bonding between nanotubes and matrix exists or not and (2) do the nanotubes still maintain their extraordinary mechanical, electrical, and thermal properties if chemical bonding exist between nanotube and matrix? To enhance the mechanical properties of advanced composite materials, many works have to be deeply investigated and this is definitely a challenging area for all people working in the composites community [278].

Health and Environmental Impacts

The National Institute for Occupational Safety and Health (NIOSH) estimates that 42% of the US workforce is at a risk of dermal exposure to hazardous materials [329]. Carbon materials, for example graphite, causes skin diseases and respiratory infections, which have been reported in different literature [329,330]. There is a general concern that nanoscale particles may have negative health and environmental impacts [2,331,332]. Few studies have been published on the effects of inhaling free manufactured nanoparticles to date. Although nanometals are actually introduced into the body for disease detection, imaging, and treatment, there are concerns about the potential toxicity of such materials [333]. The exceptional properties of carbon nanoparticles may also lead to unique health hazards [334]. This is because the size of the nanomaterials is comparable to human cells and large proteins with the result that the regular human immune system may not work against them [2,335]. While nanoparticles may enter the body by inhalation, due to skin contact, or by ingestion, the major concern is by inhalation during processing and use and reuse of these ultrafine particles [336].

Humans continually come into contact with small particles, and they are generally not hurt by being exposed to these particles. However, inhalation of micron-sized quartz particles or of asbestos fibers has proven to be quite harmful to health [2,336–338]. Similarly, nanoparticles resulting from combustion processes such as forest fires or industrial pollution have a detrimental effect [336]. In addition, studies have been conducted to observe the pulmonary toxicity of nanosized particles in rats [339]. It has been found that toxicity is related to inhalation of nanoparticles, which can penetrate into deep lung tissue. It has been suggested that the surface properties such as

surface chemistry and the area of nanoparticles and free radical generation with cell interaction play a significant role in the increased toxicity of nanoparticles [340]. Thus, the small size of the particles and the coating on these particles are both important considerations [336].

The adverse effects of carbon nanotubes (CNT) exposed to human epidermal keratinocytes (HaCaT) were evaluated [329]. Moteiro-Riveria has recently shown that MWNTs can localize within and initiate an irritation response in a target epithelial cell (human epidermal keratinocytes) [341,342]. Shvedova et al. [329] observed exposure of HaCaT cells to CNT resulted in accelerated oxidative stress and a reduction of total antioxidant reserve and vitamin E. In addition they showed ultrastructural and morphological changes in cultured skin cells followed by carbon nanotube exposure.

Deposition of ultrafine titanium dioxide (TiO_2) particles from the sunscreens was observed in the human stratum corneum within hair follicle areas and deeper parts of the hair bulb and papilla [329,344]. There is some evidence indicating that nanoparticles of TiO_2 (used in some sun protection products) do not penetrate the skin but it is not clear whether the same conclusion holds for individuals whose skin have been damaged by sun or by common diseases such as eczema [2]. TiO_2 crystals (20–100 nm) were shown to be solely deposited on the outermost surface of the stratum corneum and were not detected in deeper stratum corneum layers of the human epidermis and dermis [329,345]. Chemically modified TiO_2 nanoparticles from over-the-counter sunscreen products have been shown to induce the formation of hydroxyl radicals and oxidative DNA damage [329]. Additionally, sunlight-illuminated TiO_2 was shown to cause catalyzed DNA damage in human cells [329,346].

Combustible nanoparticles may cause an increased risk of explosion as a function of their increased surface area [2]. There has been little discussion among researchers working on plastics about the toxicological aspects of these nanofillers even though polymer nanocomposites are being used in the auto industry [336]. Polymer–clay nanocomposites have been shown to possess flame-retardant properties. However, one needs to be aware of the possibility of nanosized particles being released into the atmosphere as a result of combustion and then being inhaled by humans [336]. For PNCs used in automobiles, this may happen during an accident when the vehicle may catch fire, and it may also happen at the end of the automobile's useful life, when the discarded PNC may end up in an incinerator as a waste fuel [336]. Agarwal et al. [336] studied PNCs containing different types of surface treated nanoclays and carbon nanofibers, and burned in a *Combustion DMS500 Differential Mobility Spectrometer*. The results showed an increase in the rate of particle emission with a decrease in particle size distribution. Though in terms of safety it was not very well understood, these features are not desirable!

Introduction of novel materials into industry requires safety evaluation as well as an understanding of the impact of the nanomaterials on the environment, and human health or other biological species [339,347]. This safety information has been carried out by industry and currently has not been widely published. Fiorito et al. [348] investigated highly purified carbon nanomaterials (SWNTs-C-nanotubes, C-fullerenes) and concluded that the highly purified carbon nanomaterials possess a very low toxicity against human macrophage cells. As the determination of toxicity of C-nanoparticles is quite complicated [348], more work is needed on all of the new carbon nanomaterials to adequately assess their toxicity and health risks [349]. Another concern is the need for caution when interpreting the data obtained using these highly complex bio/nanomaterial systems [349]. Hurt et al. [349] highlighted both short-term assays and subchronic exposures. It must be

conducted in well-characterized *in vitro* (macrophage and/or epithelial cell cultures) and *in vivo* (intratracheal or inhalation in rats, mice or hamsters) models and calibrated using validated negative and positive controls [331,349]. There is an ongoing debate among toxicologists, industry, and regulatory agencies about the utility of *in vitro* cellular toxicity assay versus sub-chronic animal testing in screening for potential adverse health effects of nanomaterials [349].

Hurt et al. [349] discussed the overall status and trends of toxicology of carbon related nanomaterials. They mentioned that instead of supporting either extreme viewpoint – that nanomaterials pose no health risks, or that nanotechnology presents extreme risks that warrant cessation of development activities, it is better to continue research on toxicity and safety with a wide range of new material formulations [349]. A worthy goal for toxicologists and materials scientists is the joint development of 'green' nanomaterial formulations – those cooptimized for function and minimal health impact [349].

Future Outlook

The potential of nanocomposites in various sectors of research and application is promising and attracting increasing investment from Governments and business in many parts of the world [2]. While there are some niche applications where nanotechnology has penetrated the market, the major impact will be at least a decade away. Currently, there are a few cosmetic products made by incorporating nanoparticles on the market. To create such macroscale materials, many issues surrounding the incorporation of nanotubes into a matrix, strategies for property improvement, and the mechanisms responsible for those property improvements still remain critical. Since only a moderate success has been made over the last 20 years, researchers must continue to investigate strategies to optimize the fabrication of nanotube-enabled materials to achieve both improved mechanical and transport properties [278].

Biodegradable polymer-based nanocomposites have a great deal of future promise for potential applications as high-performance biodegradable materials. These are entirely new types of materials based on plant and nature materials (organoclay). When disposed of in compost, these are safely decomposed into CO_2, water, and humus through the activity of microorganisms. The CO_2 and water will become corn or sugarcane again through plant photosynthesis. Undoubtedly, their unique properties originating from the controlled nanostructure paves the way for a much broader range of applications (already commercially available through Unitika Ltd., Japan), and opens a new dimension for plastics and composites.

According to several sources (Chemical Business Newsbase, Plastic News), a significant increase in turnover of about 100%/year, leading to a value of about 1500 million Euro (ca. 500,000 ton/year of polymer nanocomposites) in 2009 is expected [350]. Even if these numbers are overly optimistic, they highlight the tremendous technological and economical potential associated with polymeric nanocomposites including not only clay but also other inorganic nanofillers, such as carbon nanotubes, SiO_2, SiC, and Si_3N_4. At present it is difficult to predict which, if any, market sector would not be able to benefit from this technology. Thus, it may well be that polymeric nanocomposites in the mid- and longer-term will pervade all aspects of life, similar to the way plastics did in the last century. Clearly a diverse range of sectors such as aerospace, automotive, packaging (particularly food but also solar cells), electrical and electronic goods, household goods

etc. will profit substantially from a new range of materials which would be offered by this technology. In the short term (<5 years), the commercial impact may include inkjet markets, nanoparticles in cosmetics, and automotive applications such as body moldings, engine covers and catalytic converts, batteries, computer chips [1]. In the mid-term (10 years), memory devices, biosensors for diagnostics, advances in lighting are all possible. The time-scale for automotive, aerospace, bio-nanotechnology is a long-term prospect (>15 years) as these are risk-averse sectors and thereby for large-scale production it is necessary to carry out strict testing and validation procedures [1].

ACKNOWLEDGMENTS

REFERENCES

1. RTO Lecture Series, EN-AVT-129, May 2005.
2. Nanoscience and Nanotechnologies, July 2004, The Royal Society & the Royal Academy of Engineering. (Reproduced in part with permission 2005.)
3. Oriakhi, C.O. (1998). Nano Sandwiches, *Chem. Br.*, **34**: 59–62.
4. Usuki, A., Kawasumi, M., Kojima, Y., Okada, A., Kurauchi, T. and Kamigaito, O.J. (1993). Swelling Behavior of Montmorillonite Cation Exchanged for V-amino Acids by E-caprolactam, *Mater. Res.*, **8**(5): 1174.
5. http://www.nano.gov/
6. Luo, J.J. and Daniel, I.M. (2003). Characterization and Modeling of Mechanical Behavior of Polymer/Clay Nanocomposites, *Compos. Sci. Technol.*, **63**(11): 1607–1616. (Reproduced in part with permission from Elsevier © 2006.)
7. Thostenson, E., Li, C. and Chou, T. (2005). Review Nanocomposites in Context, *Journal of Composites Science & Technology*, **65**: 491–516. (Reproduced in part with permission from Elsevier © 2006.)
8. Schmidt, D., Shah, D. and Giannelis, E.P. (2002). New Advances in Polymer/Layered Silicate Nanocomposites, *Current Opinion in Solid State and Materials Science*, **6**(3): 205–212.
9. Alexandre, M. and Dubois, P. (2000). Polymer-layered Silicate Nanocomposites: Preparation, Properties and Uses of a New Class of Materials, *Mater. Sci. Eng. Rep.*, **28**: 1–63. (Reproduced in part with permission from Elsevier © 2006.)
10. Park, C., Park, O., Lim, J. and Kim, H. (2001). The Fabrication of Syndiotactic Polystyrene/ Organophilic Clay Nanocomposites and Their Properties, *Polymer*, **42**: 7465–7475.
11. Gorga, R.E. and Cohen, R.E. (2004). Toughness Enhancements in Poly(methyl methacrylate) by Addition of Oriented Multiwall Carbon Nanotube, *J. Polym. Sci., Part B: Polym. Phys.*, **42**(14): 2690–2702.

12. Christopher, O.O. and Lerner, M. (2001). Nanocomposites and Intercalation Compound, *Encyclopedia of Physical Science and Technology*, Vol. 10, **3rd edn**. (Reproduced in part with permission from Elsevier © 2006.)

13. Mazumder, S.K. (ed.). (2002). *Composites Manufacturing, Materials, Product and Process Engineering*, CRC Taylor & Francis, ISBN 0-8493-0585-3.

14. Roy, S., Hussain, F., Lu, H. and Narasimhan, K. (2005). Characterization and Modeling of Strength Enhancement Mechanism in Polymer Clay Nanocomposites, In: *AIAA Conference Proceedings*, Texas.

15. Octeau, M.A., Yousefpour, A. and Hojjati, M. (2004). *Procedure Manual for using Resin Transfer Molding (RTM) Manufacturing Set-up*, August 2004, LM-AMTC-0025.

16. Fielding, J.C., Chen, C. and Borges, J. (2004). Vacuum Infusion Process for Nanomodified Aerospace Epoxy Resins, In: *SAMPE Symposium & Exhibition*, Long beach, CA.

17. Hussain F., Derrick, D., Haque, A. and Shamsuzzoha, A.M. (2005). S2 Glass/Vinyl Ester Polymer Nanocomposites: Manufacturing, Structures, Thermal and Mechanical Properties, *Journal of Advanced Materials*, **37**(1): 16–27.

18. Chen, J. and Tanguay, M. (2004). Autoclave Processing in the Aerospace Manufacturing Technology Center (AMTC), In: *Internal Technical Paper for, AMTC*, NRC (under reviewing).

19. Mahfuz, H., Baseer, M.A. and Zeelani, S. (2005). Fabrication, Characterization and Mechanical Properties of Nano Phased Carbon Prepag Laminates, In: *SAMPE Journal*, **41**(2).

20. Meyyappan, M. (ed.). (2004). *Carbon Nanotubes, Science and Application*, CRC. (Reproduced in part with permission from Taylor & Francis, USA © 2006.)

21. Giannelis, E.P. (1996). Polymer Layered Silicates Nanocomposites, *Adv. Mater.*, **8**: 29–35.

22. Reichert, P., Kressler, J., Thomann, R., Mulhaupt R. and Stoppelmann, G. (1998). Nanocomposites Based on a Synthetic Layer Silicate and Polyamide-12, *Acta Polymer*, **49**(2–3): 116–123.

23. Yano, K. and Usuki, A. (1993). Synthesis and Properties of Polyimide-Clay Hybrid, *J. Polym. Sci., Part A: Polym. Chem.*, **31**: 2493–2498.

24. Yano, K., Usuki, A., Okada, A. and Kurauchi, T. (1991). Synthesis and Properties of Polyimide-Clay Hybrid, *Polymer Prep. (Jpn)*, **32**(1): 65.

25. Park, J.H. and Jana, S. (2003). Mechanism of Exfoliation of Nanoclay Particles in Epoxy-Clay Nanocomposites, *Macromolecules*, **36**: 2758–2768. (Reproduced in part with permission from American Chemical Society © 2006.)

26. Chen, T.K., Tien, Y.I. and Wei, K.H. (1999). Synthesis and Characterization of Novel Segmented Polyurethane/Clay Nanocomposites via Poly (é-caprolactone)/Clay, *J. Polym. Sci., Part A: Poly. Chem.*, **37**(13): 2225–2233.

27. Scott, M.A., Carrado, K.A. and Dutta, P.K. (eds). (2004). *Hand Book of Layered Materials*. (Reproduced in part with permission from Taylor & Francis © 2006.)

28. Ray, S.S. and Okamoto, M. (2003). Polymer/layered Silicate Nanocomposite: A Review from Preparation to Processing, *Prog. Polymer Sci.*, **28**: 1539–1641. (Reproduced in part with permission from Elsevier © 2006.)

29. Shen, J.W., Chen, X.M. and Huang, W.Y. (2003). Structure and Electrical Properties of Grafted Polypropylene/Graphite Nanocomposites Prepared by Solution Intercalation, *J. App. Polym. Sci.*, **88**: 1864–1869.

30. Chung, D.D.L. (1984). Low-density Graphite-polymer Electrical Conductors, US Patent 04,704,231.

31. Chung, D.D.L. (1990). Composites of *In-situ* Exfoliated Graphite, US Patent, 4,946,892.

32. Wang, Y.S., O'Gurkis, M.A. and Lindt, J.T. (1986). Electrical Properties of Exfoliated-Graphite Filled Polyethylene Composites, *Polym. Compos.*, **7**(5): 349.

33. Foy, J.V. and Lindt, J.T. (1987). Electrical Properties of Exfoliated-Graphite Filled Polyester Based Composites, *Polym. Compos.*, **8**(6): 419.

34. Celzerd, A., McRae, E., Mareche, J.F., Furdin, G., Dufort M. and Deleuze, C. (1996). Composites Based on Micron-Sized Exfoliated Graphite Particle: Electrical Conduction, Critical Exponents, and Anisotropy, *J. Phy. Chem. Solids*, **57**(6–8): 715–718.

35. Kawasumi, M., Hasegawan, M., Usuki, A. and Okada, A. (1997). Preparation and Mechanical Properties of Polypropylene–Clay Hybrids, *Macromolecules*, **30**: 6333–6338.

36. Kornmann, X., Linderberg, H. and Bergund, L.A. (2001). Synthesis of Epoxy–Clay Nanocomposites: Influence of the Nature of the Clay on Structure, *Polymer*, **42**: 1303–1310.

37. Kornmann, X., Linderberg, H. and Bergund, L.A. (2001). Synthesis of Epoxy–Clay Nanocomposites: Influence of the Nature of the Curing Agent on Structure, *Polymer*, **42**: 4493–4499.

38. Becker, O., Cheng, Y.B., Varley, R.J. and Simon, G.P. (2003). Layered Silicate Nanocomposites Based on Various High-functionality Epoxy Resins: The Influence of Cure Temperature on Morphology, Mechanical Properties, and Free Volume, *Macromolecules*, **36**: 1616–1625.

39. Dennis, H.R., Hunter, D., Chang, D., Kim, S. and Paul, D.R. (2001). Effect of Melt Processing Condition on the Extent of Exfoliation in Organoclay-based Nanocomposites, *Polymer*, **42**: 9513–9522.

40. Okada, A. and Usuki, A. (1995). The Chemistry of Polymer-Clay Hybrids, *Mater. Sci. Eng.*, **C3**: 109–115.

41. Lan, T., Kaviratna, P.D. and Pinnavaia, T.J. (1995). Mechanism of Clay Tactoid Exfoliation in Epoxy–Clay Nanocomposites, *Chem. Mater.*, **7**(11): 2144–2150.

42. Lan, T. and Pinnavaia, T.J. (1994). On the Nature of Polyimide-Clay Hybrid Nanocomposites, *Chem. Mater.*, **6**(5): 573–575.

43. Lan, T. and Pinnavaia, T.J. (1994). Clay Reinforced Epoxy Nanocomposites, *Chem. Mater.*, **6**(12): 2216–2219.

44. Vaia, R.A., Jant, K.D., Kramer, E.J. and Giannelis E.P. (1996). Microstructural Evaluation of Melt-intercalated Polymer-Organically Modified Layered Silicate Nanocomposites, *Chem. Mater.*, **8**: 2628–2635.

45. Vaia, R.A., Ishii, H. and Giannelis, E.P. (1993). Synthesis and Properties of 2-dimensional Nanostructures by Direct Intercalation of Polymer Melts in Layered Silicates, *Chem. Mater.*, **5**: 1694–1696.

46. Lagaly, G. (1999). Introduction: from Clay Mineral-polymer Interactions to Clay Mineral-polymer Nanocomposites, *Applied Clay Sci.*, **15**: 1–9.

47. Chen, C., Cloos, L. and Rice, B.P. (2001). Carbon Fiber Composites: Part I, *SAMPE Journal*, **37**(5).

48. Pan, Y.X., Yu, Z., Ou, Y. and Hu, G. (2000). A New Process of Fabricating Electrically Conducting Nylon 6/Graphite Nanocomposites Via Intercalation Polymerization, *J. Polym. Sci., Part B: Polym. Phy.*, **38**: 1626–1633. (Reproduced in part with permission from John Wiley & Sons © 2006.)

49. Findeissen, B. and Thomasius, M. East Germany Patent DD 150739,1981.

50. Yasmin, A., Luo, J. and Daniel, I.M. (2006). Processing of Expanded Graphite Reinforced Polymer Nanocomposites, *Composites Science and Technology*, **66**(9): 1182–1189.

51. Cao, N., Shen, W., Wen, S. and Liu, Y. (1995). *New Carbon Mater.*, **4**: 51.

52. Liu, Z. and Shen, W. (1996). *New Carbon Mater.*, **11**: 34.

53. Chung, D.D.L. (1987). Exfoliation of Graphite, *J. Mater. Sci.*, **22**: 4190–4198.

54. Zhou, Q., Cao, N. and Li, Y. (1996). *New Carbon Mater.*, **11**: 42.

55. Kotov, N.A., Dekany, I. and Fendler, J.H. (1996). *Adv. Mater.*, **8**: 637.

56. Rehab, A. and Salahuddin, N. (2005). Nanocomposite Materials Based on Polyurethane Intercalated into Montmorillonite Clay, *Materials Science and Engineering A*, **399**: 368–376.

57. Beron, L., Wang, Z. and Pinnavia, T.J. (1999). Polymer-layered Silicate Nanocomposites: An Overview, *Applied Clay Science*, **15**: 11–29.

58. Halvatty, V. and Oya, A. (1994). Intercalation of Methacrylamide into Sodium, Calcium and Alkylammonium Exchanged Montmorillonites, *Appl. Clay Sci.*, **9**: 199–210.

59. Hussain, F., Dean, D. and Haque, A. (2002). Structures and Characterization of Organoclay-Epoxy-Vinyl ester Nanocomposite, *ASME International Mechanical Engineering Congress and Exposition*, IMECE 2002-33552, LA, USA.

60. Messermith, P.B. and Giannelis, E.P. (1994). Synthesis and Characterization of Layered Silicate Epoxy Nanocomposites, *Chem. Mater.*, **6**: 1719–1725.

61. http://www.nanocor.com

62. Lee, D.C. and Jang, L.W. (1998). Characterization of Epoxy–Clay Hybrid Composite Prepared by Emulsion Polymerization, *J. Applied Polymer Sci.*, **68**(12): 1997–2005.

63. Burnside, S.D. and Giannelis, E.P. (1995). Synthesis and Properties of New Poly(dimethylsiloxane) Nanocomposites, *Chem. Mater.*, **67**.

64. He, F. (1990). *New Carbon Mater.*, **4**(12).

65. Pan, Y.X., Yu, Z.Z., Qu, Y.C. and Hu, G.H. (2000). A New Process of Fabricating Electrically Conducting Nylon 6/Graphite Nanocomposites via Intercalation Polymerization, *J. Polym. Sci., Part B: Polym. Phys.*, **38**: 1626.

66. Chen, G., Wu, C. and Weng, W. (2003). Preparation of Polystyrene/Graphite Nanosheet Composite, *Polymer*, **44**: 1781–1784.

67. Chin, I.J., Thurn, A. T., Kim, H.C., Russel, T.P. and Wang, J. (2001). On Exfoliation of Montmorillonite in Epoxy, *Polymer*, **42**: 5947–5952.

68. Dean, D., Walker, R., Theodore, M., Hampton, E. and Nyairo, E. (2005). Chemorheology and Properties of Epoxy/Layered Silicate Nanocomposites, *Polymer*, **46**: 3014–3021. (Reproduced in part with permission from Elsevier © 2006.)

69. Ke, Y., Lu, J., Yi, A., Zhao, J., Qi, Z. (2000). The Effects of Promoter and Curing Process on Exfoliation Behavior of Epoxy/Clay Nanocomposites, *J. of Applied Polymer Science*, **78**(4): 808–815.

70. Wu, C.L., Zhang, M.Q., Rong, M.Z. and Friedrich, K. (2002). Tensile Performance Improvement of Low Nanoparticles Filled-Polypropylene Composites, *Comp. Sci. Tech.*, **62**: 1327.

71. Van, Vlack, L.H. (1964). *In Physical Ceramics for Engineers*, Addison Wesley, New York.

72. Jiankun, L., Yucai, K., Zongneng, Q. and Xiao, Su Y. (2001). Study on Intercalation and Exfoliation Behavior of Organoclays in Epoxy Resin, *J. Polym. Sci., Part B: Polym. Phys.*, **39**: 115–120.

73. Vaia, R.A. and Ginannelis, E.P. (1995). Kinetics of Polymer Melt Intercalation, *Macromolecules*, **28**: 8080.

74. Krisnamoorti, R. and Giannelis, E.P. (1997). Rheology of End-tethered Polymer Layered Silicate Nanocomposites, *Macromolecules*, **30**: 4097–4102.

75. Tolle, T.B. and Anderson, D.P. (2002). Morphology Development in Layered Silicate Thermoset Nanocomposites, *Compos. Sci. Tech.*, **62**: 1033–1041.

76. Brown, J.M., Curliss, D. and Vaia, R.A. (2000). Thermoset-layered Silicate Nanocomposites. Quaternary Ammonium Montmorillonite with Primary Diamine Cured Epoxies, *Chem. Mater.*, **12**: 3376

77. Pinnavaia, T.J. and Beall, G.W. (2001). *Polymer-Clay Nanocomposites*, John Wiley & Sons, USA, ISBN 0471637009.

78. Wang, Q., Song, C. and Lin, W. (2003). Study of the Exfoliation Process of Epoxy–Clay Nanocomposites by Different Curing Agents, *Journal of Applied Polymer Science*, **90**: 511–517.

79. Bension, T. and Anderson, D.P. (2004). The Role of Preconditioning on Morphology Development in Layered Silicate Thermoset Nanocomposites, *Journal of Applied Polymer Science*, **91**: 89–100.

80. Jun, H., Liang, G., Ma, X.Y. and Zhang, B.Y. (2004). Epoxy/Clay Nanocomposites: Further Exfoliation of Newly Modified Clay Induced by Shearing Force of Ball Milling, *Polymer Int.*, 53.

81. Salahuddin, N., Moet, A., Hilter, A. and Baer, E. (2002). Nanoscale Highly Filled Epoxy Nanocomposite, *Eur. Polym. J.*, **38**: 1477–1482.

82. Ahn, K.H., Kim, D.H. and Park, U. (2002). *ANTEC*, 1457.

83. Hasegawa, N., Kawasumi, M., Kato, M., Usuki, A. and Okada, A. (1998). Preparation and Mechanical Properties of Polypropylene–Clay Hybrids Using a Maleic Anhydride-Modified Polypropylene Oligomer, *Journal of Applied Polymer Science*, **67**(1): 87–92.

84. Kato, M., Usuki, A. and Okada, A. (1997). Synthesis of Polypropylene Oligomer–Clay Intercalation Compounds, *J. of Applied Polymer Science*, **66**(9): 1781–1785.

85. Hasegawa, N., Okamato, H., Kato, M. and Usuki, A. (2000). Preparation and Mechanical Properties of Polypropylene–Clay Hybrids Based on Modified Polypropylene and Organophilic Clay, *Journal of Applied Polymer Science*, **78**: 1918.

86. Ray, S.S., Yamada, K., Okamoto, M., Fujimoto, Y., Ogami, A. and Ueda, K. (2003). New Polylactide/Layered Silicate Nanocomposites. 5. Designing of Materials with Desired Properties, *Polymer*, **44**: 6631–6646.

87. Du, X.S., Xiao, M. and Meng, Y.Z. (2004). Synthesis and Characterization of Polyaniline/ Graphite Conducting Nanocomposites, *J. Polym. Sci., Part B: Polym. Phys.*, **42**: 1972–1978.

88. Chen, G.H., Wu, D.J. and Weng, W.G. (2001). Preparation of Polymer/Graphite conducting Nanocomposite by Intercalation Polymerization, *Journal of Applied Polymer Science*, **82**: 2506–2513.

89. Shioyama, H. (1997). Polymerization of Isoprene and Styrene in the Interlayer Spacing of Graphite, *Carbon*, **35**: 1664.

90. Fukushima, H. and Drazal, L.T. (2003). Graphite Nanocomposites: Structural & Electrical Properties, In: *Proceedings of the 14th International Conference on Composite Materials* (ICCM-14), San Diego, CA.

91. Cho, D., Lee, S., Yang, G., Fukushima, H. and Drzal, L.T. (2005). Dynamic Mechanical and Thermal Properties of Phenylethynyl-Terminated Polyimide Composites Reinforced With Expanded Graphite Nanoplatelets, *Macromol. Mater. Eng.*, **290**(3): 179–187.

92. Li, J., Kim, J.K. and Sham, M.L. (2005). Conductive Graphite Nanoplatelet/Epoxy Nanocomposites: Effects of Exfoliation and UV/ozone Treatment of Graphite, *Scripta Materialia*, **53**: 235–240.

93. Weng, W., Chen, G.H., Wu, D., Chen X., Lu, J., and Wang, P. (2004). Fabrication and Characterization of Nylon 6/Foliated Graphite Electrically Conducting Nanocomposite, *J. Polym. Sci., Part B: Polym. Phys.*, **42**: 2844–2856.

94. Private Communication with Professor G. Chen, Dept of Materials Science & Engineering, Huaqiao University, China.

95. Odegard, G.M. and Gates, T.S. (2006). Modeling and Testing of the Viscoelastic Properties of a Graphite Nanoplatelet/Epoxy Composite, *Journal of Intelligent Material Systems and Structures*, **17**(3): 239–246.

96. Kozima, Y., Usuki, A., Kawasumi, M., Okada, A., Fukushima, Y., Kurauchi, T. and Kamigaito, O.J. (1993). Mechanical Properties of Nylon-6 Clay Hybrid, *Journal of Material Research.*, **8**: 1185–1189.

97. Haque, A., Hussain, F., Derrick, D., Shamsuzzoha (2003). S2 Glass/Epoxy Polymer Nanocomposites: Manufacturing, Structures, Thermal and Mechanical Properties, *Journal of Composites Materials*, **37**(20): 1821–1837.

98. Xu, W.B., Bao, S.P. and He, P.S. (2002). Intercalation and Exfolation Behavior of Epoxy Resin/Curing Agent/Montmorillonite Nanocomposite, *Journal of Applied Polymer Science*, **84**: 842.

99. Hsieh, A.J. (2001). Ballistic Impact Measurements of Polycarbonate Layered Silicate Nanocomposites, *ANTEC*.

100. Koo, J. and Pilato, L. March/April (2005). Polymer Nanostructured Materials for High Temperature Applications, *SAMPE Journal*, **41**(2).

101. Chowdhury, F.H., Hosur, M.V. and Jeelani, S. (2006). Studies on the Flexural and Thermomechanical Properties of Woven Carbon/Nanoclay-Epoxy Laminates, *Materials Science and Engineering A*, **421**: 298–306.

102. Roy, S., Hussain, F., Vengadassalam, K., Lu, H. (2006). Manufacturing, Mechanical Characterization, and Modeling of a Pultruded Thermoplastic Nanocomposite, in

Nanoengineering of Structural, Functional, and Smart Materials, Schulz, M.J., Kelker, A.D. and Sunderasen, M.J. (ed.), **1st edn**., CRC Taylor & Francis, USA, ISBN 0849316537; Chapter 17.

103. Dennis, H.R., Hunter, D.L., Chang, D., Kim, S. and Cho, J.W. (2000). *ANTEC Tech Paper*, **40**: 428.

104. Vaia, R.A., Sauer, B.B., Oliver, K.T. and Giannelis, E.P. (1997). Relaxations of Confined Chains in Polymer Nanocomposites: Glass Transition Properties of Poly(ethylene oxide) Intercalated in Montmorillonite, *J. Polym. Sci., Part B: Polym. Phys.*, **35**: 59–67.

105. Gao, F. (2004). Clay/Polymer Composites: the Story, *Materials Today*, **7**(11): 50–55. (Reproduced in part with permission from Elsevier © 2006.)

106. Auto Applications of Drive Commercialization of Nanocomposites, Plastic Additives and Compounding (January 2002), 30.

107. Cox, H., et al. (September 2004). Nanocomposite Systems for Automotive Applications, In: *Presented at 4th World Congress in Nanocomposites*, EMC, San Francisco, 1–3 September 2004.

108. Patterson, F. (September 2004). Nanocomposites – Our Revolutionary Breakthrough, In: *Presented at 4th World Congress in Nanocomposites*, EMC, San Francisco, 1–3 September 2004.

109. Through the Courtesy of M. Verbrugge, General Motors.

110. Ogawa, M. and Koroda, K. (1997). *Bull. Chem. Soc.*, Jpn. **70**: 2593–2618.

111. Gliman, J.W., Kashiwgi, T. and Lichtenhan, J.D. (1997). *SAMPE Journal*, **33**: 40.

112. *Transparent Nanocomposites for Aerospace Applications*, Advanced Composites Bulletin, Feb 2004.

113. Timmerman, J., Hayes, B. and Seferis, J. (2002). Nanoclay Reinforcement Effects on the Cryogenic Micro Cracking of Carbon Fiber/Epoxy Composites, *Composites Science and Technology*, **62**: 1249–1258.

114. Bellermare, S.C. and Bureau, M.N. (2004). *Polymer Composites*, **25**(4).

115. Mallick, P.K. and Zhou, Y.X. (2003). Yield and Fatigue Behavior of Polypropylene and Polyamide-6 Nanocomposites, *Journal of Materials Science*, **38**(5): 3183–3190.

116. Juwono, A. and Graham, E. (2005). Fatigue Performance of Clay-Epoxy Nanocomposites, *International Journal of Nanoscience*, **4**(4): 501–507.

117. Ivankovic, M., Brnardic, I., Ivankovic, H. and Mencer, H.J. (2006). DSC Study of the Cure Kinetics During Nanocomposite Formation: Epoxy/Poly(oxypropylene) Diamine/Organically Modified Montmorillonite System, *Journal of Applied Polymer Science*, **99**: 550–557.

118. Bao, S., Shen, S., Liang, G., Zhai, H., Xu, W. and He, P. (2004). Curing Behavior of Epoxy Resin/Tung Oil Anhydride Exfoliated Nanocomposite by Differential Scanning Calorimetry, *J. of Applied Polymer Science*, **92**: 3822–3829.

119. Gu, A. and Liang, G. (2003). Thermal Degradation Behaviour and Kinetic Analysis of Epoxy/ Montmorillonite Nanocomposites, *Polymer Degradation and Stability*, **80**: 383–391.

120. Hu, Y.H., Chen, C.Y. and Wang, C.C. (2004). Viscoelastic Properties and Thermal Degradation Kinetics of Silica/PMMA Nanocomposites, *Polymer Degradation and Stability*, **84**(3): 545–553.

121. Gong, F., Feng, M., Zhao, C., Zhang, S. and Yang, M. (2003). Thermal Properties of Poly (Vinyl Chloride)/Montmorillonite Nanocomposites, *Polymer Degradation and Stability*, **84**(2): 289–294.

122. Hussain, M., Varley, R.J., Mathys, Z., Cheng, Y.B. and Simon, G.P. (2004). Effect of Organo-phosphorus and Nano-clay Materials on the Thermal and Fire Performance of Epoxy Resins, *Journal of Applied Polymer Science*, **91**(2): 1233–1253.

123. Chen, J.S., Christopher K.O., Weisner, U. and Giannelis, E. (2002). Study of the Interlayer Expansion Mechanism and Thermal-Mechanical Properties of Surface-initiated Epoxy Nanocomposites, *Polymer Science*, **43**: 4895–4904.

124. Tang, Y. (2003). Preparation and Thermal Stability of Polypropylene/Montmorillonite Nanocomposites, *Polymer Degradation and Stability*, **82**(1): 127–131.

125. Mehrabzadeh, M. and Kamal, M.R. (2004). Melt Processing of PA-66/Clay, HDPE/Clay and HDPE/PA-66/Clay Nanocomposites, *Polymer Engineering and Science*, **44**(6): 1152–1161.

126. Butzloff, P., D'Souza, N.A., Golden, T.D. and Garrett, D. (2001). Epoxy + Montmorillonite Nanocomposite: Effect of Composition on Reaction Kinetics, *Polymer Engineering and Science*, **41**(10): 1794–1802.

127. Zhang, M. and Sundararaj, U. (2006). Thermal, Rheological, and Mechanical Behaviors of LLDPE/PEMA/Clay Nanocomposites: Effect of Interaction Between Polymer, Compatibilizer, and Nanofiller, *Macromolecular Materials and Engineering*, **291**(6), 697–706.

128. Hussain, F., Chen, J. and Hojjati, M. (2006). Cure Monitoring and Characterization of Aerospace Epoxy Nanocomposites, *J. of Material Science & Engineering: A* (under reviewing).

129. Chen, D. and He, P. (2004). Monitoring the Curing Process of Epoxy Resin Nanocomposites Based on Organo-montmorillonite – A New Application of Resin Curemeter, *Composites Science and Technology*, **64**: 2501–2507.

130. Xu, L. and Lee, J. (2005). Kinetic Analysis and Mechanical Properties of Nanoclay Reinforced Unsaturated Polyester (UP) Resins Cured at Low Temperatures, *J. Polymer Engineering and Science*, **45**(4): 496–509

131. Xu, B.W., Zhou, Z.F., He, P.S., Pan, W.P. (2004). Cure Behavior of Epoxy Resin/MMT/ DETA Nanocomposite, *Journal of Thermal Analysis and Calorimetry*, **78**: 113–124.

132. Okamoto, M., Nam, P.H., Maiti, M., Kotaka, T., Nakayama, T., Takada, M., Ohshima, M., Usuki, A., Hasegawa, N. and Okamoto, H. (2001). Biaxial Flow-induced Alignment of Silicate Layers in Polypropylene/Clay Nanocomposite Foam, *Nano Lett.*, **1**: 503.

133. Fujimoto, Y., Ray, S.S., Okamoto, M., Ogami, A., Yamada, K. and Ueda, K. (2003). Well-Controlled Biodegradable Nanocomposite Foams: From Microcellular to Nanocellular, *Macromol. Rapid Commun.*, **24**: 457–461.

134. Nam, P.H., Okamoto, M., Maiti, P., Kotaka, T., Nakayama, T., Takada, M., Ohshima, M., Hasegawa, N. and Usuki, A. (2002). Foam Processing and Cellular Structure of Polypropylene/ Clay Nanocomposites, *Polym. Eng. Sci.*, **42**(9): 1907.

135. Mitsunaga, M., Ito Y., Okamoto, M., Ray, S. and Hironaka, K. (2003). Intercalated Polycarbonate/Clay Nanocomposites: Nanostructure Control and Foam Processing, *Macromol. Mater. Eng.*, **288**: 543.

136. Klempner, D. and Frisch, K.C. (1991). *Handbook of Polymeric Foams and Foam Technology*, Hanser Publishers, Munich, Vienna.

137. Ray, S. and Okamoto, M. (2003). Biodegradable Polylactide/Layered Silicate Nanocomposites: Opening a New Dimension for Plastics and Composites, *Macromol. Rapid Commun.*, **24**: 814–840.

138. Mohanty, A.K., Drazal, L.T. and Misra, M. (2003). Nano Reinforcements of Bio-based polymers—The Hope and the Reality, *Polym. Mater. Sci. Engg.*, **88**: 60.

139. Tetto, J.A., Steeves, D.M., Welsh, E.A. and Powell, B.E. (1999). *ANTEC*, 1628.

140. Lee, S.R., Park, H.M., Lim, H.L., Kang, T., Li, X., Cho, W.J. and Ha, C.S. (2002). Microstructures, Tensile Properties and Biodegradability of Aliphatic Polyester/Clay Nanocomposites, *Polymer*, **43**: 2495.

141. Ray, S.S., Yamada, K., Okamoto M. and Ueda, K. (2002). Polylactide-layered Silicate Nanocomposite: A Novel Biodegradable Material, *Nano Lett.*, **2**: 1093.

142. Liu, J.W., Zhao Q. and Wan, C.X. (2001). *Space Medicine and Medical Eng.*, **14**: 308.

143. Ray, S.S., Yamada, K., Okamoto, M. and Ueda, K. (2003). New Polylactide-layered Silicate Nanocomposites. II. Concurrent Improvements of Material Properties, Biodegradability and Melt Rheology, *Polymer*, **44**: 857.

144. Okamoto, K., Ray, S. and Okamoto, M. (2003). New Polyl(butylene succinate)/Layered Silicate Nanocomposites. II. Effect of Organically Modified Layered Silicates on Structure, Properties, Melt Rheology, and Biodegradability, *J. Polym. Sci., Part B: Polym. Phys.*, **41**: 3160.

145. Celzard, A., Furdin, G., Mareche, J. and McRae, E. (1994). Anisotropic Percolation in an Epoxy-Graphite Disc Composite, *Solid State Commun.*, **92**: 377.

146. Kalaitzidou, K., Fukushima, H. and Drazal, L. (2003). Graphite Nanoplatelets as Nano-reinforcements for Polymers: Comparison between a Thermoset and a thermoplastic matrix,

In: *Proceedings of the 14th International Conference on Composite Materials* (ICCM-14), San Diego, Paper no. 1751.

147. Dillon, D.R., Tenneti, K.K., Li, C.Y., Ko, F.K., Sics, I. and Hsiao, B.S. (2006). On the Structure and Morphology of Polyvinylidene Fluoride–Nanoclay Nanocomposites, *Polymer*, **47**: 1678–1688.

148. Pinnavaia, T.J., Lan, T., Wang, Z., Shi, H. and Kaviratna, P.D. (1996). *ACS Symp Ser.*, **622**: 250.

149. Wang, Z. and Pinnavaia, T.J. (1998). Nanolayer Reinforcement of Elastomeric Polyurethane, *Chem. Mater.*, **10**: 3769–3771.

150. Yao, K.J., Song, M., Hourston, D.J. and Luo, D.Z. (2002). Polymer/Layered Clay Nanocomposites: Polyurethane Nanocomposites, *Polymer*, **43**: 1017–1020.

151. Chenggang, C. and David, C. (2003). Processing and Morphological Development of Montmorillonite Epoxy Nanocomposites, *Nanotechnology*, **14**: 643–648.

152. Sheng, N., Boyce, M.C., Parks, D.M., Rutledge, G.C., Abes, J.I. and Cohen, R.E. (2004). Multiscale Micromechanical Modeling of Polymer/Clay Nanocomposites and the Effective Clay Particle, *Polymer*, **45**: 487.

153. Okamoto, M. (2003). Polymer/Layered Silicate Nanocomposites, Rapra Review Report No 163, Rapra Technology Ltd., London, p. 166.

154. Sato, H., Yamagishi, A. and Kawamura, K. (2001). Molecular Simulation for Flexibility of a Single Clay Layer, *J. Phys. Chem., B.*, **105**: 7990–7997.

155. Seo, Y.S., Ichikawa, Y. and Kawamura, K. (1999). *Mater. Sci. Res. Int.*, **5**: 13.

156. Tamura, K., Setsuda, H., Taniguchi M. and Yamagishi, A. (1999). Application of the Langmuir-Blodgett Technique to Prepare a Clay-Metal Complex Hybrid Film, *Langmuir*, **15**: 6915.

157. Kojima, Y., Usuki, A., Kawasumi, M., Okada, A., Kurauchi, T., Kamigaito, O. and Kaji, K. (1995). *J. Polym. Sci. Part B: Polym. Phys.*, **33**: 1039.

158. Yalcin, B. and Cakmak, M. (2004). Superstructural Hierarchy Developed in Coupled High Shear/High Thermal Gradient Conditions of Injection Molding in Nylon 6 Nanocomposites, *Polymer*, **45**: 2691.

159. Bafna, A., Beaucage, G., Mirabella, F. and Mehta, S. (2003). 3D Hierarchical Orientation in Polymer–Clay Nanocomposite Films, *Polymer*, **44**: 1103.

160. Roe, R. (2000). *Methods of X-ray and Neutron Scattering in Polymer Science*, Oxford University Press, New York, p. 199.

161. Bafna, A., Beaucage, G., Mirabella, F., Skillas, G. and Sukumaran, S. (2001). Optical Properties and Orientation in Polyethylene Blown Films, *J. Polym. Sci., Part B: Polym. Phys.*, **39**: 2923.

162. Ginzburg, V.V. and Balazs, A.C. (1999). Calculating Phase Diagrams of Polymer-Platelet Mixtures Using Density Functional Theory: Implications for Polymer/Clay Composites, *Macromolecules*, **32**: 5681.

163. Ginzburg, V.V., Singh, C. and Balazs, A.C. (2000). Theoretical Phase Diagrams of Polymer/Clay Composites: The Role of Grafted Organic Modifiers, *Macromolecules*, **33**: 1089.

164. Ginzburg, V.V. and Balazs, A.C. (2000). Calculating Phase Diagrams for Nanocomposites: The Effect of Adding End-Functionalized Chains to Polymer/Clay Mixtures, *Adv. Mater.*, **12**: 1805.

165. Ginzburg,V.V., Gendelman, O.V. and Manevitch, L.I. (2001). Simple ''Kink'' Model of Melt Intercalation in Polymer-clay Nanocomposites, *Phys. Rev. Lett.*, **86**: 5073–5075.

166. Totha, R., Coslanicha, A., Ferronea, M., Fermeglia, M., Pricl, S., Miertus, S. and Chiellini, E. (2004). Computer Simulation of Polypropylene/organoclay Nanocomposites: Characterization of Atomic Scale Structure and Prediction of Binding Energy, *Polymer*, **45**: 8075.

167. Sinsawat, A., Anderson, K.L., Vaia, R.A. and Farmer, B.L. (2003). Influence of Polymer Matrix Composition and Architecture on Polymer Nanocomposite Formation: Coarse-Grained Molecular Dynamics Simulation, *J. Polym. Sci., Part B: Polym. Phys.*, **41**: 3272.

168. Kuppa, V., Menakanit, S., Krishnamoorti, R. and Manias, E. (2003). Simulation Insights on the Structure of Nanoscopically Confined Poly(ethylene oxide), *J. Polym. Sci., Part B: Polym. Phys.*, **41**: 3285.

169. Zeng, Q.H., Yu, A.B., Lu, G.Q. and Standish, R.K. (2003). Molecular Dynamics Simulation of Organic-Inorganic Nanocomposites: Layering Behavior and Interlayer Structure of Organoclays, *Chem. Mater.*, **15**: 4732.

170. Sheng, N., Boyce, M.C., Parks, D.M., Rutledge, G.C., Abes, J.I. and Cohen, R.E. (2004). Multiscale Micromechanical Modeling of Polymer/Clay Nanocomposites and the Effective Clay Particle, *Polymer*, **45**: 487.

171. Iijima, S. (1991). Helical Microtubules of Graphitic Carbon, *Nature*, London, United Kingdom, **354**(6348): 56.

172. Iijima, S. and Ichihashi, T. (1993). Single-shell Carbon Nanotubes of 1-nm Diameter, *Nature*, London, United Kingdom, **363**(6430): 603–605.

173. Bower, C., Rosen, R., Jin, L., Han, J., Zhou, O. (1999). Deformation of Carbon Nanotubes in Nanotube-polymer Composites, *Applied Physics Letters*, **74**(22): 3317–3319.

174. Cooper, C.A., Ravich, D., Lips, D., Mayer, J. and Wagner, H.D. (2002). Distribution and Alignment of Carbon Nanotubes and Nanofibrils in a Polymer Matrix, *Composites Science and Technology*, **62**(7–8): 1105–1112.

175. Haggenmueller, R., Gommans, H.H., Rinzler, A.G., Fischer, J.E. and Winey, K.I. (2000). Aligned Single-wall Carbon Nanotubes in Composites by Melt Processing Methods, *Chemical Physics Letters*, **330**(3–4): 219–225.

176. Jin, L., Bower, C. and Zhou, O. (1998). Alignment of Carbon Nanotubes in a Polymer Matrix by Mechanical Stretching, *Applied Physics Letters*, **73**(9): 1197–1199.

177. Jin, Z., Pramoda, K.P., Xu, G. and Goh, S.H. (2001). Dynamic Mechanical Behavior of Melt-processed Multi-walled Carbon Nanotube/Poly (Methyl Methacrylate) Composites, *Chemical Physics Letters*, **337**(1–3): 43–47.

178. Kearns, J.C. and Shambaugh, R.L. (2002). Polypropylene Fibers Reinforced with Carbon Nanotubes, *Journal of Applied Polymer Science*, **86**(8): 2079–2084.

179. Lozano, K. and Barrera, E.V. (2001). Nanofiber-reinforced Thermoplastic Composites. Thermo Analytical and Mechanical Analyses, *Journal of Applied Polymer Science*, **79**(1): 125–133.

180. Potschke, P., Fornes, T.D. and Paul, D.R. (2002). Rheological Behavior of Multiwalled Carbon Nanotube/Polycarbonate Composites, *Polymer*, **43**(11): 3247–3255.

181. Safadi, B., Andrews, R. and Grulke, E.A. (2002). Multiwalled Carbon Nanotube Polymer Composites: Synthesis and Characterization of Thin Films, *Journal of Applied Polymer Science*, **84**(14): 2660–2669.

182. Schadler, L.S., Giannaris, S.C. and Ajayan, P.M. (1998). Load Transfer in Carbon Nanotube Epoxy Composites, *Applied Physics Letters*, **73**(26): 3842–3844.

183. Lau, K.T. and Hui, D. (2002). The Revolutionary Creation of New Advanced Materials-carbon Nanotube Composites, *Composites Part B*, **33**: 263. (Reproduced in part with permission from Elsevier © 2006.)

184. Bethune, D.S., Klang, C.H., de Vries, M.S., Gorman, G., Savoy, R., Vazquez, J. and Beyers, R. (1993). Cobalt-catalysed Growth of Carbon Nanotubes with Single-Atomic-Layer Walls, *Nature*, **363**: 605–607.

185. Dresselhaus, M.S., Dresselhaus, G. and Eklund P.C. (ed.). (1996). *Science of Fullerences and Carbon Nanotubes*, Academic Press: London.

186. Dresselhaus, M.S., et al. (2004). Electronic, Thermal and Mechanical Properties of Carbon Nanotubes, *Philosophy Transactions of the Royal Society of London A*, **362**(1098): 2065–2098.

187. Harris, P.J.F. (1999). *Carbon Nanotubes and Related Structures*, Cambridge University Press: Cambridge, UK.

188. Treacy, M.M.J., Ebbesen, T.W. and Gibson, J.M. (1996). Exceptionally High Young's Modulus Observed for Individual Carbon Nanotubes, *Nature*, **381**(6584): 678–680.

189. Lourie, O., Cox, D.M. and Wagner, H.D. (1998). Buckling and Collapse of Embedded Carbon Nanotubes, *Physical Review Letters*, **81**(8): 1638–1641.

190. Krishnan, A., Dujardin, E., Ebbesen, T.W., Yianilos, P.N. and Treacy, M.M.J. (1998). Young's Modulus of Single-walled Nanotubes, *Physical Review B*, **58**(20): 14013–14019.

191. Salvetat, J.P., Andrew, G., Briggs, D., Bonard, J.M., Bacsa, R.R., Kulik, A.J., Stöckli, T., Burnham, N.A. and Forró, L. (1999). Elastic and Shear Moduli of Single-walled Carbon Nanotube Ropes, *Physical Review Letters*, **82**(5): 944–947.

192. Walters, D.A., Ericson, L.M., Casavant, M.J., Liu, J., Colbert, D.T., Smith, K.A. and Smalley, R.E. (1999). Elastic Strain of Freely Suspended Single-wall carbon Nanotube Ropes, *Applied Physics Letters*, **74**(25): 3803–3805.

193. Li, F., Cheng, H.M., Bai, S. and Su, G. (2000). Tensile Strength of Single-walled Carbon Nanotubes Directly Measured from their Macroscopic Ropes, *Applied Physics Letters*, **77**(20): 3161–3163.

194. Pan, Z.W., Xie, S.S., Lu, L., Chang, B.H., Sun, L.F., Zhou, W.Y., Wang, G. and Zhang, D.L. (1999). Tensile Tests of Ropes of very Long Aligned Multiwall Carbon Nanotube, *Applied Physics Letters*, **74**(21): 3152–3154.

195. Lu, J.P. (1997). Elastic Properties of Single and Multilayered Nanotubes, *Journal of Physics and Chemistry of Solids*, **58**(11): 1649–1652.

196. Robertson, D.H., Brenner, D.W. and Mintmire, J.W. (1992). Energetics of Nanoscale Graphitic Tubules, *Physical Review B*, **45**(21): 12592–12595.

197. Yakobson, B.I., Brabec, C.J. and Bernholc, J. (1996). Nanomechanics of Carbon Tubes: Instabilities Beyond Linear Response, *Physical Review Letters*, **76**(14): 2511–2514.

198. Ebbesen, T.W., Lezec, H.J., Hiura, H., Bennett, J.W., Ghaemi, H.F. and Thio, T. (1996). Electrical Conductivity of Individual Carbon Nanotube, *Nature*, **382**(6586): 54–56.

199. Berber, S., Kwon, Y.K. and Tomanek, D. (2000). Unusually High Thermal Conductivity of Carbon Nanotubes, *Physical Review Letters*, **84**(20): 4613–4616.

200. Benedict, L.X., Crespi, V.H., Louie, S.G. and Cohen, M.L. (1995). Static Conductivity and Superconductivity of Carbon Nanotubes – Relations Between Tubes and Sheets, *Physical Review B*, **52**(20): 14935–14940.

201. Hone, J., Whitney, M., Piskoti, C. and Zettl, A. (1999). Thermal Conductivity of Single-walled Carbon Nanotubes, *Physical Review B*, **59**(4): R2514–R2516.

202. Liu, J., Fan, S. and Dai, H. (2004). *Recent Advances in Methods of Forming Carbon Nanotubes*, MRS Bulletin, April 2004: 244–250.

203. Thostenson, E.T., Ren, Z. and Chou, T.W. (2001). Advances in the Science and Technology of Carbon Nanotubes and their Composites: a Review, *Composites Science and Technology*, **61**(13): 1899–1912.

204. Schlittler, R.R., Seo, J.W., Gimzewski, J.K., Durkan, C., Saifullah, M.S.M. and Welland, M.E. (2001). Single Crystals of Single-walled Carbon Nanotubes formed by Self-assembly, *Science*, **292**(5519): 1136–1139.

205. Private communication with Professor Jean-Luc Meunier, Department of Chemical Engineering, McGill University, Montreal,Canada, May 2005/ Patent Application.

206. McGill Researchers Develop New Carbon Nanotube Production Method (2004). *Journal of Thermal Spray*, **13**(4): 489–490.

207. Li, H.J., Guan, L., Shi, Z. and Gu, Z. (2004). Direct Synthesis of High Purity Single-walled Carbon Nanotube Fibers by Arc Discharge, *Journal of Physical Chemistry B*, **108**(15): 4573–4575.

208. Li, Y.L., Kinloch, I.A. and Windle, A.H. (2004). Direct Spinning of Carbon Nanotube Fibers from Chemical Vapor Deposition Synthesis, *Science*, **304**(5668): 276–278.

209. Zhang, M., Atkinson, K.R. and Baughman, R.H. (2004). Multifunctional Carbon Nanotube Yarns by Downsizing an Ancient Technology, *Science*, **306**(5700): 1358–1361.

210. Ericson, L.M., Fan, H., Peng, H.Q., Davis, V.A., Zhou, W., Sulpizio, J., Wang, Y.H., Booker, R., Vavro, J., Guthy, C., Parra-Vasquez, A.N.G., Kim, M.J., Ramesh, S., Saini, R.K., Kittrell,

C., Lavin, G., Schmidt, H., Adams, W.W., Billups, W.E., Pasquali, M., Hwang, W.F., Hauge, R.H., Fischer, J.E. and Smalley, R.E. (2004). Macroscopic, Neat, Single-walled Carbon Nanotube Fiber, *Science*, **305**(5689): 1447–1450.

211. Zhou, W., Vavro, J., Guthy, C., Winey, K.I., Fischer, J.E., Ericson, L.M., Ramesh, S., Saini, R., Davis, V.A., Kittrell, C., Pasquali, M., Hauge, R.H. and Smalley, R.E. (2004). Single Wall Carbon Nanotube Fibers Extruded from Super-acid Suspensions: Preferred Orientation, Electrical, and Thermal Transport, *Journal of Applied Physics*, **95**(2): 649–655.

212. Sennett, M., Welsh, E., Wright, J.B., Li, W.Z., Wen, J.G. and Ren, J.F. (2003). Dispersion and Alignment of Carbon Nanotubes in Polycarbonate, *Applied Physics A: Materials Science & Processing*, **76**(1): 111–113.

213. Andrews, R. and Weisenberger, M.C. (2004). Carbon Nanotube Polymer Composites, *Current Opinion In Solid State & Materials Science*, **8**(1): 31–37.

214. Dondero, W.E. and Gorga, R.E. (2006). Morphological and Mechanical Properties of Carbon Nanotube/Polymer Composites via Melt Compounding, *J. Polym. Sci., Part B: Polym. Phys.*, **44**(5): 864–878.

215. Shaffer, M.S.P. and Windle, A.H. (1999). Analogies between Polymer Solutions and Carbon Nanotube Dispersions, *Macromolecules*, **32**: 6864–6866.

216. Gong, X., Liu, J. and Baskaran, S. (2000). Surfactant Assisted Processing of Carbon Nanotube/Polymer Composites, *Chem of Materials*, **12**(4): 1049–1052.

217. Jin, L. and Bower, C. (1998). Alignment of Carbon Nanotubes in a Polymer Matrix by Mechanical Stretching, *Applied Physics Letters*, **73**(9): 1197–1199.

218. Ajayan P.M., Stephan, O., Colliex, C. and Trauth, D. (1994). Aligned Carbon Nanotube Arrays Formed by Cutting a Polymer Resin Nanotube Composite, *Science*, **265**(5176): 1212–1214.

219. Chen, J., Hamon, M.A., Hu, H., Chen, Y., Rao, A.M., Eklund, P.C. and Haddon, R.C. (1998). Solution Properties of Single-walled Carbon Nanotubes, *Science*, **28**2: 95–98.

220. Mitchell, C.A., Bahr, J.L., Arepalli, S., Tour, J.M. and Krishnamoorti, R. (2002). Dispersion of Functionalized Carbon Nanotubes in Polystyrene, *Macromolecules*, **35**: 8825–8830.

221. Bubert, H., Haiber, S., Brandl, W., Marginean, G., Heintze, M. and Brüser, V. (2003). Characterization of the Uppermost Layer of Plasma-treated Carbon Nanotubes, *Diamond and Related Materials*, **12**(3–7): 811–815.

222. Eitan, A., Jiang, K., Dukes, D., Andrews, R. and Schadler, L.S. (2003). Surface Modification of Multiwalled Carbon Nanotubes: Toward the Tailoring of the Interface in Polymer Composites, *Chemistry of Materials*, **15**(16): 3198–3201.

223. Jang, J., Bae, J. and Yoon, S.H. (2003). A Study on the Effect of Surface Treatment of Carbon Nanotubes for Liquid Crystalline Epoxide-carbon Nanotube Composites, *Journal of Materials Chemistry*, **13**(4): 676–681.

224. Star, A., Stoddart, J.F., Steuerman, D., Diehl, M., Boukai, A., Wong, E.W., Yang, X., Chung, S.-W., Choi, H., Heath, J.R. (2001). Preparation and Properties of Polymer-wrapped Single-walled Carbon Nanotubes, *Angew Chem Int Ed*, **40**: 1721–1725.

225. Jia, Z., Wang, Z., Xu, C., Liang, J., We, B., Wu, D. and Zhu, S. (1999). Study on Poly(methyl methacrylate)/carbon Nanotube Composites, *Mater Sci. Eng.*, 395–400.

226. Deng, J., Ding, X., Zhang, W., Peng, Y., Wang, J., Long, X., Li, P. and Chan, A.S.C. (2002). Carbon Nanotube-polyaniline Hybrid Materials, *Eur. Polym. J*, **38**: 2497–2501.

227. Qian, D., Dickey, E.C., Andrews, R. and Rantell, T. (2000). Load Transfer and Deformation Mechanisms in Carbon Nanotube-polystyrene Composites, *Appl. Phys. Lett.*, **76**(20): 2868–2870.

228. Bhattacharyya, A.R., Sreekumar, T.V., Liu, T., Kumar, S., Ericson, L.M., Hauge, R.H. and Smalley, R.E. (2003). Crystallization and Orientation Studies in Polypropylene/Single Wall Carbon Nanotube Composite, *Polymer*, **44**(8): 2373–2377.

229. Potschke, P., Fornes, T.D. and Paul, D.R. (2002). Rheological Behaviors of Multiwalled Carbon Nanotube/Polycarbonate Composites, *Polymer*, **43**: 3247–3255.

230. Siochi, E.J., Working, D.C., Park, C., Lillehei, P.T., Rouse, J.H., Topping, C.C., Bhattacharyya, A.R. and Kumar, S. (2004). Melt Processing of SWCNT-polyimide Nanocomposite Fibers, *Composites Part B-Engineering*, **35**(5): 439–446.

231. Tang, W.Z., Santare, M.H. and Advani, S.G. (2003). Melt Processing and Mechanical Property Characterization of Multi-walled Carbon Nanotube/High Density Polyethylene (MWNT/HDPE) Composite Films, *Carbon*, **41**(14): 2779–2785.

232. Broda, J. (2003). Polymorphism in Polypropylene Fibers, *Journal of Applied Polymer Science*, **89**(12): 3364–3370.

233. Gong, X., Liu, J., Baskaran, S., Voise, R.D. and Young, S. (2000). Surfactant-assisted Processing of Carbon Nanotube/Polymer Composites, *Chem. Mater.*, **12**: 1049–1052.

234. Shaffer, M.S.P., Fan, X. and Windle, A.H. (1998). Load Transfer in Carbon Nanotube Epoxy Composites, *Carbon*, **36**: 1603–1612.

235. Dror, Y., Salalha, W., Khalfin, R.L., Cohen, Y., Yarin, A.L. and Zussman, E. (2003). Carbon Nanotubes Embedded in Oriented Polymer Nanofibers by Electrospinning, *Langmuir*, **19**(17): 7012–7020.

236. Chen, G.Z., Shaffer, M.S.P., Coleby, D., Dixon, G., Zhou, W., Fray, D.J. and Windle, A.H. (2000). Carbon Nanotube and Polypyrrole Composites: Coating and Doping, *Adv. Mater.*, **12**(7): 522–526.

237. Bin, Y.Z., Kitanaka, M., Zhu, D. and Matsuo, M. (2003). Development of Highly Oriented Polyethylene Filled with Aligned Carbon Nanotubes by Gelation/Crystallization from Solutions, *Macromolecules*, **36**(16): 6213–6219.

238. McCullen, S.D., Kinlaw, A. and Gorga, R.E. (2006). Effect of Multi-wall Nanotube Diameter on Dispersion and Mechanical Properties in Polypropylene Matrix Composites, *Journal of Applied Polymer Science* (in preparation).

239. Wilbrink, M.W.L., Argon, A.S., Cohen, R.E. and Weinberg, M. (2001). Toughen Ability of Nylon-6 with $CaCO_3$ Filler Particles: New Findings and General Principles, *Polymer*, **42**(26): 10155–10180.

240. Choi, E.S., Brooks, J.S., Eaton, D.L., Al-Haik, M.S., Hussaini, M.Y., Garmestani, H., Li, D. and Dahmen, K. (2003). Enhancement of Thermal and Electrical Properties of Carbon Nanotube Polymer Composites by Magnetic Field Processing, *Journal of Applied Physics*, **94**(9): 6034–6039.

241. Liang, Z., Shankar, K.R., Barefield, K., Zhang, C., Wang, B. and Kramer, L. (2003). Investigation of Magnetically Aligned Carbon Nanotube Bucky Paper/Epoxy Composites, In: *Conference Proceedings at SAMPE*, CA.

242. Wang, Z., Liang, Z., Wang, B., Zhang, C. and Kramer, L. (2004). Processing and Property Investigation of Single-walled Carbon Nanotube (SWNT) Buckypaper/Epoxy Resin Matrix Nanocomposites, *Composites: Part A*, **35**: 1225–1232.

243. Liang, Z., Gonnet, P., Choi, E.S., Shankar, R., Zhang, C., Brooks, J.S., Wang, B. and Kramer, L. (2005). Investigation of Thermal Conductivity of Carbon Nanotube Bucky Papers and Nanocomposites, In: *Conference Proceedings at SAMPE*.

244. Walters, D.A., Casavant M.J., Qiin, X.C., Huffman, C.B., Boul, P.J., Erickson, L.M. and Smith, K. (2001). In Plane Aligned Membranes of Carbon Nanotube, *Chem. Physics. Lett.*, **338**: 14–20.

245. Kimura, T. and Ago, H. (2002). Polymer Composites of Carbon Nanotubes Aligned by a Magnetic Field, *Adv. Mater.*, **14**(19): 1380–1383.

246. Fan, Z. and Advani, S. (2005). Characterization of Orientation State of Carbon Nanotubes in Shear Flow, *Polymer*, **46**: 5232–5240.

247. Zeng, J., Saltysiak, B., Johnson, W.S., Schiraldi, D.A. and Kumar, S. (2004). Processing and Properties of Poly (Methyl Methacrylate)/Carbon Nano Fiber Composites, *Composites Part B-Engineering*, **35**(2): 173–178.

248. Assouline, E., Lustiger, A., Barber, A.H., Cooper, C.A., Klein, E., Wachtel, E. and Wagner, H.D. (2003). Nucleation Ability of Multiwall Carbon Nanotubes in Polypropylene Composites, *J. Polym. Sci., Part B: Polym. Phys.*, **41**(5): 520–527.

249. Grady, B.P., Pompeo, F., Shambaugh, R.L. and Resasco, D.E. (2002). Nucleation of Polypropylene Crystallization by Single-walled Carbon Nanotubes, *J. Phys. Chem. B.*, **106**(23): 5852–5858.

250. Sandler, J., Broza, G., Nolte, M., Schulte, K., Lam, Y.M., Shaffer, M.S.P. (2003). Crystallization of Carbon Nanotube and Nanofiber Polypropylene Composite, *Journal of Macromolecular Science-Physics*, B**42**(3–4): 479–488.

251. Xiao, K.Q. and Zhang, L.C. (2004). The Stress Transfer Efficiency of a Single-walled Carbon Nanotube in Epoxy Matrix, *Journal of Materials Science*, **39**(14): 4481–4486.

252. Valentini, L., Puglia, D., Frulloni, E., Armentano, I., Kenny, J.M. and Santucci, S. (2004). Dielectric Behavior of Epoxy Matrix/Single-walled Carbon Nanotube Composites, *Composites Science and Technology*, **64**(1): 23–33.

253. Sandler, J., Shaffer, M.S.P., Prasse, T., Bauhofer, W., Schulte, K. and Windle, A.H. (1999). Development of a Dispersion Process for Carbon Nanotubes in an Epoxy Matrix and the Resulting Electrical Properties, *Polymer*, **40**(21): 5967–5971.

254. Martin, C.A., Sandler, J.K.W., Windle, A.H., Schwarz, M.K., Bauhofer, W., Schulte, K. and Shaffer, M.S.P. (2005). Electric Field-induced Aligned Multi-wall Carbon Nanotube Networks in Epoxy Composites, *Polymer*, **46**(3): 877–886.

255. Martin, C.A., Sandler, J.K.W., Shaffer, M.S.P., Schwarz, M.K., Bauhofer, W. Schulte, K. and Windle, A.H. (2004). Formation of Percolating Networks in Multi-wall Carbon-nanotube-epoxy Composites, *Composites Science and Technology*, **64**(15): 2309–2316.

256. Liao, Y.H., Tondin, O.M., Liang, Z., Zhang, C. and Wang, B. (2004). Investigation of the Dispersion Process of SWNTS/SC-15 Epoxy Resin Nanocomposites, *Materials Science and Engineering A*, **385**(1–2): 175–181.

257. Lau, K.T., Lu, M., Lam, C.K., Cheung, H.Y., Sheng, F.L. and Li, H.L. (2005). Thermal and Mechanical Properties of Single-walled Carbon Nanotube Bundle-reinforced Epoxy Nanocomposites: the Role of Solvent for Nanotube Dispersion, *Composites Science and Technology*, **65**(5): 719–725.

258. Gojny, F.H., Wichmann, M.H.G., Köpke, U., Fiedler, B. and Schulte, K. (2004). Carbon Nanotube-reinforced Epoxy-composites: Enhanced Stiffness and Fracture Toughness at Low Nanotube Content, *Composites Science and Technology*, **64**(15): 2363–2371.

259. Allaoui, A., Bai, S., Cheng, H.M. and Bai, J.B. (2002). Mechanical and Electrical Properties of a MWNT/Epoxy Composite, *Composites Science and Technology*, **62**(15): 1993–1998.

260. Gorga, R.E. and Tsabba, Y. (2006). Mechanical Properties of Single-wall and Multi-wall Carbon Nanotube Composites, *Textile Research Journal* (submitted).

261. Sabba, I. and Thomas, E.L. (2004). High-concentration Dispersion of Single-wall Carbon Nanotubes, *Macromolecules*, **37**(13): 4815–4820.

262. Kearns, J.C. and Shambaugh, R.L. (2002). Polypropylene Fibers Reinforced with Carbon Nanotubes, *Journal of Applied Polymer Science*, **86**(8): 2079–2084.

263. Moore, E.M., Ortiz, D.L., Marla, V.T., Shambaugh, R.L. and Grady, B.P. (2004). Enhancing the Strength of Polypropylene Fibers with Carbon Nanotubes, *Journal of Applied Polymer Science*, **93**(6): 2926–2933.

264. Coleman, J.N., Cadek, M., Blake, R., Nicolosi, V., Ryan, K.P., Belton, C., Fonseca, A., Nagy, J.B., Gun'ko, Y.K. and Blau, W.J. (2004). High-performance Nanotube-reinforced Plastics: Understanding the Mechanism of Strength Increase, *Advanced Functional Materials*, **14**(8): 791–798.

265. Xia, H.S., Xia, H., Wang, Q., Li, K. and Hu, G.H. (2004). Preparation of Polypropylene/Carbon Nanotube Composite Powder with a Solid-state Mechanochemical Pulverization Process, *Journal of Applied Polymer Science*, **93**(1): 378–386.

266. Johnson, B., Santare, M.H. and Advani, S. (2004). Manufacturing and Performance of Carbon Nanotube/High Density Polyethylene Composites, In: *International Conference on Flow Processes in Composite Materials*, July, 2004.

267. Ren, Y., Li, F., Cheng, H.M. and Liao, K. (2003). *Advanced Composites Letters*, **12**(1).

268. O'Donnell, S.E. and Sprong, K.R. AIAA 4th Aviation Technology, Integration and Operations Forum, Chicago, Sept, 2004.

269. Hsiao, K.T., Alms, J. and Advani, S. (2003). Use of Epoxy/Multiwalled Carbon Nanotubes as Adhesives to Join Graphite Fibre Reinforced Polymer Composites, *Nanotechnology*, **14**(7): 791–793.

270. Gou, J., Liang, Z., Zhang, C. and Kramer, L. (October, 2002). Nanotube Bucky Paper-epoxy Composites: Modeling, Fabrication and Characterization, In: *10th Foresight Conference on Molecular Nanotechnology*, MD, USA.

271. Patent Number: US Application #: 60-429, 955 (Utility Application No. 10/726,024)/Pending.

272. Li, C.Y. and Chou, T.W. (2003). A Structural Mechanics Approach for the Analysis of Carbon Nanotubes, *Inter. J. Solid & Struct.*, **40**: 2487–249.

273. Li, C.Y. and Chou, T.W. (2003). Elastic Moduli of Multi-walled Carbon Nanotubes and the Effect of van der Waals Forces, *Composite Science and Technology*, **63**(11): 1517–1524.

274. Frankland, S.J.V., Caglar, A., Brenner, D.W. and Griebel, M. (2002). Molecular Simulation of the Influence of Chemical Cross-links on the Shear Strength of carbon Nanotube-polymer Interfaces, *J. Phys. Chem. B.*, **106**: 3046–3048.

275. Lau, K.T. (2003). Interfacial Bonding Characteristics of Nanotube/Polymer Composites, *Chemical Physics Letters*, **370**: 399–405.

276. Tu, Z.C. and Ou-Yang, Z.C. (2002). Single-walled and Multiwalled Carbon Nanotubes Viewed as Elastic Tubes with the Effective Young's Moduli Dependent on Layer Number, *Physical Review B*, **65**: 233407.

277. Odegard, G.M., Gates, T.S., Nicholson, L.M. and Wise, K.E. (2002). Equivalent-continuum Modelling of Nano-structured Materials, *Comp. Sci. Tech.*, **62**: 1869–1880.

278. Lau, K.T., Sankar, J., Hui, D. (2006). Enhancement of the Mechanical Strength of Polymer-based Composites Using Carbon Nanotubes, in Nanoengineering of Structural, Functional, and Smart Materials, Schulz, M.J., Kelker, A.D. and Sunderasen, M.J. (ed.) **1st edn.**, CRC Taylor & Francis, USA, ISBN 0-8-8493-1653-7, Chapter 14. (Reproduced in part with permission from Taylor & Francis © 2006.)

279. Tang, J., Wang, Y., Liu, H., Xia, Y. and Schneider, B. (2003). Effect of Processing on Morphological Structure of Polyacrylonitrile Matrix Nano-ZnO Composites, *J. of Applied Polymer Science*, **90**: 1053–1057.

280. Zheng, Y.P., Zheng Y. and Ning, R.C. (2003). Effects of Nanoparticles SiO_2 on the Performance of Nanocomposites, *Materials Letters*, **57**(19): 2940–2944.

281. Private Communication with Dr Jihua Chen, at AMTC/NRC, Montreal 2005.

282. Chen, Y.C., Zhou, S.X. and Wu, L.M. (2005). *European Polymer Journal* (submitted 2005).

283. Ma, D., Hugener, T.A., Siegel, R.W., Christerson, A., Martensson, E., Onneby, C. and Schadler, L. (2005). Influence of Nanoparticle Surface Modification on the Electrical Behaviour of Polyethylene Nanocomposites, *Nanotechnology*, **16**: 724–731.

284. Chen, Y.C., Zhou, S.X., Yang, H.H. and Wu, L.M. (2005). Structure and Properties of Polyurethane/Nanosilica Composites, *Journal of Applied Polymer Science*, **95**(5): 1032–1039.

285. Zhang, M. and Singh, R. (2004). Mechanical Reinforcement of Unsaturated Polyester by AL_2O_3 Nanoparticles, *Materials Letters*, **58**: 408–412.

286. Yong, V. and Hahn, H.T. (2004). Processing and Properties of SiC/Vinyl Ester Nanocomposites, *Nanotechnology*, **15**: 1338.

287. Lao, S., Ho, W., Ngyuen, K., Koo, J.H., et al. (2005). Micro Structural Analysis of Nylon 11 Nanocomposites, *SAMPE*, Seattle, WA.

288. Wu, C.L., Zhang, M.Q., Rong, M.Z. and Friedrich, K. (2002). Tensile Performance Improvement of Low Nanoparticles Filled-polypropylene Composites, *Composite Science and Technology*, **62**: 1327–1340.

289. Zhang, Z. and Yang, J.L. (2004). Creep Resistant Polymeric Nanocomposites, *Polymer*, **45**: 3481–3485.

290. Koo, J.H., Pilato, L.A. and Wissler, G.E. (2005). Polymer Nanostructured Materials for Propulsion System, In: *Conference Proceedings for AIAA-2005-3606, 41st AIAA/ASME/SAE/ ASEE Joint Propulsion Conference & Exhibit, Tucson, AZ, 10–13 July 2005*.

291. Koo, J.H., Stretz, J., Weispfenning, Z., Luo, P. and Wootan, W. (2004). Nanocomposite Rocket Ablative Materials: Subscale Ablation Test, In: *SAMPE Symposium*, Long Beach, California, May, 2004.

292. Koo, J.H., Pilato, L.A., Wissler, G., Lee, A., Abusafieh, A. and Weispfenning, J. (2005). Epoxy Nanocomposites for Carbon Reinforced Polymer Matrix Composites, *SAMPE*, CA.

293. Ou, Y., Yang, F. and Yu, Z. (1998). A New Conception on the Toughness of Nylon 6/Silica Nanocomposites Prepared via In Situ Polymerization, *J. Polym. Sci., Part B: Polym. Phys.*, **36**: 789–795.

294. Jiang, L., Lam, Y.C., Tam, K.C., Chua, T.H., Sim, G.W. and Ang, L.S. (2005). Strengthening Acrylonitrile-Butadiene-Styrene (ABS) with Nano-sized and Micron-sized Calcium Carbonate, *Polymer*, **46**: 243–252.

295. Lopez, L. Song, B.M.K. and Hahn, H.T. *The Effect of Particles Size in Alumina Nanocomposites*, ICCM-2203 CA.

296. Chen, Y., Zhou, S., Yang, H., Gu, G. and Wu, L. (2004). Preparation and Characterization of Nanocomposites Polyurethane, *Journal of Colloid and Interface Science*, **276**(2): 370–378.

297. Lin, J.C., Chang, L.C., Nien, M.H. and Ho, H.L. (2006). Mechanical Behavior of Various Nanoparticle Filled Composites at Low-Velocity Impact, *Composite Structures*, **74**: 30–60.

298. Chisholm, N., Mahfuz, H., Rangari, V.K. and Jeelani, S. (2005). Fabrication and Mechanical Characterization of Carbon/SiC-epoxy Nanocomposites, *Composite Structures*, **67**(1): 115–124.

299. Avalle, M., Belingardi, G. and Montanini, R. (2001). Characterization of Polymeric Structural Foams under Compressive Impact Loading by means of Energy-absorption Diagram, *Int. J. Impact Engineering*, **25**(5): 455–472.

300. Mahfuz, H., Islam, M.S., Rangari, V.K. and Jeelani, S. (2004). Fabrication, Synthesis and Mechanical Characterization of Nanoparticles Infused Polyurethane Foams, *Composites: Part A*, **35**: 453–460.

301. Uddin, M., Mahfuz, H., Saha, M., Ragari, V.K. and Jeelani, S. (2004). Strain Rate Effects on Nanophased Polyurethane Foams. In: *International SAMPE Symposium and Exhibition (Proceedings)*, v 49, *SAMPE 2004 Conference Proceedings - 2004*, pp. 2291–2304.

302. Mahfuz, H., Islam, M., Saha, M.C. and Jeelani, S. (2004). Response of Sandwich Composites with Nanophased Cores Under Flexural Loading, *Composites: Part B*, **35**: 543–550.

303. Mahfuz, H., Uddin, F., and Jeelani, S. (2005). Response of Nanophased Core Materials and Sandwich Composites under Ballistic and High Strain Rate Loading. Private communication with Prof. Hasan Mahfuz, Dept. of Ocean Engineering, Florida Atlantic University, USA and Md. Farid Uddin, Grad student, Tuskegee University, 2005.

304. Jayaraman, K. (2004). Recent Advances in Polymer Nanofibers, *Journal of Nanoscience and Nanotechnology (Review article)*, **4**(1–2): 52–65.

305. Martin, C.R. (1994). Nanomaterials: A Membrane-based Synthetic Approach, *Science*, **266**: 1961–1966.

306. Martin, C.R. (1996). Membrane-based Synthesis of Nanomaterials, *Chem. Mater.*, **8**: 1739

307. Wu, C.G. and Bein, T. (1994). Conducting Polyaniline Filaments in a Mesoporous Channel Host, *Science*, **264**: 1757–1759.

308. Larrondo, L. and Manley, R.St.J. (1981). *J. Polym. Sci. Polym. Phys.*, **19**: 909.

309. Larrondo, L. and Manley, R.St.J. (1981). *J. Polym. Sci. Polym. Phys.*, **19**: 921.

310. Larrondo, L. and Manley, R.St.J. (1981). *J. Polym. Sci. Polym. Phys.*, **19**: 933.

311. Glasgow, D.G., Burton, D., Hughes, T.W. and Lake, M.L. Nanocomposites from Carbon Nanofiber, *Applied Sciences*, Inc. Cedarville, OH 45387.

312. Thomas, W., Hughes, (September 2004). *Nanocomposites 2004 Conference*, September 2004, San Francisco, CA.

313. Tandon, G.P. and Ran, Y. (2002). Influence of Vapor-Grown Carbon Nanofibers on Thermomechanical properties of Graphite-Epoxy Composites, In: *Proceedings for the 17th Annual Technical Conference ASC*.

314. Glasgow, D.G. and Tibbetts, G.G. Surface Treatment of Carbon Nanofibers for Improved Composite Mechanical Properties, *SAMPE 2004*, Longbeach, CA.

315. Lafdi, K. *SAMPE 2003*, Dayton, OH.

316. Finegan, C., Tibbetts, G.G., Glasgow, D.G., Ting, J.M. and Lake, M.L. (2003). Surface Treatments for Improving the Mechanical Properties of Carbon Nanofiber/Thermoplastic Composites, *Journal of Materials Science*, **38**: 3485–3490.

317. Gibson, T., Rice, B. and Ragland, W. Formulation and Evaluation of Carbon Nanofiber Based Conductive Adhesives, *SAMPE-2005*, Longbeach, CA.

318. Ericson, Lars, M. (2000). Strength Characterization of Suspended Single-Wall Carbon Nanotube Ropes, Masters Thesis, Rice University, Oct 2000.

319. Jana, S.C. and Jain, S. (2001). Dispersion of Nanofillers in High Performance Polymers using Reactive Solvents as Processing Aids, *Polymer*, **42**: 6897–6905.

320. Zhang, B., Xie, C., Hu, J., Wang, H. and Gui, Y.H. (2006). Novel 1–3 Metal Nanoparticle/ Polymer Composites Induced by Hybrid External Fields, *Composites Science and Technology*, **66**: 1558–1563.

321. McMorrow, B., Chartoff, R. and Klosterman, D. Processing and Characterization of a Carbon Nanofiber/Vinylster Resin Composite, *SAMPE 2003 Proceedings*, Long Beach, CA, USA.

322. Han, J., Anantram, M.P., Jaffe, R.L., Kong, J. and Dai, H. (1998). *Phys. Rev. B*, **57**: 14983.

323. Han, J. *Electrochemical Society Proceedings*, **98**(8): 875–884.

324. Han, J. and Jaffe, R.J. (1998). *Chem. Physics*, **108**: 2817.

325. Wilkins, R., et al. (2005). *Material Res. Soc. Symp. Proceedings*, 851(NN6.5).

326. Dr. Mal O' Neill, VP (2004). Chief Technical Officer, Lockheed Martin, Presentation.

327. Pham, J.Q., Mitchell, C.A., Bahr, J.L., Tour, J.M, Krishnamoorti, R. and Green, P. (2003). Glass Transition of Polymer/Single-walled Carbon Nanotube Composite Films, *J. Polym. Sci., Part B: Polym. Phys.*, **41**: 3339.

328. Ash, B.J., Schadler, L.S. and Siegel, R.W. (2002). Glass Transition Behavior of Alumina/ Polymethylmethacrylate Nanocomposites, *Mater Lett.*, **55**: 83–87.

329. Shvedova, A., Castranova, V., Kisin, E., Schwegler-Berry, D., Murray, A.R., Gandelsman, V.Z., Maynard, A. and Baron, P. (2003). Exposure to Carbon Nanotube Material: Assessment of Nanotube Cytotoxicity Using Human Keratinocyte Cells, *Journal of Toxicology and Environmental Health*, *Part A*, **66**: 1909–1926. (Reproduced in part with permission from Taylor & Francis © 2006.)

330. Eedy, D.J. (1996). *Carbon-fiber-induced Airborne Irritant Contact Dermatitis*, Contact Dermatitis **35**: 362.

331. Muller, J., Huaux, F. and Lison, D. (2006). Respiratory Toxicity of Carbon Nanotubes: How Worried Should We Be?, *Carbon*, **44**: 1048–1056. (Reproduced in part with permission from Elsevier © 2006.)

332. Warheit, D.B. (2006). What is Currently Known About the Health Risks Related to Carbon Nanotube Exposures?, *Carbon*, **44**: 1064–1069.

333. Toensmeier, P.A. (2004). *Plastics Engg.*, p. 14.

334. Borm, P.J.A. (2002). Particle Toxicology: From Coal to Nanotechnology, *Inhal. Toxicol.*, **14**: 311–324.

335. Donaldson, K., Stone, V., Tran, C.L., Kreyling, W. and Borm, P.J.A. (2004). *Occup. Environ. Med.*, **61**: 727.

336. Agarwal, S., Tatli, E., Clark, N.N. and Gupta, R. (September, 2005). *International Symposium on Polymer Nanocomposites Science and Technology*, Boucherville, Canada, September, 2005.

337. Bhattacharya, K., Dopp, E., Kakkar, P., Jaffery, F.N., Schiffmann, D., Jaurand, M.C., Rahman, I. and Rahman Q. (2005). Biomarkers in Risk Assessment of Asbestos Exposure, *Mutation Research (Review article)*, **579**: 6–21.

338. Koyama, S., Endo, M., Kim, Y.A., Hayashi, T., Yanagisawa, T., Osaka, K., Koyama, H., Haniu, H. and Kuroiwa, N. (2006). Role of Systemic T-cells and Histopathological Aspects After Subcutaneous Implantation of Various Carbon Nanotubes in Mice, *Carbon*, **44**(6): 1079–1092.

339. Shvedova, A.A., Kison, E.R. and Mercer, R. (2005). Unusual Inflammatory and Fibrogenic Pulmonery Responses to Single Walled Carbon Nanotube in Mice, *Am. J. Physiol. Lung Cell Mol. Physiol.*, 289. (Reproduced in part with permission from American Physiological Society © 2006.)

340. Warheit, D.B. (2004). Nanoparticles: Health Impact?, *Materials Today*, **7**(2): 32–35.

341. Monteiro-Riviere, N.A., Nemanich, R.J., Inman, A.O., Wang, Y.Y. and Riviere, J.E. (2005). Multi-walled Carbon Nanotube Interactions with Human Epidermal Keratinocytes, *Toxicology Letters*, **155**: 377–384.

342. Nancy, A., Monteiro-Riviere, and Alfred, O. (2006). Inman Challenges for Assessing Carbon Nanomaterial Toxicity to the Skin, *Carbon*, **44**: 1070–1078.

343. Shvedova, A.A., Kommineni, C., Jeffries, B.A., Castranova, V., Tyurina, Y.Y., Tyurin, V.A., Serbinova, E.A., Fabisiak, J.P. and Kagan, V.E. (2000). Redox Cycling of Phenol Induces Oxidative Stress in Human Epidermal Keratinocytes, *J. Invest. Dermatol.*, **114**: 354–364.

344. Lademann, J., Weigmann, H.J., et al. (1999). Penetration of Titanium dioxide Microparticles in a Sunscreen Formulation into the Horny Layer and the Follicular Orifice, *Skin Pharmacol. Appl. Skin Physiol.*, **12**: 247–256.

345. Pflucker, F. et al. *Skin Pharmacol. Appl. Skin Physiol.*, **14**(suppl. 1): 92–97.

346. Dunford, R., Salinaro, A., Cai, L., Serpone, N., Horikoshi, S., Hidaka, H. and Knowland, J. (1997). Chemical Oxidation and DNA Damage Catalyzed by Inorganic Sunscreen Ingredients, *FEBS Lett.*, **418**(1–2): 87–90.

347. Smart, S.K., Cassady, A.I., Lu, G.Q. and Martin, D.J. (2006). The Biocompatibility of Carbon Nanotubes, *Carbon*, **44**(6): 1034–1047.

348. Fiorito, S., Serafino, A., Andreola, F. and Bernier, P. (2006). Effects of Fullerenes and Single-wall Carbon Nanotubes on Murine and Human Macrophages, *Carbon*, **44**(6): 1100–1105. (Reproduced in part with permission from Elsevier © 2006.)

349. Hurt, R.H., Monthioux, M. and Kane, A. (2006). Toxicology of Carbon Nanomaterials: Status, Trends, and Perspectives on the Special Issue, *Carbon*, **44**(6): 1028–1033. (Reproduced in part with permission from Elsevier © 2006.)

350. Ebenau, A. (2002). Wirtschaftliche Perspektiven der Nanotechnologie: Enorme Markte fur kleinste Teilchen, *Journalisten und Wissenschaftler im Gesprach, Nanotechnologie in der Chemie-Experience meets Vision* Mannheim, Oct. 28–29.